QUANTITATIVE TRANSPORTATION RISK ANALYSIS BASED ON AVAILABLE DATA/DATABASES: DECISION SUPPORT TOOLS FOR HAZARDOUS MATERIALS TRANSPORTATION

A Dissertation

by

YUANHUA QIAO

Submitted to the Office of Graduate Studies of
Texas A&M University
in partial of fulfillment of the requirements for the degree of

DOCTOR OF PHILOSOPHY

May 2006

Major Subject: Chemical Engineering

QUANTITATIVE TRANSPORTATION RISK ANALYSIS BASED ON AVAILABLE DATA/DATABASES: DECISION SUPPORT TOOLS FOR HAZARDOUS MATERIALS TRANSPORTATION

A Dissertation

by

YUANHUA QIAO

Submitted to the Office of Graduate Studies of
Texas A&M University
in partial of fulfillment of the requirements for the degree of

DOCTOR OF PHILOSOPHY

Approved by:

Chair of Committee,	M. Sam Mannan
Committee Members,	Harry H. West
	Mahmoud M. El-Halwagi
	Dick B. Simmons
Head of Department,	Kenneth R. Hall

May 2006

Major Subject: Chemical Engineering

ABSTRACT

Quantitative Transportation Risk Analysis Based on Available Data/Databases: Decision

Support Tools for Hazardous Materials Transportation. (May 2006)

Yuanhua Qiao, B.En., Tianjin University, Tianjin, China;

M.S, Tianjin University, Tianjin, China

Chair of Advisory Committee: Dr. M. Sam Mannan

Historical evidence has shown that incidents due to hazardous materials (HazMat) releases during transportation can lead to severe consequences. The public and some agencies such as the Department of Transportation (DOT) show an increasing concern with the hazard associated with HazMat transportation. Many hazards may be identified and controlled or eliminated through use of risk analysis. Transportation Risk Analysis (TRA) is a powerful tool in HazMat transportation decision support system. It is helpful in choosing among alternate routes by providing information on risks associated with each route, and in selecting appropriate risk reduction alternatives by demonstrating the effectiveness of various alternatives.

Some methodologies have been developed to assess the transportation risk; however, most of those proposed methodologies are hard to employ directly by decision or policy makers. One major barrier is the lack of the match between available data/database analysis and the numerical methodologies for TRA.

In this work methodologies to assess the transportation risk are developed based on the availability of data or databases. The match between the availability of data/databases and numerical TRA methodologies is pursued. Each risk component, including frequency, release scenario, and consequence, is assessed based on the available data/databases. The risk is measured by numerical algorithms step by step in the transportation network. Based on the TRA results, decisions on HazMat transportation could be made appropriately and reasonably.

The combination of recent interest in expanding or building new facilities to receive liquefied natural gas (LNG) carriers, along with increased awareness and concern about potential terrorist action, has raised questions about the potential consequences of incidents involving LNG transportation. One of those consequences, rapid phase transition (RPT), is studied in this dissertation. The incidents and experiments of LNG-water RPT and theoretical analysis about RPT mechanism are reviewed. Some other consequences, like pool spread and vapor cloud dispersion, are analyzed by Federal Energy Regulatory Commission (FERC) model.

To

my parents
Mingke Qiao and Xiurong Zhang

my husband
Jingchao Yang

And my sister
Yuanyi Qiao

ACKNOWLEDGEMENTS

I am full of appreciation and gratefulness to everyone who helped me. This dissertation would have been a "mission impossible" without the contributions of so many people.

My deepest gratitude goes to my advisor, Dr. M. Sam Mannan, not only for his financial support, but also for everything he has done for me. He led me to this interesting research and helped me to find my career goal to be a safety specialist. He is so knowledgeable and has such a perfect character. I learned a lot from him and will benefit from continuously learning from him. I will never forget his patience and trust in me. It was my good fortune to have Dr. Mannan as my advisor. I will always have great respect and admiration for Dr. Mannan.

I am deeply grateful to Dr. Harry H. West. He liked to share his expert knowledge and experience with us, and what I learned from him is priceless and unobtainable in class. His humor made working with him an enjoyable thing. I really appreciated his help and guidance in both my research and projects. He was my second advisor. I am deeply grateful to Dr. Mahmoud M. El-Halwagi. I admire his knowledge so much. He always added great ideas to our research. I benefited so much from his ideas, his courses, and his encouragement. I really appreciate Dr. Dick B. Simmons for serving as my committee member, for his concern about my progress, and for spending time reading my proposal and dissertation.

I also want to thank the Chemical Engineering Department at Texas A&M University for admitting me into the Ph. D. program, which led me know my advisor and gave me the opportunity to work on process safety. I would like to acknowledge all the faculty for their showing me the beauty of chemical engineering, and acknowledge all the staff for their sincere help to students, especially to internationals.

I am indebted to my husband for his love. I have known him for 22 years and he is my childhood sweetheart. He has all the characteristics I have dreamed for a husband. He changed my life, leads me to a wider world, and makes my life enjoyable and meaningful. I have learned a lot from him and will continue learning from him. I am deeply grateful to my parents for their love and everything they have done for me and continue to do. Their love and wishes make my life meaningful. I feel grateful for their letting me know I cannot live without dreams and for encouraging me to make my dreams come true. I am also grateful to my sister, Yuanyi Qiao. She is such a lovely and courageous girl, and I am really proud of her. Her phone calls are pills for my homesickness. I am also grateful to all my friends, both in the U.S and in China. I appreciate the time when we share joys and sadness. My life is enjoyable because of the friendship.

TABLE OF CONTENTS

LIST OF TABLES

Page

LIST OF FIGURES

CHAPTER I

INTRODUCTION

Many conveniences taken for granted in modern civilization depend in part on HazMat. These materials must be transported from producers to end users, which creates opportunities for incidents (e.g., traffic incidents, train derailments, equipment failures) that could release hazardous chemicals into the environment. The adverse impact could occur when HazMat are released to the environment, including personal injury, property damage, and environmental contamination.

Risk is defined as a measure of human injury, environmental damage, or economic loss in terms of both the incident likelihood and the magnitude of the loss or injury (CCPS, 2000). To reduce the adverse impact associated with the HazMat transportation, it is important to assess the risk at first, and then it is necessary to develop management systems that involve procedures and actions to support strategic, tactical and operational decisions, including the transportation route selection, facility selection, emergency response in case an incident would occur, and so on and so forth. These systems can also be called decision support systems for HazMat transportation. The analysis on the transportation risk is the foundation of the decision support system.

This dissertation follows the style and format of the *Journal of Loss Prevention in the Process Industries*.

In this chapter the definition of HazMat will be introduced followed by the status of the HazMat transportation and the regulations on HazMat transportation in the U. S. Then the introduction on the techniques and concerns of TRA will be provided in comparison with the chemical process quantitative risk analysis (CPQRA). The objectives and scope of our research will be presented to define the boundaries of our work.

1.1. Hazardous Materials Transportation

1.1.1. Hazardous Materials

According to the Code of Federal Regulations, Title 49 (49 CFR), Transportation, Part 171.8, HazMat is defined as a substance or material, including a hazardous substance, which has been determined by the Secretary of Transportation to be capable of posing an unreasonable risk to health, safety, and property when transported in commerce, and has designated as hazardous under section 5103 of Federal HazMat transportation law (OHMS, 2005a). More than 3300 substances and their products have been characterized as HazMat, including flammable, corrosive, radioactive, toxic, poisonous, and explosive substances. In 49 CFR, HazMat are separated into the following classes:

- Class 1 – Explosives
- Class 2 – Gases
- Class 3 – Flammable liquids (and combustible liquids)

- Class 4 – Flammable solids; spontaneously combustible materials and dangerous when wet materials

- Class 5 – Oxidizers and organic peroxides

- Class 6 – Toxic (poison) materials and infectious substances

- Class 7 – Radioactive materials

- Class 8 – Corrosive materials

- Class 9 – Miscellaneous dangerous materials

The majority of classes are segmented into divisions. This finer categorization of HazMat is very helpful for purposes of comparing risks. For example, Explosives in Class 1 are divided into six divisions, and risk associated with different divisions should be much more different with those within one division. Table 1.1 lists all the class numbers, division numbers, class or division names and 49 CFR sections which contain definitions for classifying hazardous materials.

In subpart B of 49 CFR 171.1, the HazMat table designates the materials listed as HazMat for the purpose of transportation of those materials. For each listed material, the table identifies the hazard class, and gives the proper shipping name or directs the user to the preferred proper shipping name. In addition, the table specifies or references requirements in this subchapter pertaining to labeling, packaging, quantity limits aboard aircraft, and stowage of hazardous materials aboard vessels.

Table 1.1

Hazardous materials classes and index to 49 CFR hazard class definitions

Class No.	Division No.	Name of class or division	49 CFR reference for definitions
1	1.1	Explosives (with a mass explosion hazard)	173.50
1	1.2	Explosives (with a projection hazard)	173.50
1	1.3	Explosives (with predominately a fire hazard)	173.50
1	1.4	Explosives (with no significant blast hazard)	173.50
1	1.5	Very insensitive explosives; blasting agents	173.50
1	1.6	Extremely insensitive detonating substances	173.50
2	2.1	Flammable gas	173.115
2	2.2	Non-flammable compressed gas	173.115
2	2.3	Poisonous gas	173.115
3		Flammable and combustible liquid	173.120
4	4.1	Flammable solid	173.124
4	4.2	Spontaneously combustible material	173.124
4	4.3	Dangerous when wet material	173.124
5	5.1	Oxidizer	173.127
5	5.2	Organic peroxide	173.128
6	6.1	Poisonous materials	173.132
6	6.2	Infectious substance (Etiologic agent)	173.134
7		Radioactive material	173.403
8		Corrosive material	173.136
9		Miscellaneous hazardous material	173.140

1.1.2. HazMat Transportation Incidents

As detailed in the HazMat Shipments report from the Office of Hazardous Materials Safety (OHMS, 2005a), hazardous materials traffic levels in the U. S. now exceed 800,000 shipments per day and result in the transport of more than 3.1 billion tons of hazardous materials annually (OHMS, 2005b).

According to the DOT statistics, 156,483 HazMat transportation incidents occurred from 1995 to 2004, resulting in a total of 226 fatalities and 3,218 injuries (US DOT, 2005). The detailed statistics for different transportation modes within that period are shown in Table 1.2. Figure 1.1 shows the tendency of the number of reported HazMat incidents from 1983 to 2004.

Table 1.2

HazMat transportation incidents, fatalities, injuries, and damages from 1995 to 2004

Transportation mode	Incidents	Fatalities	Injury	Damages
Air	10,721	110	157	2,055,546
Highway	135,849	107	1,684	370,135,350
Railway	9,813	9	1,375	154,493,434
Water	100	0	2	3,873,145

Figure 1.1. Reported hazardous materials incidents.

(OHMS, 2005c)

1.1.3. HazMat Transportation Regulations

The regulations that govern the transportation of HazMat have evolved over a period of more than 100 years (US DOT, 1998). The earliest regulation was promulgated in 1886 in response to turmoil within the railroad industry by the Supreme Court of the U.S.

On January 3, 1975, the HazMat Transportation Act (HMTA), Title I of Public Law 93-633, was signed into law. The Act provided authority for the Secretary of Transportation to draw together previously fragmented regulatory and enforcement authority over the movement of HazMat in commerce into one consolidated and

coordinated effort. The HMTA was significantly amended by the Hazardous Materials Transportation Uniform Safety Act of 1990 (HMTUSA), Public Law 101-615, signed on November 16, 1990, and codified in 1994 in 49 U.S.C. §§ 5101-5127.

A number of other authorities underlie DOT's regulation of HazMat transportation: the Federal Water Pollution Control Act Amendments of 1972; the Resource Conservation and Recovery Act of 1976; the Comprehensive Environmental Response, Compensation, and Liability Act of 1980; and the Sanitary Food Transportation Act of 1990. Both HMTUSA and the HazMat Transportation Authorization Act of 1994 imposed on DOT additional responsibilities not codified in the Federal hazmat law. These laws have influenced and will continue to greatly influence the HazMat programs of all the modal administrations.

Currently, the HazMat regulations are codified in 49 CFR Parts 100-185. Those regulations set forth standards applicable to HazMat transportation, which include classification, packaging, hazard communication, emergency response information, training of hazmat employees, handling, and incident reporting.

In assessing the need for changes to the regulations, the Research and Special Programs Administration under DOT continuously monitors domestic transportation practices and experience and international regulatory developments. It evaluates requests for new or amended regulations received from the general public, the regulated industry, other Government agencies, and DOT's modal administrations. It also issues amendments to address specific safety problems, to incorporate new technology, and to respond to congressional mandates or executive orders.

1.2. Transportation Risk Analysis

1.2.1. Quantitative Risk Analysis (QRA) Methods

The techniques of chemical process quantitative risk analysis (CPQRA) are much better known than those of TRA, and there are many similarities in those two areas, so the techniques of CPQRA will be introduced first for better understanding of TRA.

CPQRA is a methodology designed to provide management with a tool to help evaluate overall process safety in the chemical process industry (CCPS, 2000). Management systems such as engineering codes, checklists and process safety management (PSM) provide layers of protection against incidents. However, the potential for serious incidents cannot be totally eliminated. CPQRA provides a quantitative method to evaluate risk and to identify areas for cost-effective risk reduction.

Many hazards may be identified and controlled or eliminated through the use of qualitative hazard analysis. Qualitative studies typically identify potentially hazardous events and their causes. In some cases, where the risks are clearly excessive and the existing safeguards are inadequate, corrective actions can be adequately identified with qualitative methods. QRA is used to help evaluate potential risks when qualitative methods cannot provide adequate understanding of the risks and more information is needed for risk management. It can also be used to evaluate alternative risk reduction strategies. The basis of QRA is to identify incident scenarios and evaluate the risk by defining the probability of failure, the probability of various consequences and the potential impact of those consequences. The risk is defined in CPQRA as a function of

probability or frequency and consequence of a particular incident scenario:

Risk = $F(s, c, f)$ (1.1)

Where,

s = hypothetical scenario

c = estimated consequence(s)

f = estimated frequency

This function can be extremely complex and there can be many numerically different risk measures (using different risk functions) calculated from a given set of s, c, f.

1.2.2 Framework of TRA

TRA methodologies have existed for about the same time period as have CPQRA methodologies, yet they are far less widely used and understood. TRA draws on many of the same tools and techniques as does CPQRA, but distribution activities are often performed in separate parts of an organization and may not be aware of all the internal resources available in risk analysis.

TRA can be conducted on a qualitative or quantitative basis. Qualitative approaches include risk screening methodologies, which are generally unique for each company. Other qualitative approaches include carrier screening programs, route and container selection, and driver training and selection programs. The quantitative approach in TRA is similar to CPQRA, which is used to help evaluate potential risks

when qualitative methods cannot provide adequate understanding of the risks. It can also be used to evaluate alternative risk reduction strategies. The general steps of TRA are described below:

- **TRA Scope Definition** converts user requirements into study goals and objectives. Risk measures and risk presentation formats are chosen in finalizing a scope of work for the TRA. A depth of study is then selected based on the specific objectives defined and the resources available.

- **Shipment Description** is the compilation of the transportation activity information needed for the risk analysis. For example, mode, container specification, weather data, number of trips, volume per container, material, shipping conditions, route or origin and destination, and population data. This data set is then used throughout the TRA.

- **Hazard or Initiating Event Identification** is a critical step in TRA. The incident-initiated events of concern can generally be identified based on historical data. Non-incident-initiated events may be identified through hazard identification techniques described in *CPQRA Guidelines* (CCPS, 2000).

- **Likelihood Estimation** is the methodology used to estimate the frequency or probability of occurrence of an incident. Estimates may be obtained from historical incident data on failure frequencies, from failure sequence models such as fault trees and event trees or from special failure models.

- **Consequence Estimation** is the methodology used to determine the potential for damage or injury from specific incidents. A single incident (e.g., rupture of a

pressurized liquid tank) can have many distinct incident outcomes, e.g., vapor cloud explosion (VCE), boiling liquid and so on.

- **Risk Estimation** combines the consequences and likelihood of all incident outcomes from all selected incidents to provide a measure of risk. The risks of all selected incidents are individually estimated and summed to give an overall measure of risk.

- **Utilization of Risk Estimates** is the process by which the results of a risk analysis are used to make decisions, either through relative ranking of risk reduction strategies or through comparison with specific risk targets.

In a screening or other qualitative analysis many of these steps are not carried out explicitly. Risk screens may be developed to implicitly take one or more of these steps into account. A screening level analysis can even be conducted by comparing the data set for the shipment of concern with the data set and results for another shipment for which a quantitative TRA has been conducted, and simply determining if the shipment of concern poses more or less risk than the previously evaluated one. In quantitative risk analyses it may be possible to take the results of other studies and use them as the basis of one or more of the steps in the TRA, but these other results may first need to be scaled or adjusted before using them, and usually all steps need to be performed to get the quantitative results.

1.2.3 Similarities to Fixed Facility Evaluations

There are both similarities and differences between transportation and fixed facility risk evaluations. As stated herein, the general process of a quantitative TRA involves: defining the scope of the analysis, describing the system or movement, identifying hazards or initiating events (accident and non-accident), numerating incidents, selecting incidents, incident outcomes, and incident outcome cases, estimating consequences, estimating frequencies, combining frequencies and consequences to estimate risk, and evaluating risk reduction alternatives. These steps are virtually the same as in a CPQRA, but there are subtleties within each step. Some of the differences are listed in the guidelines compiled by CCPS (1995). Both TRA and fixed facility risk evaluations can be qualitative or semi-quantitative as opposed to quantitative. In these cases, many of these steps are handled on a comparative basis or addressed in much less detail.

Qualitative or semi-quantitative estimates of risk generally take into account experience, judgment, good practices, training, procedures, inspection and maintenance, codes and standards, past performance, etc., whether one is dealing with fixed facilities or transportation movements.

The modeling of release consequences is largely independent of the cause of the release and is therefore basically directly transferable from the techniques of CPQRA to TRA. Risk measures are also common to the two types of quantitative risk analyses. The only real differences are in the details of how the risks are estimated and the units chosen. For example, in transportation one may wish to measure risk per trip or risk per year (or

both), while in CPQRA risks are generally measured on a per year basis or on a comparative basis with other results.

1.2.4. Differences from Fixed Facility Evaluations

The most fundamental difference between CPQRA and TRA is that TRA deals with a linear source of risk, versus a relatively discrete point source for a CPQRA. This linear source may be static as in the case of pipelines or may be a moving source for other modes of transport. In transportation, a release can occur anywhere along a route between the origin and destination. The unpredictability of the exact release location often requires the use of generalized approaches to limit the data needs and number of incident outcome cases. These generalized approaches may relate to one or more of the following:

- **Identification and selection of initiating events** – may utilize an aggregate incident rate or a limited breakdown, such as derailments and collisions, rather than a detailed breakout by failure mode.

- **Selection of incidents and incident outcomes** – particularly release sizes and rates, release orientation, material temperature and pressure at time of release. While a release in a facility is reasonably predictable in terms of the material conditions, these could change with the seasons for many HazMat transportations, and even from one end of a route to another.

- **Meteorological conditions for modeling** – wind roses and stability class distributions vary from location to location, as does the ambient temperature and

humidity.

- **Ignition probabilities** – the number, type, and proximity of ignition sources vary along a route, and it may be very difficult to get route specific data.

- **Population distribution** – not only is there usually very little, if any, buffer distance between a route and the general population, but the population density constantly changes along the route.

Generalized approaches help address these variabilities in a consistent and usually conservative manner. The ability to eliminate or prevent risks is much greater for fixed facilities. In transportation, risk reduction is generally all that can be obtained. The Office of Technology Assessment estimated that 62 percent of hazardous material incidents are due to human error. The degree of variability and influence of human performance is often cited as being much greater for some modes of transportation than others and for transportation in general in comparison to fixed sites. This is particularly true for road transportation where the route taken can vary from one trip to another. The role of outside forces such as weather and other drivers or operators can also be quite significant. For instance, extensive training of truck drivers does not change the performance of other drivers on the road. Thus, the ability to control the overall impact of human errors is diminished in transportation.

The nature of TRA data can be different from CPQRA data. They are often expressed as a function of distance traveled or per trip, transit, or visit. External event causes of accidents are generally included in the data-including such items as vandalism

for rail transport, adverse weather for marine transport, and third-party damage for pipelines.

Other difference between transportation and fixed facility risk evaluations is the nature of the risk reduction and mitigation alternatives available. By virtue of the unknown location of a transportation release (prior to its occurrence), it is much more difficult to identify and implement effective mitigative (post-release) strategies. Secondary containment via diking, selective grading, water sprays, foams, evacuations, etc. are either not feasible, or can only be initiated some significant amount of time after the release has occurred. Given the rapid dispersion of many large releases, such mitigation measures may be totally infeasible or untimely.

1.2.5. Reasons for Conducting a TRA

TRA is a powerful tool in HazMat transportation decision making system. It can help a decision maker in choosing a site for a facility or process relocation or expansion, by taking both fixed site and transportation risks into account. It is helpful in choosing among alternate routes by providing information on the relative risks associated with each route, in selecting a mode of transportation when more than one is feasible, and in selecting the most effective container or knowing if additional protective measures are warranted. Based on the TRA results, decision makers can select appropriate risk reduction alternatives by demonstrating the effectiveness of various alternatives. In case a transportation incident occurs, TRA could provide the bases for developing emergency response plans. It can also help to understand the influence of material state on risks and

make judgments about the tolerability of existing or increased movement levels.

1.3. Current Problems with TRA

Some regulations and rules have been set to regulate HazMat transportation activities; however, those regulations are mainly addressing hardware and procedures. Compliance with those regulations does not necessarily guarantee the desired reduction in the level of risk.

Significant level of risk reduction may be gained by the employment of decision support systems for HazMat transportation, for example, by selecting the route with relatively less risk. Selection for the best route for HazMat transportation involves comparisons of alternatives in the domain of risk. The TRA is the baseline for routing selection and many other actions made by decision makers.

Some numerical methodology has been developed to assess the transportation risk; however, most of those proposed methodologies were hard to employ directly by decision or policy makers. One reason is that the methodologies were proposed without input data, or the methodology was too complicated to obtain available input data. For example, incident frequency and conditional release probability data were assumed to be available in most of the methodologies, but in fact the acquisition of the required data calls for considerable effort.

Many data or databases on HazMat transportation have been analyzed to assess the risk components. Consider the Hazardous Materials Information System (HMIS) as an example. HMIS is a national database with data on HazMat transportation incidents.

Battelle (2001) analyzed this database to measure the incident rate, the severity of transportation fatalities and injuries, and the dollar loss from high-consequence transportation incidents. Such kind of data/database analysis results should be adapted to a numerical model to measure the ultimate risk level.

In many cases not all the data required by the TRA are available, thus some mathematical methodologies are needed to assess the required data based on expert experience or other information sources.

The lack of the match between the data/database analysis and the numerical methodologies for TRA has prevented decision makers from making sound actions quickly. The methodologies to assess the transportation risk according to the availability of data or databases should be developed, so that the decisions on HazMat transportation could be made appropriately and reasonably based on the TRA results.

1.4. Objectives and Scope

From the above description, it is apparent that the match between the availability of data/databases and numerical methodologies for TRA needs to be pursued. To accomplish this goal, in this paper, each risk component, including frequency, release scenario, and consequence, is assessed based on the available data/database. The risk in the transportation network is then assessed by numerical algorithms step-by-step.

The objectives of this research include:

- Transportation network analysis to define the physical environment for TRA

- Identification of HazMat transportation data/database

- Assessment of each risk component

- Development of numerical methodologies to measure the transportation risk

- Development of case study to show the application of methodologies

- Development of routing methodologies for decision support system based on TRA results

The ultimate goal of this research is to set up the framework for the assessment of transportation risk based on available data/databases, which will facilitate the set of regulations and rules, guide decision makers in HazMat transportation actions to prevent incident and reduce risk, and identify programs that can result in the greatest improvement in safety.

The scope of this research includes:

- **Highway transportation mode** – our research will focus on the highway transportation rather than all the transportation modes including railroad, air, etc, because the highway mode dominates the transportation incident occurrence. As shown in Table 1.2, historically highway transportation has been responsible for almost 90% of the transportation incidents.

- **On-road incident only** – our research only considers transportation incidents that occurred during transportation. Those that occurred during loading/unloading processes were not incorporated in our analysis, because those incidents are similar to fixed facility incidents.

- **Bulk transportation** – TRA will estimate only the incidents caused in bulk transportation, without including the non-bulk transportation. For example, anhydrous ammonia transported in cargo tanks MC 330 will be considered in our analysis, but those transported in small nurse tanks are not assessed.

- **Focused HazMat** – to compare the risks that result from transporting various hazardous materials, the nature of the risk for each commodity needs to be evaluated and understood, but it is not practical to work on all the HazMat. In this research, only those most frequently shipped HazMat and those materials representative to different classes is evaluated.

1.5. Organization of the Dissertation

This dissertation introduces a framework to assess the HazMat transportation risk step-by-step. Chapter I introduces HazMat transportation and the general framework for TRA, and introduces a broad overview of the importance of TRA.

Chapter II presents a detailed literature review of current research status of TRA. Preliminary work in this area has been categorized as procedures, data availability, risk measurement tools, and application of Geographic Information System (GIS). Fuzzy logic is employed in this research for estimation when data are not available, so the fuzzy logic models are also presented in this chapter. Chapter III characterizes the transportation network. The real transportation network is transformed into a network expressed by nodes and links, and by this way TRA can be performed in a well-defined network environment. A description of overall TRA methodology is provided in Chapter

IV in detail. The data/databases availability is analyzed at first for each of the risk components. Incident frequency and release scenario are assessed based on the analysis results. The consequence is estimated with a commercially available software, CANARY. Individual risk and societal risk for HazMat transportation are determined by numerical models. Chapter V presents the case study to illustrate the employment of our TRA methodologies in the real world. Based on the TRA, the optimized routing methodology is presented in Chapter VI. It proves that the TRA have the ability to benefit decision support systems in HazMat transportation. LNG plays an increasingly important role in the natural gas industry and energy markets. The combination of recent interest in expanding or building new facilities to receive LNG carriers, along with increased awareness and concern about potential terrorist actions, has raised questions about the potential consequences of incidents involving LNG marine transportation. Chapter VII describes the consequence analysis results for marine transportation of liquefied natural gas (LNG).

CHAPTER II

BACKGROUND

2.1. Previous Work on TRA

Risk analysis is a sequential process, beginning with an understanding of the level of involvement of risk, the frequency and type of incident, and the consequence for a given incident scenario. The way those components are defined and determined should depend on the data available and the purpose of the risk assessment. In the past two decades, attention has been focused on risk analysis of HazMat within transportation networks, and the techniques of QRA initially developed for fixed plants have been extended to TRA.

2.1.1. Procedures for Developing TRA Methodology

Risk is defined in Chapter I in terms of two parameters: the likelihood of occurrence of an incident scenario and the magnitude of the incident consequence. Rowe (1983) characterizes quantitative risk analysis methodologies for transportation in three ways: (i) how they combine the two parameters to arrive at risk; (ii) the level of detail; and (iii) the methods for obtaining data and modeling parameters. As described in Chapter I, usually the framework for TRA includes the following steps: (i) TRA scope definition; (ii) shipment description; (iii) hazard or initiating event identification; (iv)

likelihood estimation; (v) consequence estimation; (vi) risk estimation; and (vii) utilization of risk estimation. In principle, these steps have to be repeated every time that any of the parameters involved in the above calculations changes along the itinerary, so usually a great deal of computation time is required to achieve the TRA goal. Researchers in this field have executed substantial efforts to explore the practical and reasonable methods to measure the risk associated with HazMat transportation.

Ang (1989) suggested a general framework for risk analysis in transportation that decomposed the problem into three separate stages: (i) determination of an undesirable event, (ii) estimation of the level of potential exposure, and (iii) assessment of the magnitude of consequences.

Abkowitz and Cheng (1988) attempted to measure the risk of hazardous material transportation by summing the cost of fatalities, major injuries, minor injuries, and damage to property. The risk was expressed as a risk profile, which is a probability distribution of incident likelihood and severity.

Purdy (1993) estimated the impact to humans from flammable substances and toxic gases. The entire population that may be affected by a HazMat incident was considered in their model, including motorists on a road where an incident occurs, travelers on trains, and people who live near the transportation route.

Erkut and Verter (1995) proposed that an assessment of HazMat transportation is a two-stage process that involves: (i) representation of risk via a quantitative model; and (ii) estimation of the model parameters. A basic model for risk assessment was presented in their work.

Kara, Erkut, and Verter (2003) pointed out that what differentiates HazMat transport models from other transport models is the explicit modeling of transport risk which usually consists of one or both of the following two factors: incident (i.e., spill, fire) probability and population impacted. They focused on modeling the incident probability and modeling the population exposure to quantify the risk along the transportation route.

Vayiokas and Pitsiava-Latinopoulo (2004) developed a methodology for the risk assessment during road transportation of HazMat. Two critical factors have been taken into consideration: the probability of an outcome during incident occurrence and the consequences of the outcome. Theoretical risk source release model, exposure model, and consequence model were set up for the ultimate risk estimates.

Erkut and Verter (1995) and Leonelli, Bonvicini, and Spadoni (1999) proposed that a path between a given origin-destination pair can be represented by a set of road segments, where the road characteristics are uniform within each segment. The risk imposed on an individual due to a HazMat shipment can be estimated as the probability of an incident during transport multiplied by the probability of the individual experiencing the consequence as a result of the incident. At the same year, Spadoni, Leonelli, Verlicchi, and Fiore (1995) also proposed that the risk resulting from the transport of HazMat has to be calculated considering all the incidents occurring at any point of the road network, namely a set of linear source risk. The technique they used to perform linear source risk calculations is to divide each route into arcs, each then being considered as a point risk source. Next, a reassembling methodology has to be applied to

perform calculations of indicators of the area risk.

Fabiano, Curro, Palazzi, and Pastorino (2002) developed a site-oriented framework of general applicability at local level. The evaluation of frequency took into account on one side inherent factors (e.g., slope, characteristics of neighborhood, etc.) on the other side factors correlated to the traffic conditions (e.g., dangerous goods trucks, etc.). The simple theoretical models were given to express both the incident frequency and the fatality number.

Depending on the scope of the analysis, approximate as well as detailed approaches to TRA can be used. The former could be kept as simple as possible, in principle allowing also non-specialists to carry out the analysis and to immediately use its results for a basic evaluation of the risk level of the transport activity under consideration. The latter could be kept as accurate as possible, enabling a specialist to properly assess the risk, to investigate the presence of highly hazardous spots and to suggest effective mitigation measures. Bubbico, Cave, and Mazzarotta (2004a) proposed a simplified approach to TRA. Only limited number of incident scenarios and release consequences need to be estimated in this simplified approach. In this manner, TRA could be performed very rapidly to obtain the relevant risk measures, which can be then used for a preliminary assessment of the case.

2.1.2. Risk Measurement Tools

In CPQRA, a number of numerically different measures of risk can be derived from the same set of incident frequency and consequence data. Three commonly used

ways of combining incident frequency and consequence data to produce risk estimates are risk indices, individual risk, and societal risk (CCPS, 2000).

Risk indices are single numbers or tabulations of numbers which are correlated to the magnitude of risk. Some risk indices are relative values with no specific units, which only have meaning within the context of the risk index calculation methodology. Other risk indices are calculated from various individual or societal risk data sets and represent a condensation of the information contained in the corresponding data set.

Individual risk measures can be single numbers or a set of risk estimates for various individuals or geographic locations. In general, they consider the risk to an individual who may be in the effect zone of an incident or set of incidents. The size of the incident, in terms of the number of people impacted by a single event, does not affect individual risk.

Societal risk measures are single number measures, tabular sets of numbers, or graphical summaries which estimate risk to a group of people located in the effect zone of an incident or set of incidents. Societal risk estimates include a measure of incident size (for example, in terms of the number of people impacted by the incident or set of incidents considered). Some societal risk measures are designed to reflect the observation that people tend to be more concerned about the risk of large incidents than small incidents, and may place a greater weight on large incidents.

In the area of truck transport of HazMat, there have been widely varying applications of risk analysis since 1980s. They have been characterized by generic

treatment of HazMat or focus on a single substance or class, and have included a diverse set of risk measures.

Abkowitz and Cheng (1988) measured the risk of HazMat transportation by summing the cost of fatalities, major injuries, minor injuries, and damage to property.

Purdy (1993) estimated the risk through assessing the impact to humans from flammable substances and toxic gases. The entire population that may be affected by a HazMat incident was the measure of the risk level.

Erkut and Verter (1998) used the expected undesirable consequences of HazMat transport as a measure of the associated societal risk, that is, their societal risk of HazMat transportation was defined as the probability of a release event during transport, multiplied by the consequence of that event. This societal risk of HazMat transport was calculated as an aggregation of the risks imposed on each individual living near the road used for transportation. They proposed each population center as a point on the plane whose population is assumed to be concentrated. This approach presumes that each individual in a population center will incur the same kind of risk due to the HazMat transportation. The risk imposed on an individual was calculated as a sum of the risks associated with each road segment on path. In general, a path between a given origin-destination pair can be represented as a set of road segments, where the road characteristics are uniform within each segment.

The most common risk measurements used to perform a quantitative risk analysis for a major incident in a plant, i.e., individual risk and societal risk, were also employed in TRA. Individual risk reflects the frequency of a specific health effect at a

geographical location. Its predictions are used to answer the question: how does the risk to an individual vary with location? Societal risk represents the overall risk associated with an activity to a particular population. The most common societal risk presentation technique is an f-N curve, which is a graph of the number of fatalities (N) on the abscissa and frequency (f) of N or more fatalities on the ordinate (CCPS, 1995). Methodology has been developed to evaluate individual and societal risk for a transportation network by a variety of authors (Fabiano, Curro, Palazzi, and Pastorino, 2002; Vayiokas and Pitsiava-Latinopoulo, 2004). Advisory Committee on Dangerous Substances (1991) has pointed out that individual risk and societal risk are powerful tools for the measurement of transportation hazard impact.

Spadoni, Leonelli, Verlicchi, and Fiore (1995) discussed the importance of the acceptability of risk criteria. Some European countries have adopted threshold values for individual risk by referring to statistical data on death probability either for natural events or for incidents not connected to industrial activities. The UK Health and Safety Executive has fixed a limit of 10^{-4}, above which individual risk cannot be accepted under any circumstances and a limit value of 10^{-6} below which individual risk is considered broadly acceptable to members of the public. For the societal risk, the UK Health and Safety Executive has suggested for use as an upper maximum tolerable risk level a line of slope -1 through the point N=500, F=$2*10^{-4}$ (per year) and, as a negligible risk level, a line of the same slope at three orders of magnitude below. The Dutch Government utilizes as an upper maximum tolerable level a line of slope -2 through the point N=10, F=10^{-5} (per year) and a parallel line two orders of magnitude below as negligible risk.

2.1.3. Data Availability in TRA

Harwood and Russell (1990) made the first well-recognized attempt to assess the incident rate and the release probability based on certain databases. An analysis of existing incident, and exposure data before 1990 were presented in their report. The frequency, causes, circumstances, and consequences of HazMat transport have been characterized based on 5 years of data (1981-1985) from the HMIS. The analysis of exposure data were performed on the data available from the 1982 Truck Inventory and Use Survey conducted by the Bureau of Census.

To develop system-wide truck incident rates, the data from three state highway agencies were analyzed by Harwood and Russell (1990). These agencies were the California, Illiouis, and Michigan Departments of Transportation. The incident rates, incident severity distributions, and incident type distributions for different highway and area type classes obtained in the analysis were presented. Some of the data analysis results were published later by Harwood, Viner, and Russell (1993).

Rhyne (1994) compared the Harwood and Russell' results with others performed earlier, and noted that the estimates of Harwood and Russell were reasonable for many risk calculations. Their results are still the most popularly cited for current research in TRA.

Battelle (2001) analyzed HMIS database and utilized several sources of data to adjust the incidents reported in the HMIS. Data from 1990 through 1999 were used to create an annual portrait of HazMat impacts. This provided a large quantity of HazMat incident data from which consequence and likelihood values were obtained. Incident

number and impact results for HazMat transportation were broken down by HazMat classes. The incident rate and incident cost for each 12 HazMat classes were presented separately in this report. The results showed that more detail can be developed for some categories of HazMat because those classes or divisions have more incident exposure.

2.1.4. Application of Geographic Information System (GIS) in TRA

In order to perform an accurate TRA, the knowledge of territorial information of comparable accuracy is of paramount importance. In particular, data are needed about local distribution of population, incident rates, and weather conditions. Lepofsky, Abkowitz and Cheng (1993) first proposed to integrate GIS into TRA to manage those kinds of information. GIS is a system of computer software, hardware, and data that manipulates, analyzes, and presents information that is tied to a spatial location. GIS contain both geometry data (coordinates and topological information) and attribute data, i.e., information describing the properties of geometrical spatial objects such as points, lines, and areas. In the work of Lepofsky, Abkowitz, and Cheng (1993), GIS was employed to develop transportation networks that incorporate both physical and operational characteristics, and overlay these networks on other spatially referenced data.

Fedra (1998) proposed to employ GIS in the spatial TRA. In GIS, the basic concept is one of location, of spatial distribution and relationships; the basic elements are spatial objects. GIS and its capability to map risks is clearly a powerful tool for risk assessment. The integration of GIS and simulation models, together with the necessary databases and expert systems, within a common and interactive graphical user interface

could make for more powerful, easy-to-use and easy-to-understand risk information systems. Based on a dedicated GIS as the central tool and user interface, databases of hazardous installations and hazardous chemicals are linked in a hypertext structure. They include tools for spatial risk assessment based on externally generated risk contours, and links to models describing accidental and continuous atmospheric releases, spills into surface water systems, and transportation risk analysis.

The dispersion models were suggested by Zhang, Hodgson, and Erkut (2000) to incorporate into route selection for HazMat transportation. To find minimal risk paths on a network, the Gaussian plume model is employed to model the air pollution dispersion. The information on surrounding locations in the model is treated by adopting raster GIS framework. The raster framework transforms a continuous space into a discrete one by modeling it as a tessellation of square arid cells called pixels. Raster is commonly used to approximate continuous surfaces in GIS. Raster GIS are organized as a number of layers, one assigned to each characteristic of interest. The traditional raster GIS overlay techniques were used to predict the spatial consequences of potential releases of airborne HazMat in a network.

Verter and Kara (2001) set up a model to assess the total transport risk as well as the equity of its spatial distribution. They employed GIS to manage territorial information during the risk analysis of transportation network. A GIS-based model that was suitable for representing the HazMat transportation was constructed for Quebec and Ontario areas. Bubbico, Cave, and Mazzarotta (2002, 2004a) pointed out that the TRA tool developed based on the GIS approach allows risk assessment for various

transportation modes and permits to rapidly investigate possible benefits resulting from changes of routes.

2.2. Fuzzy Logic and Fuzzy Logic Models

Conventionally, a mathematical model of a system is constructed by analyzing input-output measurements from the system. However, additional important source of information on engineering systems is human expert knowledge. This knowledge is known as linguistic information. It provides qualitative instructions and descriptions of the system. While conventional mathematical model fails to include this type of information, fuzzy logic model can incorporate it conveniently.

The core technique of fuzzy logic is based on three basic concepts: (1) fuzzy set: set with smooth boundary. Unlike the crisp set, fuzzy set has a smooth boundary, i.e., the elements of the fuzzy set can be partly within the set. Membership functions are employed to provide gradual transition from regions completely outside a set to regions completely in the set. (2) Linguistic variables: variables that are qualitatively as well as quantitatively described by a fuzzy set. Similar to a conventional set, a fuzzy set can be used to describe the value of a variable. (3) Fuzzy "if-then" rules: scheme, describing a functional mapping or a logic formula that generalizes an implication of two-valued logic. The main feature of the application of fuzzy "if-then" rules is its capability to perform inference under partial matching. It computes the degree the input data matches the condition of a rule. This matching degree is combined with the consequence of the rule to form a conclusion inferred by the fuzzy rule.

A fuzzy "if-then" rule associates a given condition to a conclusion, using linguistic variable and fuzzy sets. The most common fuzzy model, Mamdani model (Yen and Langari, 1999), consists of the following fuzzy "if-then" rules that describe a mapping from $U_1 \times U_2 \times ... \times U_r$ to W:

$$R_i : \text{If } x_1 \text{ is } A_{i1}, \ldots, \text{ and } x_r \text{ is } A_{ir}, \text{ then } y \text{ is } C_i \tag{2.1}$$

Where,

x_j ($j = 1,2,...,r$): input variables

y : output variable

A_{ij} : fuzzy sets for x_j

C_i : fuzzy sets for y

The relationship between the various parameters and the accident is hard to be expressed by a function; however, it is possible to express the relationship among parameters by the fuzzy if-then rules. For example, if a driver is not experienced, then accident frequency is high. This type of association can be incorporated conveniently in fuzzy models. This characteristic is especially important given the complexity of transportation conditions and the level of human experience/knowledge on the system.

2.3. Summary of Chapter II

A comprehensive review of the research work done on TRA has been presented in this chapter. Efforts have been carried out to set up models to combine two parameters

of risk, likelihood of incident and the incident consequences, and to arrive at the measurements of risk. However, none of these methods has been extensively used in practice. The main reason is the unavailability and the lack of matching of the required input data to those models.

Analysis has been performed on some historical databases to obtain the information on both the incident rate and the incident impact to personal health, properties and environment, but those data obtained could only be applied for qualitative comparisons between different transportation activities, and it is not enough for models to quantitatively evaluate potential risks or to evaluate alternative risk reduction strategies.

This research is aimed at developing a practical and efficient TRA methodology based on available data/databases and expert knowledge. Historical data/databases are carefully observed and analyzed to derive the data according to the requirement of the model. Given the conditions where no enough data exist, some mathematical methods including fuzzy logic are employed to incorporate human linguistic information. The development of fuzzy logic model has been presented in this chapter. The TRA models are then set up based on the data analysis results. By matching the available data with the model set up, the TRA methodology can be applied directly in the decision support system to guide the operations of HazMat transportation.

CHAPTER III

TRA METHODOLOGY

3.1. Overview

This chapter provides a general quantitative risk assessment methodology used to develop the risk profile. As presented in Chapter I, there are seven steps to perform TRA, including TRA scope definition, shipment description, hazard or initiating event identification, likelihood estimation, consequence estimation, risk estimation, and utilization of risk estimates. In our methodology development, some changes are made to this TRA framework due to our objectives/purposes.

A general TRA methodology is developed in our study, which is expected to apply to the transportation of various HazMat. The shipment description is different according to the kinds of materials, so it is not included in our methodology. Only in the case study part, the shipment description is presented before the TRA.

The development of our methodology takes account of the availability of data/databases. Hazard or initiating event identification is not performed in our study. From our incident frequency and release probability analysis, the hazard or initiating event is changed with the type of HazMat, tank condition, and other factors, and it affects the risk analysis result by changing incident frequency, release probability and consequence scenario. In our study the incident frequency, release probability and

consequence scenario are assessed based on the analysis of available data/databases, the effects of different kinds of HazMat, tank condition and other factors are considered in these steps, thus it is not necessary to perform the hazard or initiating event identification, and the release probability and consequence scenario analysis are included in our methodology.

The whole TRA process is performed in transportation network, and some models and methodologies for network analysis are employed in our study, so it is necessary to characterize the transportation network at first.

Based on above analysis, the TRA framework in our study is presented in Figure 3.1.
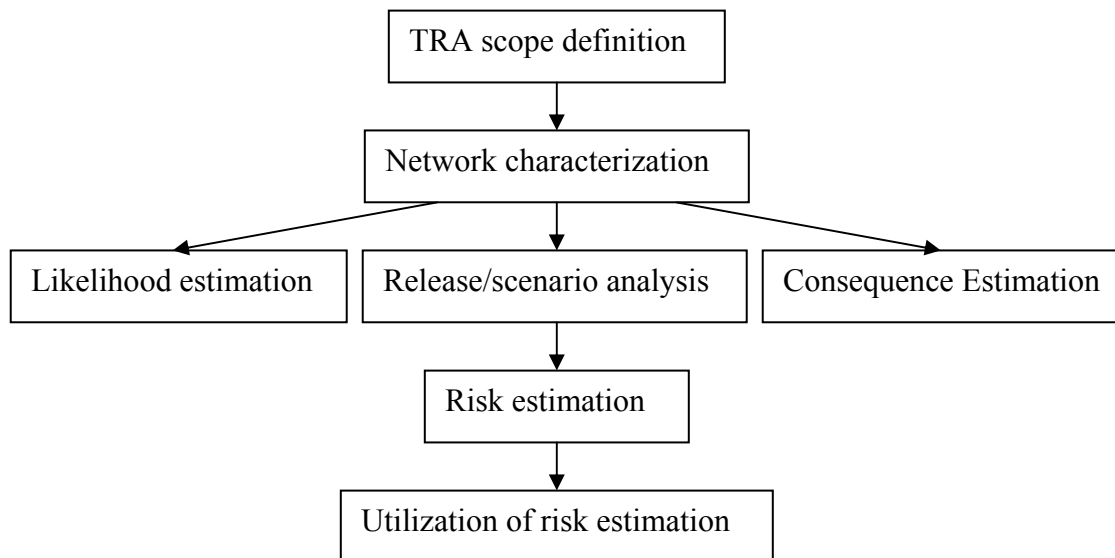
Figure 3.1. Framework for comprehensive TRA.

3.2. Network Characterization

3.2.1. Network Transformation

Analyzing risks from HazMat transportation is significantly complicated because the factors that influence the risk, such as incident probability, release amount, meteorology, and population density, vary both temporally and geographically. TRA is performed in transportation network, so all of those parameters need to be characterized in the network before the risk calculation.

In Industrial Engineering, network is defined as interconnected set of nodes and links. Node is the point where flow is created, relayed or terminated. Link is channel for moving flow between two directly connected nodes. A transportation route can be considered as composed of links and nodes, and the set of transportation routes is regarded as transportation network. Before performing TRA on certain transportation activities, we need to transform the real highway network into network expressed by nodes and links.

The principle for the network transformation is that each link has to have uniform properties at all its points, i.e., road condition, traffic volume, and other properties associated with road should be the same in one link. By this way all points in one link will cause the same potential of transportation incident when a vehicle passes through them, and each link can be considered as a unit when performing TRA.

The other principle is that each link has to be straight. This principle is to simplify the risk integration through all points of a link. This condition can easily be obtained without any loss in generality by adding fictitious nodes to the network.

Based on those principles, the transportation road network can be transformed into the network expressed by nodes and links. Set in such a network defined by a set of nodes and links, all parameters on risk assessment can be easily characterized, which makes the overall risk assessment easy. On the other hand, decision makers can guide transportation activities by employing abundant algorithms and models developed for network circumstance. For example, the network "minimum cost flow" model can easily be employed in selecting the transportation route under certain conditions.

3.2.2. Network Characterization

Risk assessment is typically structured as a process resulting from the interaction between (i) the transportation network, (ii) the vehicle or traveling risk source, and (iii) the impact area.

When performing the transportation risk analysis each link has to be characterized by some properties. For a link l of a set N_{link}, the link properties to take into account are the following:

- The geographical position in the impact area; to do this a Cartesian reference frame X/Y with origin $O_{X/Y}$ has to be arbitrarily overlapped on the impact area.

- The amount of the yearly shipments $N_{ship}(v)$ traveling on each link for each vehicle typology v, i.e., on a specific conveyance means carrying a specific substance.

- The incident frequency $P_{incident}$, expressed in events/(km.vehicle). This variable is generally a function of the route features, the traffic conditions, environmental conditions, and driver status.

As already mentioned therein, a transportation route can be viewed as a linear risk source, since a release can occur at each of its points; this means that each of its points can be considered as a point risk source, or, in other words, the generic vehicle has to be considered as a traveling risk source. Therefore the second step in transportation risk analysis is the vehicle or traveling risk source characterization.

In order to perform this description, the concept of "vehicle typology" has to be introduced. Vehicle typology is a certain kind of vehicle conveying certain kind of HazMat which could caused hazard if a release occurs during the transportation. For example, a truck tanker conveying ammonia is a kind of vehicle typology. The combination of link and vehicle typology could define the risk source associated with each link. The properties associated with the link-vehicle typology pair for TRA purpose are defined as:

- The release probability for each vehicle typology. That is the probability of having a release once an incident has happened. Vehicle construction standards strongly depend on the features of the transported substance; in other words the

release probability depends on the vehicle typology. Furthermore it can also depend on the link since it can be higher on high speed than on low speed route segments.

In order to identify and quantify incident scenarios referred to each traveling risk source and to predict the consequence of each incident scenario, the following parameters are required:

- The transportation conditions for each substance, i. e., the temperature and pressure values at which the substance is stored in the transportation vehicle and the vehicle capacity.

- The probability of the size of the equivalent holes which have been chosen to describe all possible releases from each vehicle typology. For each vehicle typology and for each rupture size a physical aspect of the outcome and a release rate, or a release quantity in case of instantaneous release, have to be evaluated.

- The final outcomes to which each hole size of each vehicle typology can lead, that is if a toxic cloud arises, or an explosive one, or a pool flame, or a jet-fire and so on. Each vehicle typology can lead to N_o final outcomes.

- The probability of having the final outcome once a release has occurred, P_o, i.e., the product of the probability of the release being of a specific equivalence size, once the releae has occurred, and the probability of having final outcome, once the release of this specific equivalence hole has occurred.

The impact area characterization includes both the definition of some parameters which influence the release effects evaluation and the description of the population distribution.

To perform the release effects evaluation, it is necessary to define:

- Some physical parameters, like the air temperature and air humidity; the average terrain roughness, the terrain typology, the grade of confinement and so on.

- Meteorological conditions characterizing the impact area, given by atmospheric stability class and wind speed.

- Wind probability density distribution that is the wind rise in the impact area, for each meteorological condition. The angle θ is used to mark a wind direction.

All the parameters influencing the effects evaluation can vary from zone to zone of the impact area, especially when considering very large areas, and the procedure takes into account these variations.

The distribution of the population on the impact area is an essential input for calculating societal risk. A population map is composed of zones, where people may be considered uniformly distributed, and of aggregation centers, where people are clustered. The total numbers of these zones and centers and their population density need to be determined.

3.2.3. Risk Analysis for Network Transportation

Sine risk is additive, in transportation network the risk caused by a vehicle transporting along a highway route is the sum of risk caused by vehicle passing each link in the route, and the risk caused by each link is the sum of the risk caused by each point in that link. The framework for risk analysis in transportation network is shown in Figure 3.2.
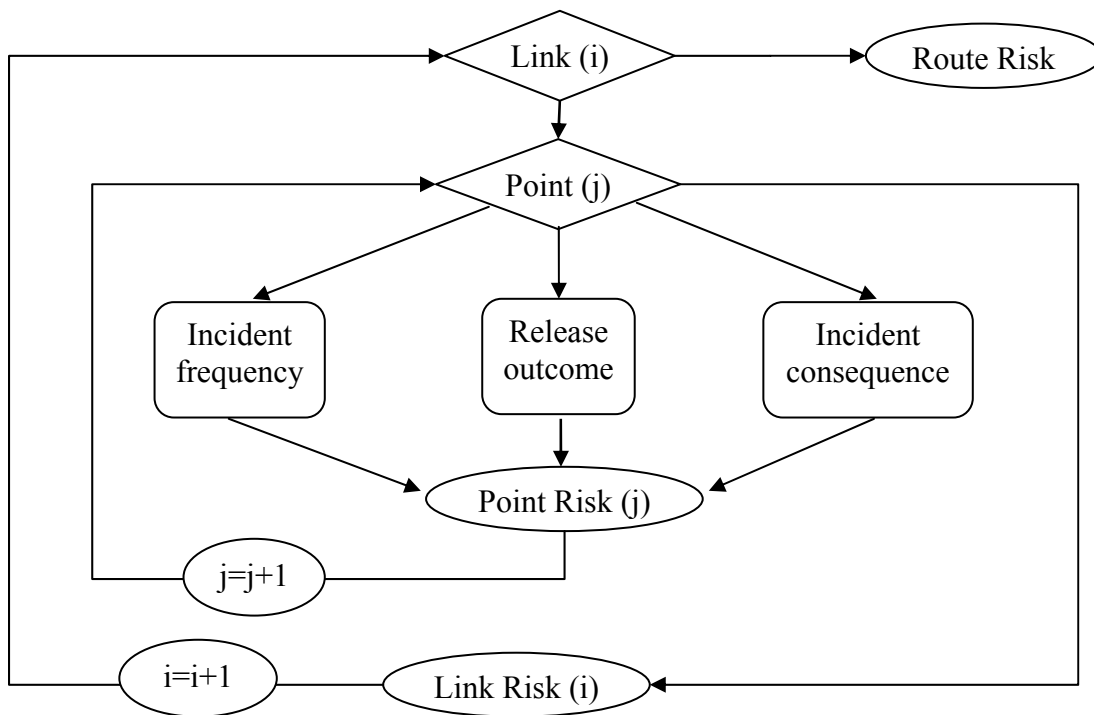
Figure 3.2. Network TRA process.

3.3. Incident Frequency Analysis

Risk is a combination of two parameters: frequency and the magnitude of the consequence. A quantitative risk analysis incorporates numerical estimates of the frequency and the consequences in a sophisticated but approximate manner. The specification of incident frequency has been the subject of extensive efforts in the risk assessment community. Currently, the most popular cited data for incident frequency took only few factors into consideration. We develop an approach on the basis of an analysis of national commodity flow information and HazMat incident data. The methodology is presented to predict the incident frequency for different types of roads by incorporating the effects of a large number of parameters, including the nature of truck configurations, operation conditions, environmental factors, and road conditions.

3.3.1. Background on Incident Frequency Assessment

Incident frequency can be defined as the number of incidents occurred per unit of road (mile, kilometer, etc.). It can be computed by dividing the number of incidents by the number of vehicle miles, which is the corresponding exposure measure of opportunities for an incident to occur.

There are three basic options to assess incident frequency with reasonable accuracy (Rhyne, 1994). The first is to obtain one database (or more) and to perform analysis to determine both incident data and exposure data for the specific conditions under investigation (assuming that the dataset is structured to support distinction

between the desired variables). Second option is to access state databases for specific routes. States frequently have incident data and exposure data for the major state highways. A third option is to use an existing limited analysis of databases and apply the results to a specific route of interest.

Detailed analyses of several publicly available databases have made it possible to specify incident frequency on a per-mile basis. One of the most detailed analyses of such data was conducted by Harwood and Russell (1990). On the basis of computerized data files from three states – California, Illinois, and Michigan, Harwood and Russell calculated the incident frequency by using the number of reported incidents and the total number of truck-miles exposed. The incident frequency is assessed as a function of road type, truck type, and population density. Brown and Dunn (2000) analyzed Harwood and Russell's data and divided their statistics into two road categories – interstates and non-interstates (state highways) – and three population density categories – urban, suburban, and rural. Bubbico, Cave, and Mazzarotta (2004b) have pointed out that both route-independent and route-dependent parameters affect risk.

Several problems exist in above analysis on incident frequency. The first one is that the well-accepted data on incident frequency, that is, the statistics of Harwood and Russell (1990), was obtained based on the analysis of incident databases of 1980s. The status of transportation incidents has changed over the last two decades as shown in Figure 1.1. So did the incident reporting system with the heightened consciousness on the risk of HazMat transportation incidents. The statistics of Harwood and Russell (1990) are to a large extent, update to take into account the changes since 1980s. The second

problem is that the neglect of the premier effect of transportation road on incident frequency. When performing database analysis to derive incident frequency, we should try to disaggregate the incident database for different road rather than for different kinds of HazMat or other parameters. The third problem is that these above analyses failed to improve the frequency data sensitivity by incorporating parameters describing the nature of the roads, characteristics of the trucks, environmental factors, and driver conditions. In our research an integrated methodology to predict incident frequency is developed by incorporating the effects of various parameters, including both route-dependent and route-independent variables.

3.3.2. Data and Database Analysis

Both incident and vehicle-mile data are required to assess the incident frequency. HMIS is the national database with data on HazMat transportation incidents. Container types, consequences of incidents, and other information are available in this database. However, incidents that occurred on intrastate roads and incidents not resulting in spill are not recorded in this database. Battelle (2001), in a report to the Federal Motor Carrier Safety Administration, suggested supplementing HMIS with additional databases that consist of data on non-spill incidents and other spill incidents (especially intrastate incidents).

The Departments of Public Safety (DPS) incident databases from each state consist of incident data gathered from state highways. Since these databases are collected by state DPS, the probabilities of underreporting on intrastate incidents are

much less. These databases can be disaggregated into various sub-databases, with each sub-database corresponding to a road. This capability makes it relatively easy to assess the incident frequency for a specific road.

In our research state DPS databases are analyzed to determine incident frequency. A sub-database associated with a certain road is formed by subtracting all incidents occurring on that road. Incidents recorded in DPS databases are described by parameters on road and environmental conditions. Several parameters that affect incident frequency are as follows:

- Lane number (x_1)

- Weather (x_2)

- Population density (x_3)

Incident frequency specific for a road is predicted based on analysis on its sub-database. This frequency is a function of above route-dependent parameters.

Several route-independent parameters that affect incident frequency, but are not available in DPS databases, are as follows:

- Truck configuration (y_1)

- Container capacity (y_2)

- Driver experience (y_3)

The frequency obtained by considering route-dependent parameters has to be modified by incorporating route-independent parameters, i.e., the assessment of the

frequency needs to incorporate data from different sets as follows: basic incident frequency is derived from DPS database initially; only the route-dependent parameters are considered; the effects of route-independent parameters on incident frequency are derived from other database such as HMIS or from expert knowledge. Then the final incident frequency is a function of both route-dependent and route-independent parameters. It is essential to use fuzzy logic in the modification process for the following two reasons: (i) the information available in HMIS is on nationwide transportation activities, while the data derived from DPS is for specific roads, i.e., data obtained from HMIS cannot be applied directly; (ii) the effects of several of the parameters on the frequency cannot be derived from any database; thus, expert judgment has to be employed in the assessment.

In addition to the number of incidents, the number of miles traveled (exposure data) is needed. The most common cited exposure data source is the Commodity Flow Survey (CFS) (US Census Bureau, 2004). CFS is based on 5-year economic census. The most up-to-date CFS is that of 2002. It provides information on commodities shipped, their value, weight, and mode of transportation. Exposure data on state highways can also be obtained from state DOT or transportation institutes (TI). In many cases both the data from CFS and data from state DOT or TI are needed to assess the exposure data for specific roads.

3.3.3. Incident Frequency Analysis Methodology

Based on the analysis above, incident frequency can be predicted as follows:

- Number of incidents is derived from the DPS databases as a function of route-dependent parameters.

- The corresponding vehicle-mile data are obtained from states DOT or TI and from the 2002 CFS. The basic incident frequency is obtained by dividing the number of incidents by the number of miles traveled.

- The basic incident frequency is modified by considering the effects of route-independent parameters. Fuzzy logic is employed to incorporate the expert knowledge. The membership functions of these parameters are built based on the data available in the HMIS database or based on expert experience.

The flow chart in Figure 3.3 presents the process of utilizing the variety of data sources to establish an incident frequency assessor.

A case study is presented following the development of the methodology. HazMat incident frequency on US Highway 290 in Texas is predicted to illustrate the performance of our methodology.
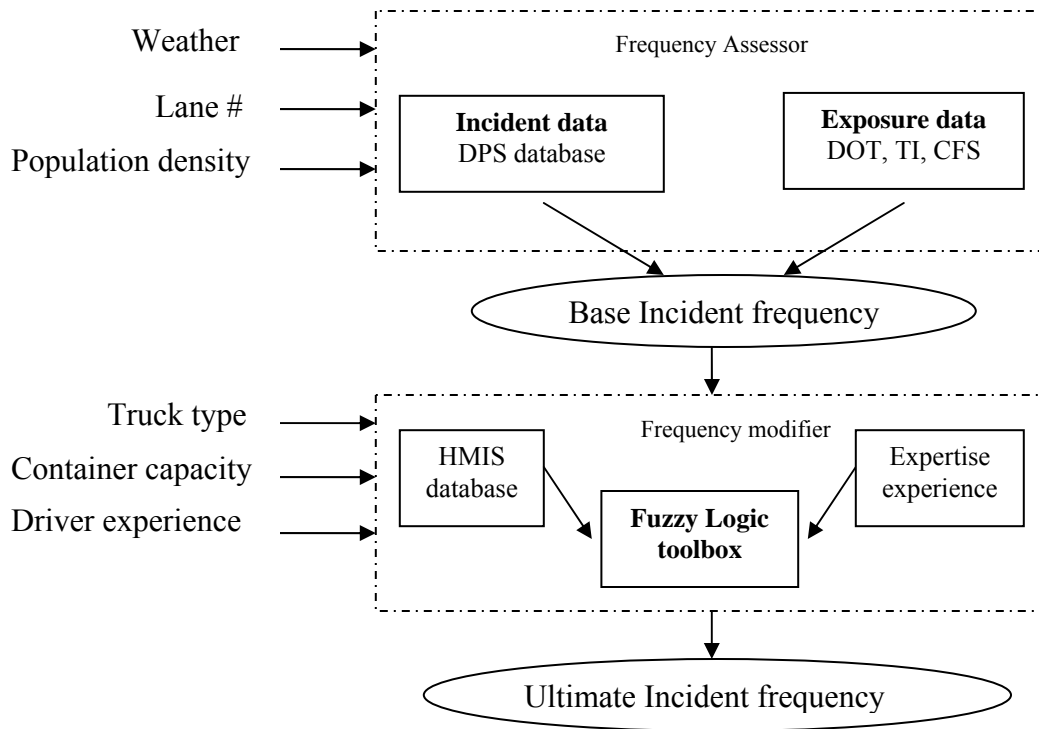
Figure 3.3. Prediction of incident frequency – a flow chart.

3.3.3.1. Basic Incident Frequency Assessment

Table 3.1 shows the structure of DPS database. It consists of data extracted from Texas DPS, and this sub-database contains records on incidents that occurred on US Highway 290. There are more than three parameters that describe the conditions of each incident. These parameters are listed in the first row in the table. The parameters are treated as linguistic variables, and the numeric values in the table are designated to represent the values of those linguistic parameters. For example, the variable "*surface condition*" has four linguistic values: 1-dry, 2-wet, 3-muddy, and 4-snowy/icy.

Table 3.1

DPS incident database – sample of records of incidents occurring on US Highway 290

COUNTY district	MILE 1 milepoint	WEATHER	SURF_CON	ROAD_CON	INVEST	ROADWAY	INTRSECT	..
101	315	1	1	0	3	1	4	..
101	356	2	2	0	3	1	3	..
101	313	1	1	0	2	1	2	..
101	332	1	1	0	3	1	4	..
101	381	2	4	5	6	3	4	..
101	364	8	4	5	2	3	4	..
101	384	8	4	5	6	1	4	..
101	308	8	4	5	5	3	4	..
101	243	8	4	5	6	1	4	..
101	211	3	1	4	5	9	3	..
101	367	2	2	2	5	9	3	..
…	…	…	…	…	…	…	…	..

DPS data for ten years (from 1992 to 2001) are utilized in this study. The data are sorted by using Matlab at first to obtain the number of incidents under all the given conditions in the databases. Then the number of incidents under any conditions needs to be estimated as a function of those three route-dependent parameters. An appropriate count data model is needed for this estimation. Four approaches were considered for this purpose: linear regression, Poisson regression, negative binomial model, and Bayesian estimation. The following paragraphs discuss these approaches.

- Many of the early works in empirical analysis have been done using multiple linear regression models. However, these models suffer from several methodological limitations and practical inconsistencies. The two major

deficiencies are: a) linear regression assumes a normal distribution of the dependent variable, which is not valid for count (incident) data; b) linear regression may produce negative estimates for the dependent variable.

- Poisson model has several advantages in comparison to normal regression model. It assumes that the data follows a Poisson distribution, a distribution frequently encountered when events are counted. Despite its advantages, Poisson regression assumes that the variance and mean of the dependent variable are equal. However, it is quite common to have the variance of data that is substantially higher than the mean. This phenomenon is known as "over-dispersion". Over-dispersion leads to invalid t-tests of the estimated parameters. This restriction can be avoided by using negative binomial regression, which allows the variance of the dependent variable to be larger than the mean.

- Bayesian estimation can combine sample information with other information that may be available prior to collecting the sample. In Bayesian model, each input independent variable has a probability distribution that is a function of one parameter (known as prior). This approach is useful when uncertainty exists in input variables. However, in DPS databases, the four affecting parameters have been defined and categorized.

Therefore, the negative binomial regression model is the best choice to assess the number of incidents. The regression model is derived from the statistical software SAS.

Then the number of incidents under any condition is estimated using the model established by SAS.

Exposure data is obtained from state DOT or TI and the 2002 CFS. Since the number of incidents is a function of several parameters, the corresponding number of miles traveled needs to consider the effects of the same parameters, i.e., the exposure data have to be disaggregated by the same factors.

Finally, the basic incident frequency is obtained by dividing the number of incidents by the number of miles traveled. This frequency is expressed as $f_{basic}(x_1, x_2, x_3)$. Figure 3.4 consists of schematic presentation of the algorithm of prediction of basic incident frequency.

3.3.3.2. Modification to the Basic Incident Frequency Data

Basic frequency data need to be modified to incorporate the effects of the following parameters: *Truck configuration (y_1), Container capacity (y_2),* and *Driver experience (y_3)*. These three parameters are not road-related variables, and their effects on the frequency are independent from road condition. In this study Fuzzy Mamdani models are employed to assess the effects of y_1, y_2, and y_3 on the frequency. MatLab software is employed to help the model setup. A modifier, expressed as $m_i (i = 1,2,3)$, is generated for each of these 3 parameters, and then the ultimate incident frequency is expressed as: $f_{ultimate} = f_{basic} \times (m_1 \times m_2 \times m_3)$.
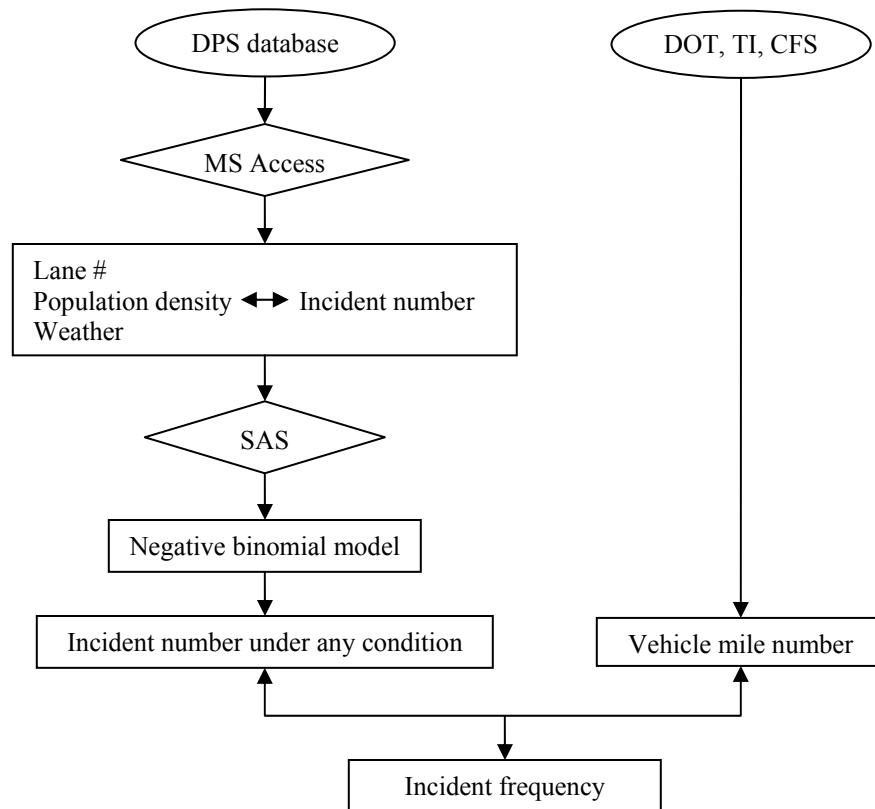
Figure 3.4. Schematic presentation of an algorithm of prediction of basic incident frequency.

y_1, y_2, and y_3 are treated as linguistic variables. The frequency modifiers are viewed as linguistic variables as well. Each linguistic variable is defined by several fuzzy sets. The membership function for each fuzzy set is determined either by expert experience or from available data. Analysis is performed on the HMIS database to develop the membership functions for *Truck configuration*. The membership functions for *Driver experience* and *Container capacity* are determined based on expert experience. Then, the fuzzy "if-then" rules are built to associate each affecting variable, y_i, to the

corresponding modifier, m_i. For example, *driver experience (y_3)*, as shown in Figure 3.5, is expressed by three fuzzy sets: novice, medium, and experienced. The *driver experience modifier* variable (m_4) also includes three fuzzy sets: low, medium, and high.
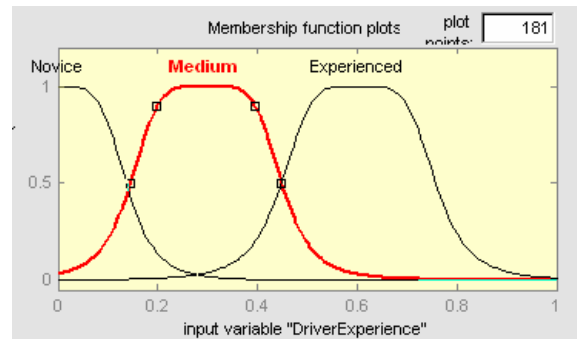
Figure 3.5. Driver experience membership function.

The "if-then" rules are set up as:

If *driver experience* is novice, then the *driver experience modifier* is high,

If *driver experience* is medium, then the *driver experience modifier* is medium,

If *driver experience* is experienced, then the *driver experience modifier* is low.

Fis editor in Matlab is used to defuzzify the process based on input data in order to derive the output modifier. After the set-up of these rules, *driver experience* data can be input to the model. Then, defuzzification is performed in order to obtain a numerical

output value. The value obtained after the defuzzification is the *driver experience modifier* (m_3) as shown in Figure 3.6. Other modifiers are obtained similarly.
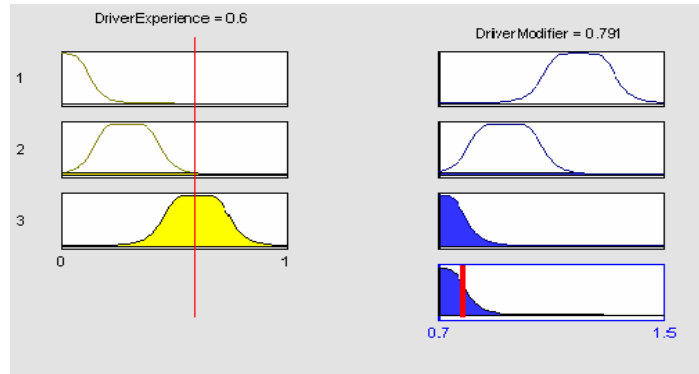
Figure 3.6. Defuzzification process in Matlab.

3.3.4. Case Study

3.3.4.1. Calculation of Number of Incidents by SAS

As mentioned earlier, this case study will address sections from US Highway 290 in Texas, a road connecting Houston and Austin. Figure 3.7 presents the control section map for Houston area. The sections under study are between Highway 6 and Highway 610 as shown in the figure.

DPS databases from 1992 to 2001 are employed in this study. 9536 incidents are recorded for this period. The data was sorted by Matlab and input into SAS.
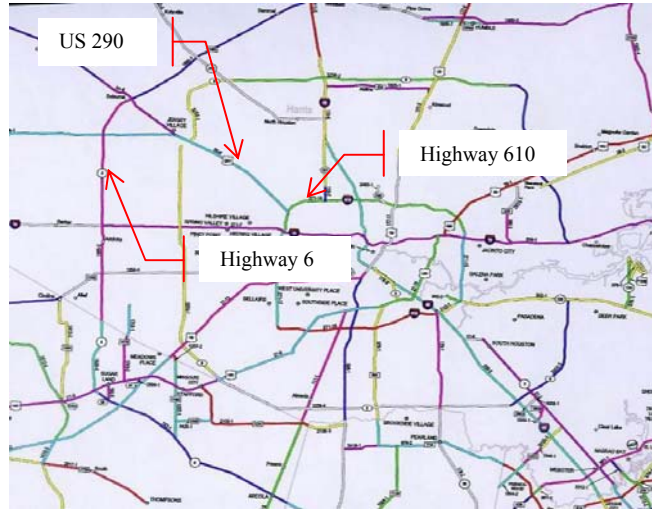
Figure 3.7. Control section map for Houston TX.

The parameter estimations are shown in Table 3.2. The definitions of each value of the parameters of DPS are given in Table 3.3. The number of incidents under any conditions (denoted as POP, NUMN_LN, and WERATHER) is estimated by the following equation:

$$N(i,j,k) = e^{(\beta_0 + \beta_{1i} + \beta_{2j} + \beta_{3k})} \tag{3.1}$$

Where,

N: number of incidents

i: linguistic value of *population density*, 0, 1, 3, 4, or 9

j: linguistic value of *number of lanes*, 4, 5, 6, 8, or 10

k: linguistic value of *weather condition*, 1 or 2

β_0: intercept of regression equation

β_1 : regression coefficient for variable *population density*

β_2 : regression coefficient for variable *number of lanes*

β_3 : regression coefficient for variable *weather condition*

Pearson's chi-square is used to calculate goodness of fit. The P-value for the Pearson's chi-square is computed from the output of SAS. The calculated P-value is 0.1976, which is larger than 0.05. Thus, the derived negative binomial models pass the chi-square goodness-of-fit test at the 0.05 confidence level, i.e., the level of fitness of the negative binomial model is acceptable.

Table 3.2

Parameter estimation

Parameter	Parameter categories	Parameter estimates
POP (β_1)	0	-1.5727
	1	-6.0371
	3	-1.7244
	4	-2.2201
	9	0.0000
NUMN_LN (β_2)	4	2.3151
	5	-2.3590
	6	2.6869
	8	2.5499
	10	0.0000
WEATHER (β_3)	1	1.9717
	2	0.0000
$\beta_0 = 3.1703$		

Table 3.3

Parameter meaning in DPS

Parameter	Parameter categories	Parameter meaning
POP (β_1)	0	Rural
	1	Town under 2,499 pop.
	3	2,500-4,999 pop.
	4	5,000-9,999 pop.
	9	250,000 pop. and over
NUMN_LN (β_2)	4	Number of lanes = 4
	5	Number of lanes = 5
	6	Number of lanes = 6
	8	Number of lanes = 8
	10	Number of lanes = 10
WEATHER (β_3)	1	Clear (cloudy)
	2	Raining (other)

The test for detecting over-dispersion in the Poisson process is performed in order to verify that either Poisson regression or negative binomial regression can be used to analyze DPS database. Table 3.4 and Table 3.5 provide the fit statistics for Poisson and negative binomial models. For Poisson model, the values of Pearson Chi-sq and deviance divided by the degrees of freedom are significantly larger than 1, i.e., this is a case of over-dispersion (Cameron and Trivedi, 1998), and Poisson models cannot be used. Since negative binomial models are not restricted by over-dispersion, it should be used in the methodology.

Table 3.4

Criteria for assessing goodness of fit for Poisson regression

Criterion	DF	Value	Value/DF
Deviance	15	2827.9395	188.5293
Scaled Deviance	15	2827.9395	188.5293
Pearson Chi-Square	15	2626.1428	175.0762
Scaled Pearson X2	15	2626.1428	175.0762
Log Likelihood		56708.2067	

Table 3.5

Criteria for assessing goodness of fit for negative binomial regression

Criterion	DF	Value	Value/DF
Deviance	15	26.9834	1.7989
Scaled Deviance	15	26.9834	1.7989
Pearson Chi-Square	15	10.4236	0.6949
Scaled Pearson X2	15	10.4236	0.6949
Log Likelihood		58058.0075	

3.3.4.2. Exposure Data Assessment

Exposure data for US Highway 290 are obtained from Texas Transportation Institute (TTI). The exposure data could be disaggregated by the number of lanes and population density group. The data disaggregated need to be segmented further to incorporate the effect of weather.

According to the National Climate Data Center (2005), the normal annual precipitation is 47.84 inches. The rain rate is modeled by Crane (2005). His study shows that the percentage of raining time over a year in Houston area is about 3.9%. The

annual precipitation assessed by multiplying the raining rate by the raining time is about 53.3 inches, very close to the data reported by the National Climate Data Center. Thus, the assessment by Crane is employed here, but was approximated as 5% of the raining percentage over a year. We assume the weather condition would affect the corresponding vehicle mile data equally over the number of lanes and population group.

The completely disaggregated exposure data are shown in Table 3.6. By dividing the estimated number of incidents with the corresponding exposure data, the basic incident frequency is calculated.

Table 3.6

Exposure (vehicle miles) data for control section 58 and 59 on US Highway 290

Exposure data (vehicle miles)				NUM_LN				
				4	5	6	8	10
Weather	1	POP	0	498870024	1405378	951118019	/	3931089
			1	/	/	4152767	/	/
			3	444307187	/	14353884654	/	/
			4	243085504	/	213621596	/	/
			9	54087951	/	2601401642	1447712804	249977292
	2	POP	0	26256317	73967	50058843	/	206899
			1	/	/	218566	/	/
			3	23384589	/	755467613	/	/
			4	12793974	/	11243242	/	/
			9	2846734	/	136915876	76195410	13156700

3.3.4.3 Fuzzy Logic Modification

The basic frequency data need to be modified to incorporate the effects of *Truck configuration (y_1), Container capacity (y_2),* and *Driver experience (y_3)*. y_1, y_2, and y_3, are treated as linguistic variables. The frequency modifiers are viewed as linguistic variables

as well. Each linguistic variable is defined by several fuzzy sets, and the membership functions for each fuzzy set are determined either by experts or from data.

The effects of *driver experience* and the *container capacity* on the incident frequency is assessed utilizing expert experience. The membership functions plots and the corresponding modifiers plots are shown in Figures 3.5, 3.8, 3.9, and 3.10.

Harwood and Russell (1990) studied the effects of truck configuration on the incident frequency. Based on their result, triangular membership functions are set for four different vehicle configurations and their modifiers as shown in Figures 3.11 and 3.12.

After the determination of membership functions, the fuzzy "if-then" rules are set using expert experience and the Harwood and Russell work (1990). Given any input data of the route-independent parameters, the corresponding modifier is derived from this fuzzy model. This process is the defuzzification process. Figure 3.6 illustrates the defuzzification process to derive the modifier for driver experience.
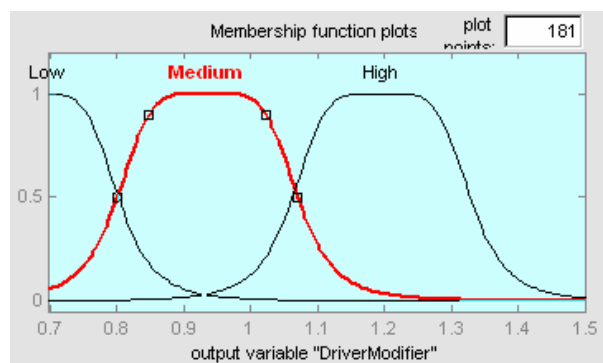
Figure 3.8. Driver modifier membership function.
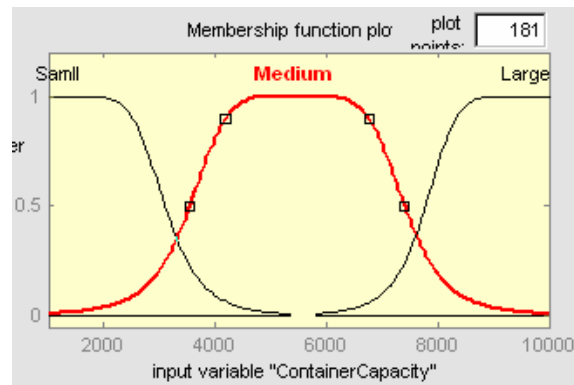
Figure 3.9. Container capacity membership function.
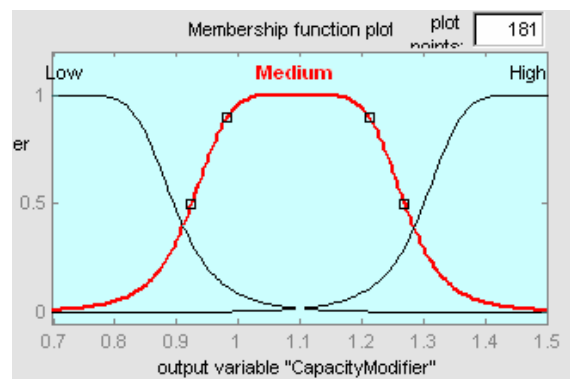
Figure 3.10. Container modifier membership function.
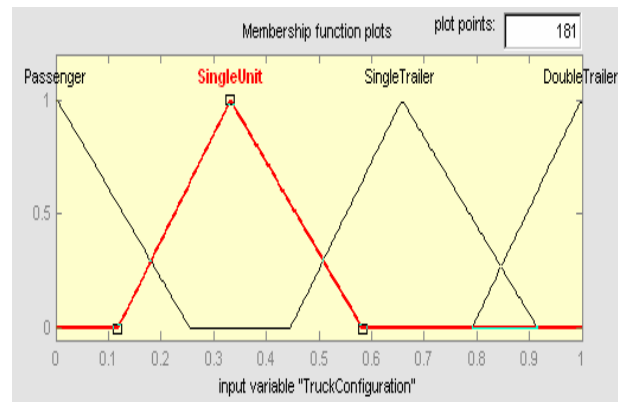
Figure 3.11. Truck configuration membership function.
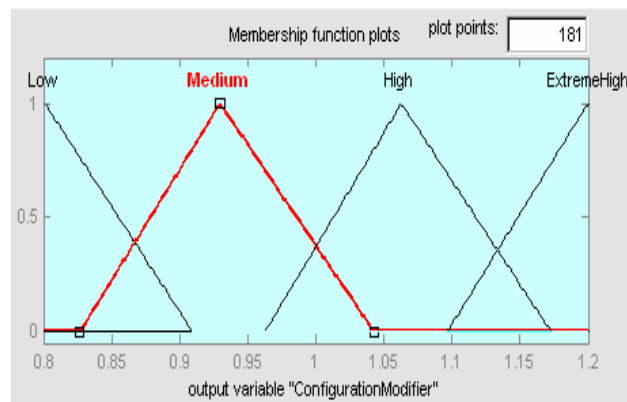
Figure 3.12. Configuration modifier membership function.

3.3.4.4. Effect of Various Parameters on Incident Frequency

Figures 3.13, 3.14, and 3.15 and Table 3.7 present the effect of *number of lanes, truck configuration, population density,* and *road condition* on the incident frequency.

An increase in population density increases the frequency as shown in Figure 3.13. When the number of lanes changed from 4 to 6, the incident frequency decreases somewhat when the population group is 0; however it increases for the other population groups. Incident frequency is relatively low in rural areas, so the effects of number of lanes are not prominent. Other reason for this inconsistency may be poor data sample. Our study focus on control section 58 and 59 for US Highway 290. Study on more sections may be able to obtain the effects of number of lanes on the frequency in rural area. Figure 3.15 shows that weather conditions affects the frequency significantly. The frequency increases under rainy weather in comparison to the frequency under clear weather. The increase is more significant when the number of lanes is 6 and the population group is between 5,000 and 10,000. This may be the case, or may not be accurate due to the inadequacy of the data sample.

As for route-independent parameters, an increase in both the complexity of vehicle configuration and container capacity increases the frequency (shown in Figure 3.14). Table 3.7 illustrates the effects of driver experience. The accumulation of driver experience is helpful in decreasing the probability of incident.
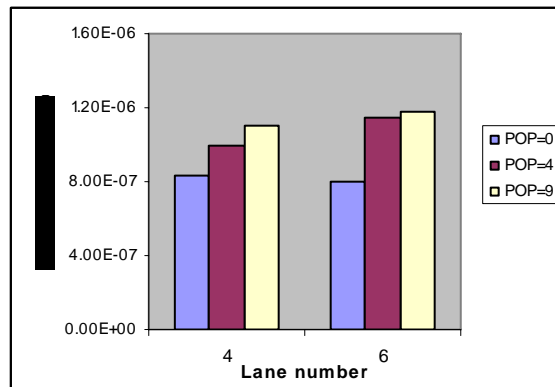
Figure 3.13. Effects of number of lanes and population density on the incident frequency.

Figure 3.14. Effects of container capacity and truck configuration on the incident frequency.

Table 3.7

Effects of driver experience on the incident frequency

Driver experience	Driver modifier	Incident frequency (Incident/vehicle mile)
0.1	1.14	1.65821E-06
0.6	0.791	1.15057E-06
0.8	0.86	1.25093E-06
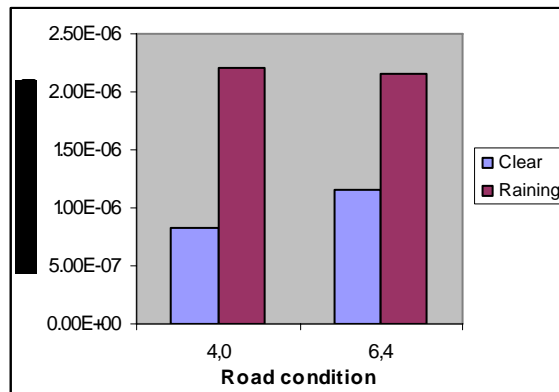
(4,0): Number of lanes=4

Pop group =0

(6,4): Number of lanes=6

Pop group =4

Figure 3.15. Effects of weather condition on the incident frequency.

A methodology to predict incident frequency of HazMat transportation has been presented in this section based on empirical data. The integrated models incorporate the effects of both route-dependent and route-independent variables. This methodology can be applied to predict frequencies associated with a given road as long as data with incident records and exposure information are available for this type of road.

3.4. Release Scenario Analysis

3.4.1. Conditional Probability of Release

The release probability is a conditional probability that a release will occur following an incident. The probability of a release in a case of transportation of HazMat is affected by the following four parameters:

- Vehicle characteristics

- The nature of the incident

- Characteristics of the transported material

- The conditions of transport

Vehicle characteristics include the strength and integrity of the container, as well as specific mitigation factors such as antisloshing devices and the height of the center of gravity of the loaded vehicle. Strength and integrity are functions of the material and wall thickness of the container, the presence or absence of a double wall, compartmentalization of cargo, and the use of any protective shielding devices. These measures either affect the potential for container rupture or puncture or, in the event of container failure, they affect the quantity of material released.

Incidents can be classified as follows: (i) High speed collision, (ii) Low speed collision, (iii) Overturning, and (iv) Non-incident initiated release.

The type of the HazMat and the conditions of transport also affect the release probability. These factors mainly affect the size of the release. Other factors are the material phase (liquid or gas), the temperature, and the pressure. While pressurized gas will increase the rate of the release, the size of the release area is the main factor that dictates the release rate.

Rhyne (1994) has studied the incident force types and force magnitudes to evaluate the conditional failure probabilities for a spectrum of release sizes. However, it is still difficult to predict the size of the release by analyzing the impact of the mechanical force.

Due to the limitation in performing analysis of the impact of the mechanical force, a statistical inference will be used to extract the conditional probability of release. This methodology is based on sufficient historical data that allow inferring the conditional probability for the variety of containers. The selection of container for HazMat transport has been regulated in 49 CFR. Brown and Dunn (2000) also mentioned the information on the containers utilized to transport the selected HazMat. The selected HazMat include Chlorine, Ammonia, LPG, gasoline, and other explosives. By using the release data from the HMIS database, Brown and Dunn (2000) estimated the release probability by dividing the number of reported releases by the estimated number of incidents. Although this approach has a considerable degree of uncertainty, it provides a large statistical sample that consists of data on specific container types. The results of this analysis are used to obtain the conditional probability of release in our study.

3.4.2. Consequence Scenario Analysis

The size of a release affects the magnitude of the severity of the consequences. HMIS consists of information on whether a release occurred, as well as on the size of the release and on the resulting consequences. This combination of parameters is required to quantify the probability of release for a variety of consequence scenarios.

Event Tree Analysis (ETA) is employed in our methodology in order to develop the propagation sequence of each of the variety of scenarios, and to calculate the final probability of each type of consequences. HMIS will be disaggregated for each

hazardous material and each type of container. For a variety of common hazardous materials, including ammonia, chlorine, LNG, LPG, and gasoline, data will be analyzed and substituted in the appropriate branches on the tree.

ETA enables the assessment of multiple, co-existing system faults and failures as well. It functions simultaneously in the failure and success domains. Here the event tree has three possible release magnitudes:

- A rupture: release area equal to the area of a 4-inch diameter hole

- A puncture: release area equal to the area of a 1-inch diameter hole

- A leak: release area equal to the area of a ¼ -inch diameter hole

One or more hazards may be created by each of these failure categories. In LPG, for example, the possible consequences upon release are:

- Torch fire: results from immediate ignition of the release

- Flash fire: may result from delayed ignition of the release

- Vapor dissipation: no ignition occurs after the release

Figure 3.16 is an example of event tree of propagation of a release of propane.

Conditional release occurs	Release magnitude	Immediate fire	Delayed fire	Probability	Outcome
		Yes 0.15		$P_1=1.08*10^{-4}$	Torch fire from rupture
	Rupture 0.03		**Yes 0.12**	$P_2=7.34*10^{-5}$	Flash fire from rupture
		No 0.85	**No 0.88**	$P_3=5.38*10^{-4}$	Dissipation from rupture
		Yes 0.10		$P_3=6.00*10^{-4}$	Torch fire from puncture
LPG Release	**Puncture 0.25**		**Yes 0.17**	$P_3=9.18*10^{-4}$	Flash fire from puncture
0.024 release/incident		**No 0.90**	**No 0.83**	$P_6=4.48*10^{-3}$	Dissipation from puncture
		Yes 0.02		$P_7=3.46*10^{-4}$	Torch fire from leak
	Leak 0.72		**Yes 0.03**	$P_8=5.08*10^{-4}$	Flash fire from leak
		No 0.98	**No 0.97**	$P_9=1.64*10^{-2}$	Dissipation from leak

Figure 3.16.Example of event tree of propagation of a release of propane.

3.5. Consequence Analysis

Several factors govern the severity of the consequences. Among these factors are the amount of material released, toxicity of the chemical, health effects of the released materials, characteristics of the population and the environment adjacent to the site of the incident, and the weather conditions at the time of the incident. The interplay among these factors produces a risk spectrum.

A variety of consequence analysis software is available in the market. In this study we utilize CANARY^{TM}, consequence analysis package, to assess the consequence. CANARY^{TM} calculates the consequences, based on the physical properties and based on consequence models that are available in the literature. Given a release occurs during transportation, the majority of potential hazards can be modeled. These include toxic vapor cloud, flammable vapor cloud, unconfined vapor cloud explosion, pool fire, torch fire, flare, BLEVE, and confined explosion.

3.6. Individual Risk Analysis

A personal consequence could be minor injury, major injury, or fatality. This document concentrates on incurring the probability of death as a basis for assessing risk. The consequences resulting from an incident are obtained from CANARY^{TM}, including overpressure due to explosion, toxic vapor density, and/or radiant heat flux. It is combined with the proper exposure times to obtain the corresponding received doses. Doses are then converted to fatalities using Probit Correlations (CCPS, 2000). Thus, the fatality probability can be estimated for any given point.

Among the parameters that are considered in the risk analysis, are incident frequency and weather conditions. These variables are rarely constant along a route. To get a more accurate estimate of the risk, the transportation route is broken into a set of links. As presented in the network characterization part of this chapter, a basic assumption is that all factors are constant along a link. The individual risk at point *M(x, y)*

is the sum of all risk sources from all links in the transportation route. The following steps should be employed to obtain the overall risk along a route of transportation:

- Summing the risks created by all points on a link, and

- Summing the risks of all links in the route.
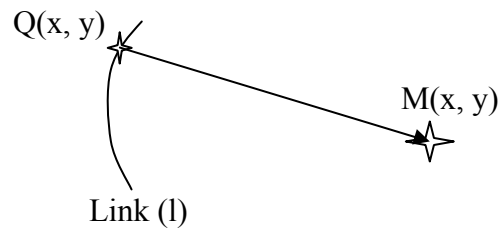
Figure 3.17. Graphical presentation of the relationships between Link (l), point of release Q(x, y) and point of exposure M(x, y).

As shown in Figure 3.17, a vehicle transporting HazMat is passing through point $Q(x, y)$ on link l. As a result, a risk is posed on point $M(x, y)$. In order to calculate the annual individual risk (fatalities/year) at $M(x, y)$, the following input data are required:

- *Incident frequency*. It is a function of the following parameters: *Lane number (x_1), Weather (x_2), Surface condition (x_3), Alignment (x_4), Truck type (y_1), Container capacity (y_2), Container type (y_3),* and *Driver experience (y_4)*. For a given transportation activity and a given link, all the parameters are constant, except the *Weather (x_2)*, which is changing over the year. Therefore, the frequency at

point Q(x, y) is a function of the *Weather (x₂)* for given transportation activity. $P_{incident}$(*weather)* denotes incident frequency. The number of weather conditions is denoted by $N_{weather}$, and the probability for each weather condition is $P_{weather}$.

- *Outcome probability.* If a release occurs following an incident, various outcomes caused by different magnitudes of release are possible. The probability of each outcome has been estimated using ETA as described in 3.2. The total number of outcomes is marked as N_o, and the probability for each outcome is marked as P_o.

- *Fatality.* The fatality probability is a function of the consequence and of the exposure time (the exposure time is assumed constant for a given consequence scenario). The consequence is a function of the nature of the HazMat, type of release outcome, weather condition, and wind direction. Therefore, for the transportation of a given HazMat, the fatality probability is a function of release outcome and the wind direction noted as *F(weather, o, w)*. The number of wind directions is noted as N_w, and the probability of each wind direction is P_w.

The individual risk at point *M(x, y)* caused by the point risk source *Q(x, y)* is calculated by integrating the consequences associated with each wind direction over all wind directions, release outcomes, and weather conditions. This individual risk caused by a point risk source is known as a point individual risk (*PIR*):

$$PIR = \sum_{1}^{N_{weather}} \left\{ P_{weather} \times P_{incident}(weather) \times \sum_{1}^{N_o} \left\{ P_o \times \sum_{1}^{N_w} \left[F(weather, o, w) \times P_w \right] \right\} \right\} \quad (3.2)$$

In the calculation above we assumed that the vehicle is a stationary source at $P(x, y)$. However, vehicles are in motion, and the effect of the velocity should be incorporated into the model. A linear integration along the link, with respect to time (dt), will incorporate the component of travel time on the link risk value. The link individual risk (*LIR*) will then have the following form:

$$LIR = \int_l (PIR)dt \qquad (3.3)$$

The sum of *LIR*s along the entire transportation route will represent the total individual risk (*IR*) posed on point *M(x, y)*. The total individual risk (*IR*) then can be expressed as follows:

$$IR = \sum_{l=1}^{N_{link}} LIR \qquad (3.4)$$

3.7. Societal Risk Analysis

Societal risk is the risk to a population. It reflects the frequency of health effects (usually fatalities) in a specific population, occurring as the result of exposure to a specific hazardous material. The societal risk is often expressed in terms of frequency distribution of multiple fatalities (f-N curve). The population map for the transportation network needs to be defined in order to calculate the societal risk. The population map is composed of zones where people are assumed to be uniformly distributed. Aggregation centers are points where people are clustered. Zones can have rectangular shape or can be linear. Rectangular areas describe the off-route residential quarters, while linear zones

represent the road network where motorists are present. Aggregation centers refer to particular areas where people are clustered, like schools, hospitals, commercial centers, and other similar locations.

The total number of rectangle zones and the total number of linear zones in the network are marked as N_r and N_l, and the uniform population densities are denoted as ρ_r (persons/m^2) and ρ_l (persons/m) respectively. The total number of aggregation centers is N_c, and the total number of persons in each center is P_c.

The number of fatalities in a linear zone is obtained by linear integration (first segment of Equation (3.5)) of the fatalities along the line, and it is a function of an outcome and a wind direction noted as $F_L(wind, o, w)$. In rectangular zones, the number of fatalities is obtained by integration (second segment of Equation (3.5)) over the area of the rectangle noted as $F_R(wind, o, w)$. In an aggregation center, the number of fatalities is the fatality probability in the center multiplied by the number of people (third segment of Equation (3.5)) in the center noted as $F_C(wind, o, w)$.

The number of fatalities over all zones, caused by a risk source $Q(x, y)$, under given release outcome and given wind direction, is calculated as follows:

$$
\begin{aligned}
N(weather, o, w) = & \sum_{1}^{N_L} \left[\rho_L \times \int_L F_L(weather, o, w) dl \right] \\
& + \sum_{1}^{N_R} \left[\rho_R \times \int_A F_R(weather, o, w) dA \right] + \sum_{1}^{N_C} \left[P_C \times F_C(weather, o, w) \right]
\end{aligned}
\tag{3.5}
$$

The probability of having N fatalities under a given weather condition, release outcome, and wind direction is estimated by Equation (3.6):

$$F\big(N(weather, o, w)\big) = P_{incident} \times P_{weather} \times P_o \times P_w \qquad (3.6)$$

By taking into account all wind directions, it is possible to evaluate the probability of having N_n (or more) fatalities for given weather condition and release outcome:

$$F\big(N_n(weather, o)\big) = \sum_{1}^{N_w} \big[P_{weather} \times \delta_n(weather, o, w)\big] \qquad (3.7)$$

Where

$$\delta_n = \begin{cases} F\big(N(weather, o, w)\big), & N(weather, o, w) \geq N_n \\ 0, & N(weather, o, w) < N_n \end{cases}$$

Considering the motion of the vehicle over all the links and the effects of all release outcomes and weather conditions, the probability of having N_n fatalities is calculated as follows:

$$F(N_n) = \sum_{1}^{N_{weather}} \sum_{1}^{N_o} \sum_{1}^{N_L} \int_L F\big(N_n(weather, o)dt\big) \qquad (3.8)$$

Equation (3.8) is actually an F-N curve.

3.8. Conclusion on Chapter III

This chapter has been dedicated to describe the basic modeling technique and overall methodology. The basic idea of the proposed methodology is to capture the

matching of data/databases availability with TRA techniques and to set up an applicable framework to assess transportation risk step by step.

Risk assessment is a process resulting from the interaction between the transportation network, the vehicle or traveling risk source, and the impact area. All our risk components, including incident frequency, release probability, consequence scenario, and fatality, are carefully observed to determine their contributing factors and to figure out the proper data/databases for analysis. Mathematical models and risk analysis techniques like ETA are employed for each risk component assessment. Numerical models are presented to measure individual risk and societal risk caused by HazMat transportation network.

The overall methodology is developed from available data/databases, which makes it an applicable and accountable resource in transportation decision support system. This generic method could be applied for most of TRA within the scopes described in Section 1.4. Decision makers could modify the methodology when dealing with different HazMat. The methodology could be simplified or elaborated further based on the requirement of users.

CHAPTER IV

TRA CASE STUDY

This chapter does not address all HazMat. It contains two representative case studies that use the TRA techniques presented in Chapter III.

Historical data provide valuable clues to the risks of transporting hazardous materials. However, they do not necessarily reflect the actual distribution of risk among various hazardous materials because the risks associated with certain materials are largely driven by rarely occurring catastrophic events. For example, historical data for the past 20 years show that fatalities are more likely to result from events associated with the transportation of gasoline and other flammable materials than from other transportation incidents. Risk from flammable materials like propane is driven by frequently occurring incidents that involve number of injuries and fatalities. These types of incidents are called high-probability/low consequence events.

Transporting toxic-by-inhalation materials poses significantly different risks than are associated with transporting propane or other flammable materials. Risks associated with toxic materials are strongly influenced by rarely occurring catastrophic incidents, such as the rupture of a tank that contains chlorine near a populated area in adverse atmospheric conditions. Such incidents are called low-probability/high-consequence events.

Because the historical record contains information on many propane incidents and because the maximum potential impacts from an incident involving propane are limited, these historical data provide an accurate measure of risk. However, for toxic materials, because of strong influence of low-probability events on the overall risk profile and because too few incidents have occurred to support statistical characterization, experience does not provide an adequate basis for defining toxic transportation risks. In this chapter, we illustrate how our methodology is employed for these two different cases: propane TRA and chlorine TRA.

In reality, each study might require over 100 pages of calculations and documentation, while here we want to show the performance of our methodology, so some assumptions are used besides the exact data, and the assumptions used in an actual analysis are situation specific.

4.1. Road Analysis

The transportation route selected in our case study is sections of US Highway 290. As explained in Chapter III, the incident data and information on road conditions (e.g., number of lanes) are obtained from TTI. The release and consequence scenario probabilities are derived from HMIS. The surrounding area information is required to measure the societal risk. GIS is employed in our study to characterize the population distribution. On a paper map, we cannot peel cities away from countries, or countries away from the ocean, but on a GIS map we can. A GIS map is made up of layers, or

collections of geographic objects that are alike. To make a map, we can add as many layers as we want.

For our case study purpose, we peel Texas highway information from GIS and create the highway layer. A second layer on population distribution is also added to the map. Figure 4.1 is the two-layer GIS map for US Highway 290 sections between Highway 610 and Highway 6. Population blocks in the map can be characterized by both overall population and density. The area of each block is also available in GIS. Dividing population data into classes requires we choose both the number of classes and a method to determine where one class ends and another begins.

GIS has six classification methods: natural break, equal interval, defined interval, quantile, standard deviation, and manual. Manual method is chosen in our study in order to have the same classification as data provided by TTI. Same as TTI data, the population distribution is divided into five classes. Figure 4.1 illustrates population distribution after classifying the data in the same way as TTI system.

However, compared with TTI data, the population blocks along Highway 290 are not in the same classes. From example, according to TTI, Highway 290 segment that has 8 lanes has a population class of 9, i.e., the population blocks along the 8-lane segment have population of more than 250,000 people, while in GIS, population blocks for that part have less than 2,499 people. We believe the difference is caused because these two systems use different areas in define blocks. GIS records more information so that it is possible to assess each block in a smaller size.
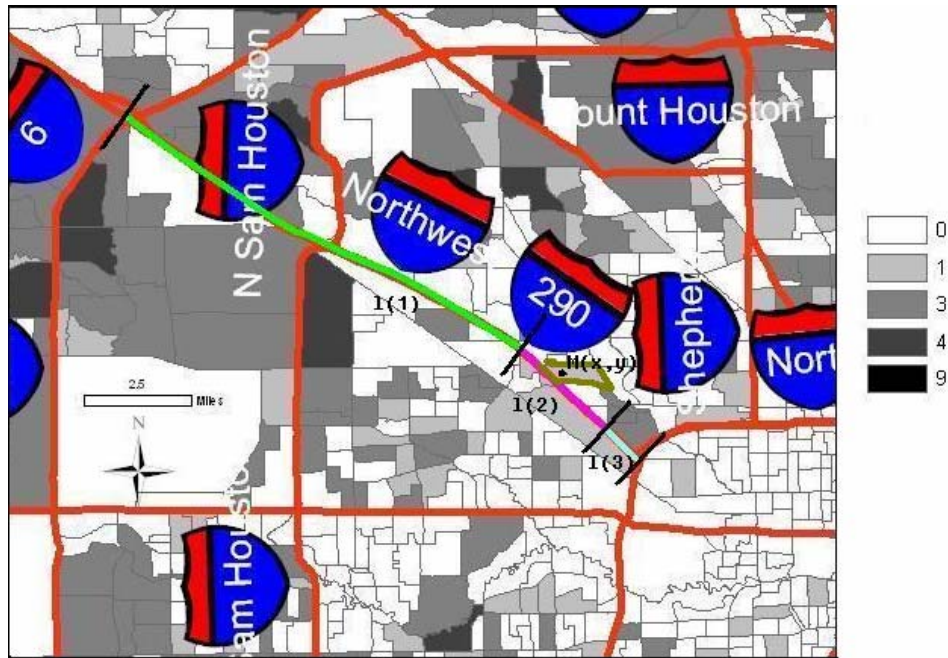
Figure 4.1. GIS map with population block information for Highway 290 surrounding area.

Before performing TRA associated with transportation on Highway 290, the transportation route needs to be divided into several links. As analyzed in Chapter III, unlike incident frequency, release probability, consequence scenario, and consequence are affected little by road condition. Incident frequency is a function of Lane number (x_1), Weather (x_2), Population density (x_3), Truck configuration (y_1), Container capacity (y_2), and Driver experience (y_3). Lane number(x_1) and Population density (x_3) are road features, so the dividing is based on the lane number and population group.

As shown in Figure 4.1, the selected route can be divided into three parts based on the number of lanes. These three parts are denoted as l(1), l(2), and l(3). The population groups along l(2) and l(3) are uniform. Two different population groups are

associated with l(1). Only Figure 4.1 black markers separate different links, with each link denoted in blue. By referring to the incident frequency calculation in Chapter III, the population group does not affect incident frequency much when the number of lanes is 6, so we do not divide l(1) further based on population groups. Thus, the selected route is divided into three links for risk assessment purpose.

The notation on population group for each link is defined based on TTI data rather than on GIS, because TTI data has been employed therein and it is not necessary to spend more time for little improvement of accuracy. Table 4.1 is the definition for three links of this transportation route.

Table 4.1

Link definition

Link	Number of Lanes	Population Group
l(1)	6	3
l(2)	8	9
l(3)	10	9

4.2. Propane TRA

4.2.1. Description

Propane is one of the nation's most versatile sources of energy and supplies 3 to 4 percent of our total energy needs. Nearly 11 billion gallons of propane are consumed annually in the U.S. by more than 60 million Americans (NPGA, 2005). The situation of

concern in this section is that involving the transportation of propane along transportation route as highlighted in Figure 4.1. Propane is commonly transported under pressure as a flammable liquid which vaporizes rapidly if releases. Table 4.2 describes the properties of propane.

Table 4.2

Properties of propane

Lower flammable limit	2.1%
Upper flammable limit	9.5%
Boiling point	-44 ^{o}F
Molecular weight	44.1

Two types of trucks are used for propane transportation: a highway transport (which typically carries 7,000 to 12,000 gallons) and a smaller bulk delivery truck, called a "bobtail" (which carries 1,000 to 5,000+ gallons). In our case study the container capacity is assumed to be 10,000 gallons. One-third of the nation's propane is produced in Texas, so the number of trips per year on Highway 290 is assumed to be 1,000. Table 4.3 describes the specifics associated with this case.

4.2.2. Incident Frequency Estimation

As detailed in Chapter III, the base incident frequency for these three links in the studied route can be assessed by the developed models. Table 4.4 lists the data calculated based on the model.

Table 4.3

Tank truck example description

Product	Propane
Contain type	MC331
Container capacity	10,000 gallons
Container temperature	70 ^{o}F
Container pressure	125 psia
Truck type	Truck with single trailer
Trips per year	1,000

Table 4.4

Incident frequency for different links

Link	Link length (mile)	Population Group	Number of Lanes	Weather	Basic Incident frequency	Ultimate incident frequency
l(1)	9.7	3	6	1	$3.1*10^{-8}$	$4.6*10^{-8}$
				2	$8.2*10^{-8}$	$1.2*10^{-7}$
l(2)	2.4	9	8	1	$1.5*10^{-6}$	$2.3*10^{-6}$
				2	$4.0*10^{-6}$	$5.9*10^{-6}$
l(3)	0.9	9	10	1	$6.8*10^{-7}$	$1.0*10^{-6}$
				2	$1.8*10^{-6}$	$2.7*10^{-6}$

The modifying parameters are Truck configuration (y_1), Container capacity (y_2), and Driver experience (y_3). In this study the modifier associated with driver experience is assume to be 1, i.e., the driver has average experience. The other two modifiers are assessed from fuzzy models built in Chapter III, and the values of modifiers are 1.39 for y_2 and 1.07 for y_3. The ultimate incident frequencies for these three links are shown in Table 4.4.

4.2.3. Release and Consequence Scenario Analysis

Since propane is flammable, flammability hazards and the potential for explosions must be addressed in the consequence analysis. As discussed in CCPS (1995), BLEVE is not a typical outcome unless there is a secondary source of fuel. Only consequences related with flammability are considered. The release probability and consequence scenarios have been analyzed in the example shown in Chapter III. Nine different consequence scenarios result after the release of propane from the tank. Torch fires/flash fires consequence resulting after propane releases have different dimensions and affect different areas, which are closely related with the release scenario. The probabilities of different consequence scenarios were derived from ETA.

4.2.4. Consequence Simulation

The consequence caused by each of these scenarios is simulated using CANARY. For all of these hazards, the concern of study is the fatalities caused by heat

flux. Table 4.5 is the CANARY output for heat flux of the center line along wind direction. Figure 4.2 shows the radiation flux vs. distance in the targeted ground level.

The heat fluxes for other scenarios are simulated in the same way. With the changing of release orifice size, the heat flux along the wind direction also changes. The smaller the orifice, the less the heat flux at the same distance from the release source.

Table 4.5

Heat flux at the center line along wind direction vs. distance

Downwind Distance (feet)	Flux (Btu/hr-sq.ft)
16.4	4723
18.1	4689
20.0	4611
22.1	4484
24.4	4302
26.9	4066
29.8	3775
32.9	3439
36.3	3068
40.1	2678
44.3	2289
48.9	1918
54.0	1579
59.6	1280
65.9	1026
72.7	815
80.3	644
88.7	507
98.0	398
108.2	312
Downwind Distances to Endpoints	
24.4	4300
53.2	1600
89.2	500
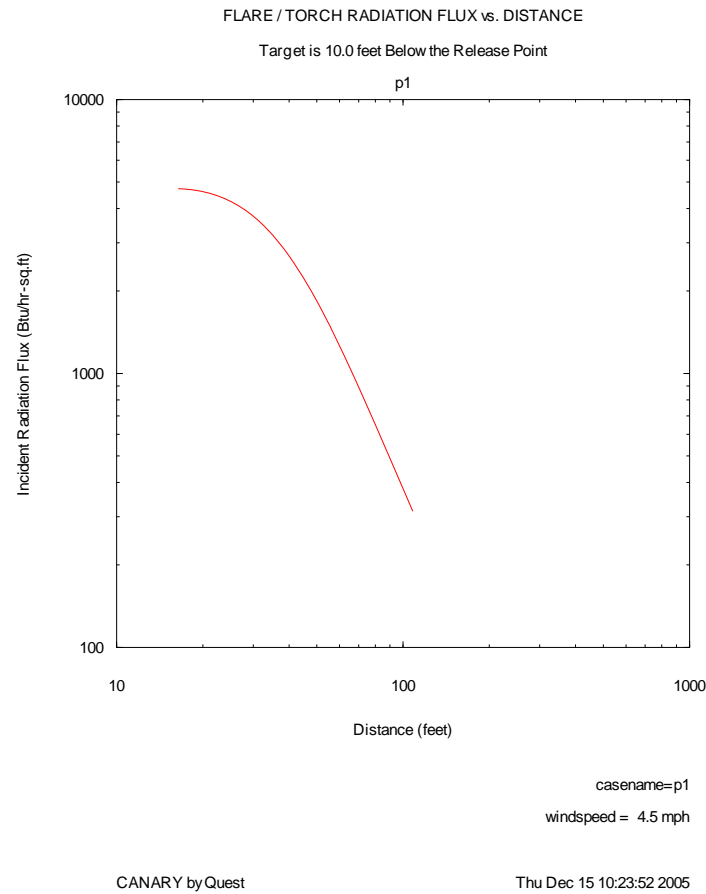
Figure 4.2. Radiation flux vs. distance in the targeted ground level.

4.2.5. Risk Estimation

The point individual risk is estimated by Equation (3.2). After obtaining all the

probabilities present in the equation, the only missing item is the Fatality. These data are

obtained from probit correlations. The fatality associated with flash fire is caused by heat

radiation. The probit correlation for burn deaths from flash fire is (Crowl, 2002):

$$Y = -14.9 + 2.56 \times \ln(V) \qquad (4.1)$$

$$V = t_e I_e^{4/3} / 10^4$$

t_e = effective time duration (s)

I_e = effective radiation intensity (W/m^2)

To assess the individual risk, the observed point has to be defined in the network first, i.e., at that point a person is supposed to be stationed there for a whole year. The fatality probability of that individual is the individual risk for that point.

This point M is chosen to be located in the highlighted block as shown in Figure 4.1, because this point is next to l(2) whose incident frequency is a little bit larger than the other two. The distance of point M to l(2) is 30 feet. That is a reasonable distance for individuals to be stationed, and at that distance the heat flux is still high enough for worst scenario analysis.

Figure 4.3 shows that the wind direction does not affect the heat flux much at a distance of 30 feet. So the wind direction is not considered any more. When weather is in class 1, and the consequence scenario is flash fire occurring after rupture, the heat flux is assessed to be 3775 Btu/hr.ft^2. The effective time duration is supposed to be 60 seconds. Then the probit under such conditions is calculated to be 4.005 according to Equation (4.1). The corresponding fatality probability is 10.6% (Crowl, 2002).
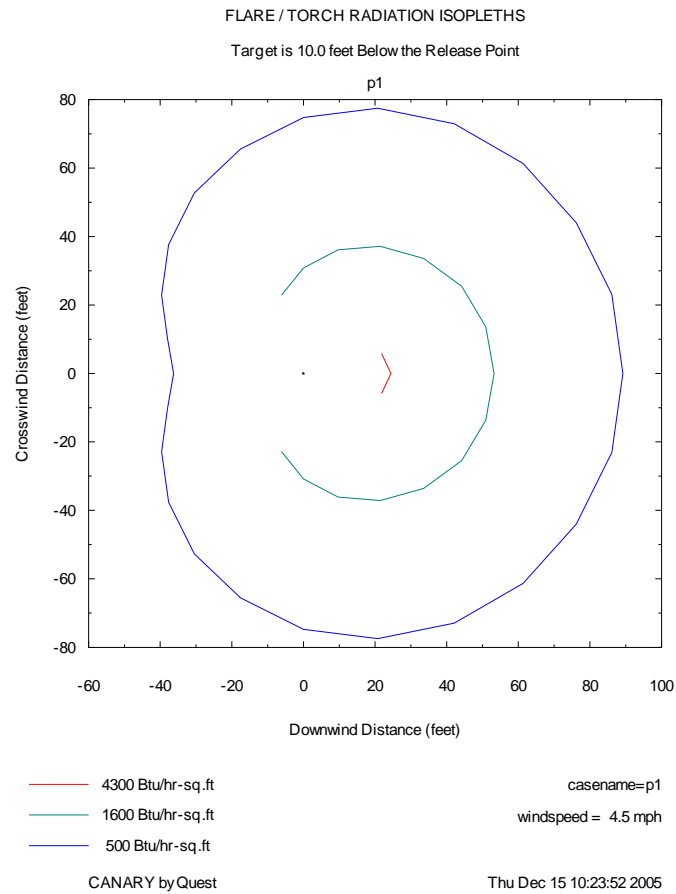
Figure 4.3. Flare radiation isopleths.

Since the consequence scenario is flash fire, fatality is not supposed to occur when weather condition is rainy, so only one weather condition is taken into account in the risk assessment. Without considering weather and wind condition in Equation (3.2), only fatalities associated with all other consequence scenarios need to be measured to get

the point individual risk, but the vapor distribution is not included in the calculation. Fatalities for other consequence scenarios are listed in Table 4.6.

Table 4.6

Fatalities caused by different scenarios

Consequence scenario obtained from ETA	Fatality (%)
P_1	10.6
P_2	10.6
P_4	1
P_5	1
P_7	<1
P_8	<1

The overall point individual risk is calculated to be:

$$
\begin{aligned}
PIR &= P_{weather} \times P_{incident} \times \sum_{1}^{N_O}\left(P_O \times F(o)\right) \\
&= 0.95 \times 2.3 \times 10^{-6} \frac{incident}{vehicle \bullet mile} \times 3.5 \times 10^{-5} \frac{death}{incident} \\
&= 7.6 \times 10^{-11} \ death\big/vehicle \bullet mile
\end{aligned}
\tag{4.2}
$$

The link risk is to integrate the point risk through the whole link. Usually, when the heat flux is less than 500 Btu/hr.ft^2 (1,562W/m^2), we will not consider its effect on fatality. According to CANARY output shown in Table 4.5, the heat flux meets this level at distance of 89.2 ft. Thus only these points on link (2) whose distance to M is less than 89.2 ft are considered to contribute link risk. This requirement results in a

contributing segment whose length is 168 feet. To simplify the calculation, each point is

assumed to create the same risk to point M, thus the link risk is calculated to be:

$$
\begin{aligned}
LIR &= PIR \times l \\
&= \frac{7.6 \times 10^{-11} \; death}{vehicle \bullet mile} \times 168 \; ft \times \frac{1 \; mile}{5280 \; ft} \\
&= 2.4 \times 10^{-12} \; death/vehicle
\end{aligned}
\tag{4.3}
$$

Considering the trips per year, the overall risks to an individual in a year is:

$$
\begin{aligned}
RIR &= LIR \times Trip \\
&= \frac{2.4 \times 10^{-12} \; death}{vehicle} \times \frac{1000 \; vehicle}{year} \\
&= 2.4 \times 10^{-9} \; death/year
\end{aligned}
\tag{4.4}
$$

This result illustrates that the transportation risk associated with propane

transportation does not result in high risk level if people are 30 feet away from the

highway. The same method is utilized to assess risk caused at other point in the network.

When people are very near to the transportation route, the risk could be very high due to

the high heat flux of flash fire.

4.3. Chlorine TRA

4.3.1. Description

Chlorine is a toxic gas that has a pungent suffocating odor. It is extremely toxic

by inhalation and is heavier than air. Container for transporting chlorine on highway is

MC331, which is the same as propane. To compare risk caused by chlorine with that of propane, the chlorine shipment condition is chosen similar to propane transportation. Table 4.7 summarizes the shipment information through the route highlighted in Figure 4.1. As addressed in Chapter III, the incident frequency is affected by road condition, truck/container configuration, environmental condition, and driver status. The type of HazMat affects the incident frequency little, and if there is any, it is because the type of HazMat requires the change of these four, especially the first three kinds of parameters. Therefore, the data on incident frequency along the highlighted route in Figure 4.1 are assessed in the same way as shown in Section 4.2.2.

Table 4.7

Chlorine shipment on Highway 290

Product	Propane
Contain type	MC331
Container capacity	10,000 gallons
Container temperature	70 ^{o}F
Container pressure	105 psia
Truck type	Truck with single trailer
Trips per year	1,000

4.3.2. Release and Consequence Scenario Analysis

According to the Chlorine Institute (2003), chlorine production averaged 10.5 million tons per year in the U.S. over the 1979-1987 period, and there were an estimated

60,000 to 90,000 separate sites in the U.S. using chlorine. There were also approximately one million containers of chlorine shipped each year in the U.S. including barges, railroad tank cars, tank trucks, ton containers, and 100 and 150 pound cylinders. Since 1989, there have been approximately 50,000 shipments per year of chlorine in 90-ton rail tank car. Rail is the most common transportation mode for chlorine shipment.

According to HMIS, there were 7 incidents associated with chlorine transportation from 1993 to 2002. The lack of enough data makes it impossible to employ the method presented in Chapter III to assess the release probability and consequence scenario. On the other hand, most of these chlorine highway incidents were related to non-bulk container, so the chlorine incident information recorded in HMIS is not within our research scope.

In this research we assume the conditional release probability of chlorine upon the occurrence of an incident is the same as that of propane. This assumption is based on the similarities in container type and condition. For both propane and chlorine, MC331 is the mainly used container, both of them are liquefied gas, and they are under similar high pressure during transportation process. Based on this reason, the probabilities for rupture, puncture, and leakage are also assumed the same as those of propane.

4.3.3. Consequence Simulation

No matter what the release size, the consequence scenarios associated with chlorine are the toxic vapor dispersion and potential fatalities or injuries and environment damage. The toxic vapor dispersion is modeled using CANARY. For

rupture scenario, the release is assumed to be continuous, and the release time is 10 min, which is used as operator's response time in risk management. CANARY output shows that the ground level concentration is $5*10^5$ ppm at 30 ft downwind distance.

The probit correlation on chlorine toxic death is (Crowl, 2002):

$$Y = -17.1 + 1.69 \times \ln(V) \tag{4.5}$$

$$V = \sum C^{2.75} T$$

C = concentration (ppm)

T = time interval (min)

The time interval is assumed to be 10 min, same as the usual response time. Point M is at 30 feet away from release source and in wind direction; the death probability for individual at that point is 100%. For puncture release and leakage scenario, the fatality is calculated to be 100% as well.

4.3.4. Risk Estimation

The calculation of point risk requires the probability distributions of weather class, consequence scenario, and wind direction. However, CANARY does not have the capacity to assess the vapor dispersion under rain climate, so the weather effect is neglected here. There are three consequence scenarios corresponding to three different release scenarios, but the fatalities associated with all scenarios are 100%. Therefore it is

not necessary to consider each scenario's probability. The wind direction varies throughout a year. For conservative analysis, in this research we use 90% as the probability of wind directing toward individual at point M. The point risk is equal to:

$$PIR = \sum_1^{N_{weather}} \left\{ P_{weather} \times P_{incident}(weather) \times \sum_1^{N_o} \left\{ P_o \times \sum_1^{N_w} [F(weather, o, w) \times P_w] \right\} \right\}$$

$$= 2.3 \times 10^{-6} \frac{incident}{vehicle \bullet mile} \times 0.024 \times 0.9 = 5.0 \times 10^{-8} / (vehicle \bullet mile)$$

(4.6)

The Time Weighted Average (TWA) for chlorine is 0.5. According to CANARY output for rupture release consequence, the distance of vapor dispersed is 30,000 feet (5.7 mile) before the concentration becomes less than 0.5 ppm. That is, when chlorine truck is passing a certain segment in this route, fatality could be caused, but beyond that segment, transportation cannot cause fatality at point M. The length of that segment is 11.4 mile. Here we assume M is located in such a way that all links in that segment are as those shown in Table 4.8. Part of l(1) next to Highway 6 does not contribute the risk caused at point M.

Table 4.8

Links characterization for risk assessment

Link	Link length (mile)	Ultimate incident frequency
l(1)	8.1	$4.6 * 10^{-8}$
l(2)	2.4	$2.3 * 10^{-6}$
l(3)	0.9	$1.0 * 10^{-6}$

Each link risk (LIR) is to integrate point risk along that link. Point risk should be assessed for every point in the link. For simplifying the process, here we use the uniform point risk to derive the route risk (RIR). By considering the trips per year, the risk associated with this route is:

$$
\begin{aligned}
RIR &= Trip \times PIR \times L \\
&= \frac{5.0 \times 10^{-8}\ death}{vehicle} \times \frac{1000\ vehicle}{year} \times 11.4 \\
&= 5.7 \times 10^{-4}\ death/year
\end{aligned}
\tag{4.7}
$$

4.4. Comparison between Propane and Chlorine Transportation

Because of strong influence of low-probability events on the overall risk profile and because too few incidents have occurred to support statistical characterization, experience does not provide an adequate basis for defining toxic transportation risks. The fact that the number of deaths and injuries for any given decades is small does not necessarily mean that the risk is small. Rather, it may reflect the good fortune that no large toxic releases have occurred near population area. As a result, the number of injuries or fatalities in a given time period can differ substantially from an average based on the distribution of possible incidents that accounts for low-probability/high-consequence events.

These terms of low probability and high probability are proposed in respect to the amount of material transported. The more popular usage and shipment of propane draws the conception that propane is much easier to result in incident or fatality than chlorine. However, causing more incidents does not mean the incident frequency is higher or the

transportation is more dangerous. The high number of incidents associated with propane transportation is mainly due to the large amount of trips. If all the transportation conditions (e.g., container type, container capacity, truck configuration) are the same for both propane and chlorine, the vehicles will have the same probability to be involved in transportation incidents in a trip.

The consequence of toxic materials and flammable materials are very different. The heat radiation of flash/torch fire decreases rapidly with distance, and the exposure to that heat radiation is not lethal if the individual is not too close to the release source. However, the fatality is very high if the individual is exposed to even small amounts of chlorine. Therefore, the consequence would be severe if large amount of chlorine is released in the transportation.

CHAPTER V

OPTIMUM ROUTING METHODOLOGY

TRA aims at providing baseline for risk management on HazMat transportation activities. To reduce the risk associated with the handling of HazMat, it is important to develop risk management systems that involve procedures and actions for supporting strategic, tactical, and operational decisions that aim in reducing risk. such a risk management system is also called decision support system for risk management decisions, and it must be developed based on TRA results and take into consideration the transportation characteristics.

Risk could be mitigated by the implementation of incident prevention actions, i.e., (i) judicious selection of route, (ii) alteration of vehicle/container design to reduce release severity, and (iii) improvement of driver training to reduce incident probability. In this chapter, network routing methodologies are addressed to provide risk mitigation tools for decision makers and to illustrate the importance of TRA in decision support system.

5.1. Background

The routing of HazMat operations is a complex, multiobjective problem involving environmental, engineering, economic, and political concerns. When

considering the simplest deterministic case, Abkowitz and Cheng (1988) and many other authors proposed to solve the routing problems by employing the classic shortest path algorithm. It involves finding the route from an origin to a destination which minimizes a single measure. The measure must be additive across links. The risk draws much concern as well as cost to be used as the measure. However, the methodologies did not explicitly consider the tradeoff between risks and cost. List and Mirchandani (1991) analyzed tradeoff between risk & cost. Zografos and Androutsopoulos (2004), Iakovou (2001), and List and Mirchandani (1991) proposed bi-objective models to address the effects of both cost and risk in routing decision.

In some cases the bi-objective model causes problems to decision makers, i.e., combining both the transportation cost and risk is hard for the decision makers to determine weights that would make such a combination meaningful; it is also hard to choose the weights that would differentiate equitably between the risk and the transport cost for the entire network.

Perceived risk reflects more the opinions of individuals or groups and is greatly influenced by feelings, perceptions, and emotions toward a specific problem. In our study, two optimum models are presented by taking account of decision makers' perception and avoiding the tradeoffs between cost and risk. The optimum models could be developed and solved in optimization software LINGO.

5.2. Fuzzy Logic Optimum Routing Model

5.2.1. Fuzzy Sets on Risk and Cost

Many existing mathematical models indirectly address aspects of human perception in the decision making process. Yet, none of these models has an effective method of measuring the public's perceptions and incorporating these perceptions into the strict mathematical framework required by optimization techniques. Fuzzy logic provides one way of directly integrating perceptions.

Figure 5.1 and Figure 5.2 depict the linear fuzzy sets used to represent the public's acceptance of any policy with respect to the cost and risk associated with that option. If a policy option has zero risk, its acceptability with respect to risk, μ_r, is unity. As risk exceeds the value B_r, the acceptability decreases linearly to zero at B_r'. A similar fuzzy membership function is used for acceptability with respect to cost. The mathematical expression of the fuzzy risk membership function depicted in Figure 5.1 is:

$$\mu_r \leq \frac{S_r - (Risk - B_r)}{S_r} \tag{5.1}$$

Similarly, a fuzzy cost constraint is formulated as:

$$\mu_c \leq \frac{S_c - (Cost - B_c)}{S_c} \tag{5.2}$$
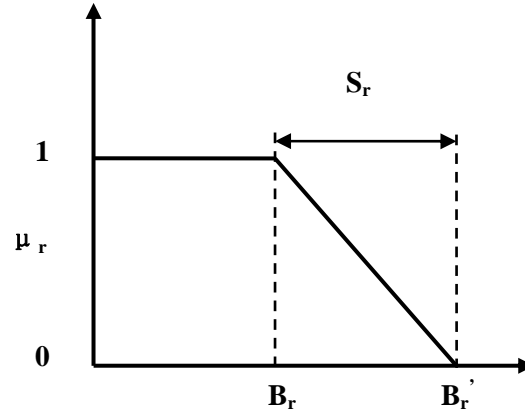
Figure 5.1. Linear risk fuzzy membership function.
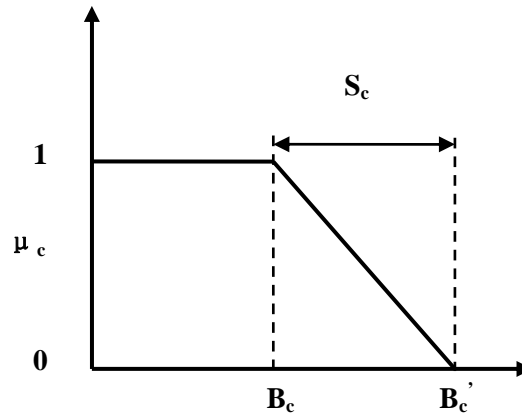
Figure 5.2. Linear cost fuzzy membership function.

5.2.2. Fuzzy Logic Optimum Model Setup

For model setup, perceptions on risk and cost are incorporated into the model using fuzzy sets. A single, non-controversial, non-fuzzy objective function is formulated

while all fuzzy sets are represented as constraints. In this manner, the algorithm can be used to arrive at a solution that optimizes the objective function subject to the fuzzy constraints as well as the physical constraints governing the transport and HazMat.

The network needs to be defined a little bit in routing process different than in the TRA process. The characterization process is shown in the following part.

- Network G={N, L}

- Link (i, j): from node i to node j

    l (i, j): length of link (i, j)

    C (i, j): link cost;   R (i, j): link risk

    T (i, j): number of trucks traveling on link (i, j)

    Cap (i, j): capacity of link (i, j)

- Node (i)

    b(i): truck's supply or demand

    b(i)>0 for supply nodes, <0 for demand nodes, =0 for other nodes

All the above parameters are known or could be determined directly by users except the capacity of link (i, j). It is determined by combing the risk acceptance and the risk associated with the link. The Dutch government has general risk criteria for fixed facility, which is the individual risk less than 10^{-6}. This criterion is implemented in transportation decisions in our study. Since transportation risk is additive, the individual risk caused by each link, R(i, j) should be less than 10^{-6} to ensure that the overall risk

associated with the whole transportation route can meet this criterion. Thus the capacity of link is determined as:

$$Cap(i, j) = \frac{10^{-6}}{R(i, j)} \qquad (5.3)$$

The objective is to maximize the overall acceptability of the routing solution with respect to cost and risk. Mathematically, this objective is expressed as

$$\max = \mu_r + \mu_c \qquad (5.4)$$

This objective function is subject to several mathematical constraints that are necessary to physically define the HazMat transportation problems:

- Mass balance for node

- Link capacity constraint for each link

- Fuzzy membership function for total cost and risk

The first constraint ensures that all the HazMat originating at the origin is transported though the transportation route and delivered to the destination, and the truck's supply and demand in the intermediate nodes are 0. The constraint is expressed as:

$$\sum_{(i,j) \in A} T(i, j) - \sum_{(i,j) \in A} T(j, i) = b(i) \qquad (5.5)$$

$$b(0) = Number\ (Transportation\ Truck)$$
$$b(i) = 0, \qquad (1 \leq i \leq N - 1)$$
$$b(N) = -Transportation\ Truck$$

The second constraint guarantees the truck transport capacity for each link. The number of trucks passing through each link can not exceed the capacity of that link. By this way the risk associated with this segment is guaranteed not beyond the risk acceptance level.

$$0 \leq T(i,j) \leq Cap(i,j) \tag{5.6}$$

The acceptability of the policy includes acceptability with respect to both cost and risk. The overall cost reflects the total cost of transporting HazMat. Mathematically, the cost is defined as:

$$Cost = \sum_{(i,j)\in A} T(i,j) \times C(i,j) \tag{5.7}$$

The acceptance level to cost is defined in Equation (5.1).

The overall policy risk also reflects the total risk associated with the HazMat transportation. Assuming independence, this objective is mathematically defined as:

$$Risk = \sum_{(i,j)\in A} T(i,j) \times R(i,j) \tag{5.8}$$

The acceptance level to cost is defined in Equation (5.2).

Solutions to this model formulation completely specify the routing strategy corresponding to the maximum acceptance. The model solutions are governed by the physical constraints defining the routing process and driven by overall risk and cost considerations. The solution could be obtained from optimization software LINGO once all data are input to the model.

5.3. Alternative Users' Determiner Optimum Model

Fuzzy logic optimum model presented in Section 5.2 is a good routing approach when users already have the perception towards the risk and cost associated with HazMat transportation and the acceptance levels of risk and cost can be changed to some degree.

However, if the decision makers already have a concept about the exact data of maximum acceptable risk, the model presented above needs to be modified to meet users' demand. In this section, the optimum route under given risk tolerance is selected based on an alternative optimum model.

Since the maximum acceptable risk has been defined by users, the objective function in the model is only the cost associated with the transportation activity:

$$\min = Cost = \sum_{(i,j) \in A} T(i,j) \times C(i,j) \tag{5.9}$$

The constraints to the objective function include:

- Risk constraint set by decision maker

- Mass balance for each node i

- Link capacity constraint for link (i, j)

The first constraint is defined by decision makers regarding the acceptance of risk:

$$Risk = \sum_{(i,j) \in A} T(i,j) \times R(i,j) \le R_{constra\,int} \tag{5.10}$$

Here $R_{constraint}$ is given by decision maker.

The constraints on mass balance and link capacity are the same as those described in Section 5.2.

After the setup of the model, the optimum route can be obtained by using LINGO to get the solution to the input model. With the change of risk acceptance level, different routes can be utilized to ensure the minimum cost. The decision makers can thenchoose the optimum routes based on their own requirements for acceptable risk level.

CHAPTER VI

LNG TRANSPORTATION CONSEQUENCE ANALYSIS[*]

Liquefied natural gas (LNG) plays an increasingly important role in the natural gas industry and energy markets. Taking the U.S market as example, industry analysts predict that LNG imports could increase to 5% of the total U. S. gas supply by 2007 (California Energy Commission, 2003). Marine transportation of LNG has been carried out with a very good safety record since 1959 (Otterman, 1975; ABS, 2004). However, the risks associated with LNG have been debated for decades. After September 11, 2001 there is a heightened sense of concern over the potential for terrorist attacks on LNG tankers. No LNG tanker or land-based LNG facility has been attacked by terrorists. However, similar natural gas and oil facilities have been favored terror targets internationally. In October 2002, the French oil tanker Limberg was attacked off the Yemeni coast by a bomb-laden boat (Parfomak, 2003). The combination of recent interest in expanding or building new facilities to receive LNG carriers, along with increased awareness and concern about potential terrorist action, has raised questions about the potential consequences of incidents involving LNG marine transportation.

---

[*] Portions of this chapter reprinted with permission from "Assessment of the effects of release variables on the consequences of LNG spillage onto water using FERC models" by Qiao, Y., West, H., Mannan, M., Johnson, D., and Cornwell, J., 2006. *Journal of Hazardous Materials*, in press. Copyright (2006) by Elsevier; "LNG-water rapid phase transition: A literature review" by West, H., Qiao, Y., and Mannan, M., 2005. *LNG Journal*, May, 21-24. Copyright (2005).

The major hazards of an LNG spill on water include:

- Pool fires: If LNG spills near an ignition source, the evaporating gas in a combustible gas-air concentration will burn above the LNG pool (Methane, the main component of LNG, burns in gas-to-air ratios between 5% and 15%). The resulting pool fire would spread as the LNG pool expanded away from its source and continued evaporating.

- Flammable vapor clouds: If LNG spills but does not immediately ignite, the evaporating natural gas will form a vapor cloud that may drift some distance from the spill site. If the cloud subsequently encounters an ignition source, those portions of the cloud with a combustible gas-air concentration would burn. The vapor cloud fire would burn its way back to the LNG spill where the vapors originated and then continue to burn as a pool fire.

- Rapid phase transition or flameless explosion: The phenomenon of rapid vapor formation with concomitant loud "bangs" has been observed when LNG was released on water. This non-flaming physical interaction is referred to as "rapid phase transition (RPT)" or "flameless explosion." West, Qiao, and Mannan (2005) believe that the rapid phase transition will not propagate into a significantly larger damage scenario.

- Confined space explosions: If significant confinement of the vapor cloud occurs after an accidental LNG release, damaging overpressures (explosion) may occur.

In the first part of this chapter LNG-water RPT is analyzed and previous experiments and theoretical work on RPT are reviewed. In the second part we will focus on the flammable vapor clouds dispersion process. The related processes, including LNG spillage and pool spread and evaporation, will also be considered. The effects of tank conditions, release scenarios and environmental conditions on the LNG spillage, spread and dispersion processes will be evaluated.

6.1. Rapid Phase Transition

In addition to a fire and/or explosion hazard when natural gas is mixed with air, there is the possibility of a low temperature, non-chemical interaction of the LNG with water. This type of interaction is often referred to as flameless vapor explosion, or as RPT as used herein. RPT takes place when a liquid rapidly changes phase to vapor. The large increase in volume causes a localized pressure increase, which can give rise to an air or waterborne boom. Though RPT results in shock waves, it is less powerful than what one usually associates with a chemical explosion.

A report by Burgess, Murphy, and Zabetakis (1970) provided the impetus for efforts of many investigators in this field. After September 11, 2001, this issue is under focus again due to the consideration of homeland security issues. No LNG tanker or land-based LNG facility has been attacked by terrorists. However, similar natural gas and oil facilities have been favored terror targets internationally. Two occurrences have been addressed by Parfomak a report for Congress (Parfomak, 2003).

In this chapter the incidents and experiments of LNG-water RPT are reviewed. Theoretical analysis about the LNG RPT mechanism and quantitative LNG RPT damage assessments are presented. Conclusions are drawn based on literature review and the available theoretical/quantitative analysis results.

Most of the LNG RPT work was reviewed here; however, since some experimental results were never published, and many of the comments result from informal, but not proprietary sources, such a review is undoubtedly incomplete, but it is considered that the basic facts presented in this article are correct.

6.1.1. Accidents Analysis and Experimental Results

The earliest reported observations of LNG RPT on water were made by Constock Liquid Methane Corporation at Bayou Long, Louisiana in 1956. LNG was intermittently pumped with flow rates of 0.23 m^3/min maintained for periods of several days and on short occasions exceeded 0.95 m^3/minute for a period of several hours. It is estimated that about 3785 m^3 of LNG were spilled in a period of about 3 months during which 3 or 4 very audible eruptions, loud enough to be heard 402 m away, occurred. Since none of these RPTs damaged standard window glass panes erected for these tests less than 15.2 m from the spill area, it was concluded that this phenomenon was unlikely to constitute a hazard.

On April 26, 1959, Constock Methane conducted jettison tests at sea in which 18.5 m^3 of LNG were pumped overboard in a period of 7 minutes. No audible eruptions were reported.

Tokyo Gas had conducted over 1000 small scale tests, starting in 1967, and the work has been addressed by Nakanishi and Reid (1971) and Burgess, Biordi, ad Murphy (1972) ,. The LNG quantities were 0.0012 or 0.0024 m^3. Although they observed small pops near the end of the evaporation of the spill, they never encountered a violent eruption or RPT.

In 1968 and 1969, the U. S. Bureau of Mines Safety Research Center conducted a series of tests on spilling LNG on water (Burgess and Murphy, 1970). One set of tests consisted of dumping 0.0038 to 0.0076 m^3 of LNG on 0.0189 m^3 of water or brine contained in an aquarium of 0.0566 m^3 capacity. 54 such tests were conducted with water followed by 2 tests with brine on the second of which RPT occurred which shattered the aquarium. Another series of 12 tests consisted of spilling 0.00378 to 0.472 m^3 of LNG on an artificial pond. In one of these tests, scheduled to be a 0.265 m^3 test, RPT occurred within an eighth of a second after the spill bucket had been tripped; it was estimated that at most 0.0945 m^3 were spilled. One observer standing on shore compared the RPT to a stick of dynamite. These noise observations are not a reliable indication of energy release as noted later in Section .

Subsequently, the Bureau conducted about 40 spills of LNG, totaling 1.13 m^3, on their artificial pond with no instances of visible or audible RPTs (Burgess, Biordi, and Murphy, 1972). In addition, they performed tests using other hydrocarbons and variable compositions of LNG. In some cases weak RPTs, probably comparable to the one that shattered the aquarium, have been reproduced.

Experiments were conducted by Garland and Atkinson (1971) at the University of Maryland. Small amounts (5-20 ml) of LNG were dropped onto water, water/organic liquid mixtures, or, in certain cases, one-component organic liquid. No RPT was observed during all of those tests. When larger amounts of LNG (10-100ml) were poured onto a liquid mixture consisting of a 1 mm film of Hexane on 100 ml water, RPT occurred every time.

Esso Research Laboratories in New Jersey carried out tests during 1971, and the results were reviewed by Atallah (1997) and the LNG Research Center, MIT (1977). As found in other tests, pouring LNG on top of water did not lead to RPT. However, when LNG was poured into a dry container and allowed to evaporate until only a foam remained, upon suddenly adding water to the foam, RPTs were produced which on occasion ruptured the container. Continental Oil Company had observed a similar phenomenon in their "dry- bucket" experiments in 1965 and 1971. Esso has since conducted numerous other tests including dumping LNG on liquids other than water. Weak RPT was sometimes noted if 3% sodium chloride salt solutions were employed. If LNG was poured on pentane or hexane, RPT was still observed.

A related test program was carried out by Nakanishi and Reid (1971) at MIT. No evidence of RPT was noted throughout the process for the small scale spills of LNG on cold or hot water. When, however, 10 to 100 ml of LNG was spilled on hexane, RPT occurred with a violent crack-like noise and the residual LNG was thrown violently out of the Dewar flask. RPT also occurred when LNG was spilled on water coated by

hexane usually 1 to 2 second after the start, though occasionally a delay of 5 to 10 second was noted.

Beginning in 1970, the research laboratories of Shell Pipeline Company in Houston conducted about 300 laboratory tests consisting of spills from 30 ml to 6 l of cryogens on water (Enger and Hartman, 1972a). Weak RPT or pops occurred within one to two minutes after the spillage of LNG. The higher the temperature of the water, the less elapsed evaporation time was required for the pops to occur. Presumably, these pops are related to the persistence of the Leidenfrost film boiling into a metastable region, which ultimately terminates explosively in the transition boiling regime as demonstrated by Baumeistor, Hendrick, and Hamill (1966).

Shell has reported their work on larger spill tests. Reproducible RPT was obtained only with weathered LNG containing less than 40 percent methane (Enger and Hartman, 1972b).

LNG Research Center, MIT (1977) finished a report under contract to American Gas Association. Spills were made with six pure hydrocarbons on water and other fluids. RPT occurred under certain substrate temperatures for most of the spilled liquid-substrate pairs. At temperatures less than those necessary for RPT, there was generally nucleate boiling and sometimes the substrate froze. At temperatures above the RPT, film boiling took place. Five binary hydrocarbon mixtures of ethane or ethene with a heavier hydrocarbon were studied with water as the only substrate. RPT was observed for every binary system under certain temperatures. If RPT did not occur, ice always formed rapidly.

In 1980 the Burro series were conducted by Lawrence Livermore National Laboratory (LLNL) primarily to study vapor cloud dispersion (Koopman, et. al., 1982). The spill volume ranged from 24 to 39 m^3, the spill rate from 11.3 to 18.4 m^3/min. Energetic RPT explosions, though not expected, did occur during the Burro 6 and 9 tests. In test 9 the most severe RPT event produced blast overpressure of 0.05 bar measured at distance of about 30 m. The air-blast TNT equivalents of the observed RPTs were calculated from peak overpressures measured at known distances from the spill point. By this calculation the surface shock wave reflection produces an overestimate of the explosive energy by a factor of 1.8. In earlier reports the surface reflection reduction was not imposed. The maximum TNT equivalent was originally calculated to be equal to 6.3 kg by Koopman et. al. (1982). After considering the surface reflection reduction, Goldwire et. al. (1983) and McRae, Goldwire, and Koopman (1984) estimated the maximum TNT equivalence for Burro test RPT explosion was 3.5 kg. It is most notable in Burro test 9 that RPT damaged the spill plate and spill pipe support structures.

In 1981 the Coyote series tests were performed in order to further study the RPT explosions (Goldwire et. al., 1983; McRae, Goldwire, and Koopman, 1984). Thirteen spills of 3-14 m^3 with flow rates of 6-19 m^3/min were performed with fuel of varying ratios of methane, propane and ethane. Five spills of 8-28 m^3 with flow rates of 14-17 m^3/min were also performed to obtain dispersion and combustion data. Six of the eighteen spills produced RPT explosions. The maximum overpressure measured at distance of 24.3 m from the spill source was 0.09 bar, which was estimated to have maximum TNT equivalence of 5.5 kg if the surface reflection reduction was not imposed

(Goldwire et. al., 1983; McRae, Goldwire, and Koopman, 1984). After imposing the surface reflection reduction effect, the maximum TNT equivalence was estimated to be 3.0 kg . However, the maximum TNT equivalence of 5.4 kg and 6.3 kg ware noted by Atallah (1997) and Sandia (2004) respectively. Based on the LLNL report, which should be the most reliable source since they were published by the laboratory that conducted the Coyote series tests, the maximum TNT equivalence noted in the Sandia report may not account for the surface reflection reduction effect, while the data provided by Atallah may come from Burro tests rather than Coyote tests.

In 1980 LNG tests were conducted at Maplin Sands, England by the National Maritime Institute to obtain dispersion and thermal radiation data on 20 spills of LNG and 14 spills of propane onto water (Blackmore, Eyre, and Summers, 1982). The maximum spill size of 20 m^3 was chosen for the experiments, both of LNG and refrigerated propane. RPTs were observed in one of the instantaneous LNG spills, and it is believed that the barge was damaged by the series of RPTs (Sandia, 2004).

Gaz de France has done a lot of research in this area (Gabillard, Dahlsveen, and Cronin,1996; Cleaver, Dahlsveen, and Heiersted, 1998; Nedelka, Sauter, Goanvic, and Ohba, 2003). In 1981, Gaz de France performed continuous spillages of LNG onto the sea at Lorient, France, with flow-rates up to 50 m^3/h to reproduce the conditions of an LNG leakage from a loading/unloading arm. In a partnership with Shell Research in 1982 and with British Gas in 1984, complete ruptures of a loading/unloading arm were simulated during 28 instantaneous spillages of volumes between 1 and 9 m^3. The maximum RPT recorded was evaluated to be equivalent to 4.15 kg of TNT (Nedelka,

Sauter, Goanvic, and Ohba, 2003). However, the maximum measured overpressure and the corresponding distance to the source was not specified by Sandia (2004), Blackmore, Eyre, and Summers (1982) or Gabillard, Dahlsveen, and Cronin (1996), so that it is hard to evaluate the validity of the TNT equivalence data.

In 1987 the Falcon tests were conducted at Frenchman Flat in Nevada by LLNL (Shin, Meroney, and Neff, 1991). The Falcon tests were also addressed by Sandia (2004). The testing was performed on a 40 by 60 m pond, enclosed by an 88 m long by 44 m wide by 9.1 m high vapor fence. A 22 m wide by 13.7 m high barrier was erected upwind of the pond, in order to simulate the obstruction of a storage tank. Five tests were performed with spill rates of 8.7-30.3 m^3/min (20.6-66.4 m^3), and methane concentrations of 88-94.7%. Large RPT explosions occurred approximately 60 seconds after the spill, and a fireball started inside the vapor fence at 81 seconds for Falcon test #5, which had a spill rate of 30.3 m^3/min, total volume of 43.9 m^3, and methane content of 88%. RPT also occurred with Falcon 3, with a spill rate of 18.9 m^3/min, total volume of 50.7 m^3, and methane content of 91%.

The Falcon test is significant because it is the only case where RPT was considered an ignition source. However, there are two theories. One theory claims sufficient energy release to cause methane ignition, whilst the other theory suggests an aerosol formation, which then ignited surrounding gas by an electrostatic mechanism.

6.1.2. Hot Liquid-Water RPT

To explore the mechanism of RPT, some investigators also tried to use other liquid-liquid systems that can interact similar to the LNG/Hydrocarbons-water system. For example, Anderson and Armstrong at the Argonne National Laboratory worked on water-molten NaCl and Sodium-molten UO_2 systems to produce RPT with well-defined fluid geometry (Anderson and Armstrong, 1973).

In retrospect, the violent interaction of LNG with water is probably quite similar to the steam explosions that have been observed for many years in almost every industry where very hot liquids are handled such as the aluminum, copper, paper (soda and Kraft smelt), nuclear, and the iron and steel industries. A critical review of these physical explosions, including a postulated mechanism and a mathematical model, has been published by Genco and Lemmon (1970). Although this work constitutes an excellent frame of reference for analyzing the consequences of such explosions, their mathematical model is not directly applicable to the LNG-water eruptions, particularly with respect to the scale-up parameters.

A significant point of difference between the liquid metal-water explosions and the LNG-water combination is that the former can be reproduced consistently in the laboratory at conditions comparable to those encountered in actual practice. On the other hand, as is evident from the summaries in the preceding paragraphs, LNG-water RPT can be reproduced with any degree of consistency only when the experimental variables and procedures are carefully controlled under conditions which are not likely to be encountered in actual practice. It is also significant to note that despite the occurrence of

explosions in these other industries under conditions of actual practice, they have continued to operate in a relatively safe and prudent manner.

6.1.3. The Audible Pop Phenomenon

It is essential to recognize clearly that two separate phenomena have been observed under the category of LNG-water eruptions: (1) the audible burst or pop, and (2) RPT. These two phenomena have at least one element in common in that superheating of the LNG is a contributing factor, which culminates in an eruption, although of different magnitudes, in both instances. However, beyond this premise, the detailed mechanisms leading to the RPT could conceivably be different since the elapsed time differs by at least three orders of magnitude (about a factor of a thousand) for these two phenomena. For example, in the small-scale Shell experiments, which have also been observed by others, an elapsed time of about 75 to 125 seconds was required to achieve a pop after LNG (usually around 30 ml) at −161 °C was poured onto water (or brine) having an initial temperature of 15 °C to 86 °C. The shorter times are associated with the higher water temperatures, and the reproducibility of the results when correlated as elapsed time versus initial water (or brine) temperature was quite remarkable (Enger and Hartman,1972a; Enger and Hartman,1972b). Similarly, the Bureau of Mines observed in pouring LNG continuously at a rate of 0.45 kg/s onto water that no audible activity was encountered during the first 60 seconds. However, after 120 to 180 seconds, audible pops were observed about every 30 to 60 seconds for the entire period of 600 seconds involved in the continuous spill (Burgess, Murphy, and Zabetakis, 1970). On the other

hand, the single, major RPT observed by the Bureau of Mines on their Bruceton pond transpired within a fraction of a second after the LNG first contacted the water. It is significant to note that this almost instantaneous interaction has not been reproduced in experiments except under carefully controlled, unusual conditions as demonstrated by Shell. Some idea of the probability of obtaining a substantial RPT can be gleaned from the aforementioned Bayou Long tests by Constock. Since 3 or 4 RPTs were noted over a period of several months, during which LNG was spilled continuously at rates of 0.23 m^3/min to 0.95 m^3/min, it is estimated that on the average one very audible eruption was encountered for every 950 m^3 spilled.

6.1.4. RPT Conditions and Mechanism

The composition of spilled hydrocarbons has great effect on the occurrence of RPT. As reviewed by the LNG Research Center, MIT (1977), previous studies by Esso Research Laboratories have shown that LNG with a high methane content (> 40%) does not undergo a RPT when spilled on ambient water. Natural gas typically consists of at least 80% methane, and LNG is usually over 90% methane. It may contain other hydrocarbon gases (e.g., propane) and nitrogen. This may explain why large scale LNG RPT have not been reported. In no case did a RPT occur when the methane concentration was greater than 40%. Methane need not be present for a RPT to take place.

On the other hand, Esso Research Laboratories were able to obtain RPT in quite small scale spills of LNG on hot water with initial methane concentrations in excess of

50%. After spillage, there was 4 to 15 seconds of film boiling before the occurrence of RPT, which was, therefore, sufficient time to boil off much of the methane as the original thickness of the LNG layer was only 2-4 mm (LNG Research Center, MIT, 1977)

Shell Pipeline also concluded from their experiments that RPT from LNG spilled onto open water at ambient temperature can only occur if the methane content of the LNG is less than 40 mole% (Enger and Hartman, 1972b). Furthermore, RPT will not occur if the mole ratio of propane to ethane in the LNG is 1.3 or greater.

LNG can eventually age in a storage tank, by boiling off methane, to reach the composition required to produce a RPT on ambient water. In the Maplin Sands tests, Blackmore et al. believe that operational delays encountered in this particular test allowed the LNG to age sufficiently for RPT to occur (Blackmore, Eyre, and Summers, 1982). However, if the initial methane content is 95 mole%, for example, only 10% of the initial volume of the liquid will remain when the LNG has aged to the critical composition. At this time the normal boiling point of the liquid remaining will be –148 °C or higher, about 13°C hotter than normal LNG.

Temperature is another important factor for RPT. Enger and Hartman (1972a) noted that the water had to have an initial temperature between 54 °C and 70 °C for RPT to occur when liquid propane was spilled on water. In the tests conducted by the LNG Research Center, MIT, various hydrocarbons were spilled onto different host liquids. It was also noted that the temperature of host liquid must fall within a certain range on RPT occurrence (LNG Research Center, MIT, 1977). For example, when 2-

Methylpropane was spilled onto the ethylene glycol/water mixture, RPT occurred only when the substrate temperature is from 101 °C to 106 °C, with violent boil noted from 97 °C to 100 °C and film boil observed from 108 °C to 115 °C.

The requirement for weathering directs suspicion on the heavier hydrocarbons which are usually present in LNG. It is further reinforced by the fact that no RPT has, as yet, been reported with pure liquid methane on water. Nevertheless, it does not necessarily follow that pure liquid methane (or other pure liquids, for that matter) will not have RPT when dumped on liquids having an appropriate temperature difference across the interface.

The amount of LNG spillage has a minor effect on RPT occurrence. During the experiments conducted by the LNG Research Center, MIT (1977), no RPT was observed when very small amounts of LNG were spilled on hexane, while when 10-100 ml of LNG was spilled on hexane, RPT occurred.

Esso research laboratories also found in their several experiments, in which LNG was spilled on hexane films on water, that the amount of LNG required to obtain RPT on a 1.5 cm film was 4 l (LNG Research Center, MIT, 1977).

Impact force may be another minor factor for this phenomenon. Porteous and Reid (1976) pointed that impacting the cold, volatile liquid upon the hot liquid may lead to very destructive RPT or to RPT that would not have occurred if the liquids were contacted in a gentler fashion.

While there are considerable variations in both the spilled liquid and the host liquid, all RPTs seem to have at least one common characteristic, that is, RPT occurs

only when the substrate temperature reaches between that necessary to give film boiling and that in nucleate boiling. This is based on visual observations of the boiling phenomena. Not only is the substrate temperature important, but also its melting point. In 1973, Yang (1973) reported the results of spills of LNG onto various organic liquids, that is, the hydrocarbon substrates, and his work was addressed by LNG Research Center, MIT (1977). It was found in Yang's tests that, with a few exceptions, RPT occurred with organics which had melting points below −51 °C. Substrates that have high melting points can freeze almost as soon as LNG is poured on them. A frozen surface provides nucleation sites which prevent RPT.

A generally accepted explanation for RPT mechanism was proposed by Katz and Sliepcevich (1971). The essence of their explanation is that RPT results from superheating of LNG. Using the literature on pool boiling and superheating of liquids, they have qualitatively explained many of the observed phenomena surrounding LNG-water reactions. Take the delayed RPT as an example. Here the composition of the hydrocarbon is such that when it reaches the water, it is in film boiling. Boiling changes the composition of the hydrocarbon as with the platelets so that the temperature rises and the temperature difference between the water and the hydrocarbon decreases. After boiling for a period of time, the temperature difference due to the changing hydrocarbon temperature reaches the Leidenfrost Point and enters the liquid-liquid superheat temperature difference region where without any phase change, the liquid film reaches the limit of superheat and RPT occurs. Katz (1972) gave a figure to describe this process. A similar explanation was given by LNG Research Center, MIT (1977).

6.1.5. RPT Models

Some fundamental aspects of heat transfer and nucleation characteristics in liquid-liquid systems were discussed by Fauske (1974) in an attempt to predict RPT. Rausch and Levine carried out the analysis using a geometric thermodynamic model to predict RPT. The physical basis of the model is that a second order phase transition takes place when a system passes through a critical region. In passing through a critical region, thermodynamic stability conditions are violated. The critical region marks the point of separation between definite stability and definite instability and consequently a second order phase transition may be looked upon as corresponding to incipient instability (Rausch and Levine, 1973).

Atallah (1997) reviewed several RPT models, including McRae's analysis of four models for cryogen-water RPT, with respect to a possible application in explaining the China Lake results. Atallah (1997) pointed out that a numerical solution to the transient heat equation is necessary for small volumes of cryogen. However, calculation of transient superheating of a drop composed of a mixture of cryogens of different volatilities must include species mass transport. Evaporation of the more volatile species will result in surface enrichment of the less volatile species, if the diffusion rates are slower than the evaporation rates, but no experiment or calculation using the surface enrichment effect has been carried out for LNG-water mixtures. LNG-water mixing code and RPT propagation code were compiled by Gaz de France to provide an insight into the possible hazards presented by RPT events and a quantified estimation, expressed in

terms of TNT equivalence, of the associated risks (Nedelka, Sauter, Goanvic, and Ohba, 2003).

As proposed in reports by the Federal Energy Regulatory Commission (FERC) (2004) and ABS Consulting Inc. (ABS, 2004), the modeling of RPT could be helpful in two aspects: (1) understanding overpressures resulting from the RPT and (2) understanding dispersion of the "puff" of LNG expelled into the atmosphere by the RPT. The sizes of the overpressure events have been generally small, and it is not expected to cause significant damage to an LNG vessel. However, RPT may increase the rate of LNG pool spreading and the LNG vaporization rate. No theoretical or experimental basis could be identified for modeling either the overpressure or source term effects. A possible example dispersion analysis was performed to examine the importance of an RPT in estimating downwind flammable concentrations. The ABS analysis results indicated that the total evaporation duration time will decrease significantly (due to bigger pool contact area), but the downwind distance to LFL will increase only slightly.

Sandia (2004) reviewed several theoretical models that have been proposed to explain the formation of RPT, and it was postulated that much different behavior may occur at larger scales, which could not be predicted from smaller scale studies. It was concluded that the impacts of RPT will be localized near the spill source and should not cause extensive structural damage.

The consortium of BG, Gaz de France and the University of Trondheim have not yet released the commercial version of a computer program, called CRYO-CULDESAC, which purports to model the RPT phenomena.

6.1.6. Damage Assessment

6.1.6.1. Uncertainty of RPT Magnitude Estimation by Sound Waves

The RPT occurred in one of those series of tests conducted by the U. S. Bureau of Mines. The magnitude was comparable to the explosion of a stick of dynamite according to one of the observers standing onshore. However, this estimation of the magnitude of the blast should be viewed with suspicion since the loudness of an explosion is a very unreliable measure of its absolute intensity. As explained by Cook (1958), if two sound waves of a single and equal frequency are compared, the loudness varies somewhat as a function of the intensity level. On the other hand, noise, such as that produced by RPT, possesses a continuum of frequencies, and the loudness sensation from such waves will not be related directly to the intensity level since the ear is a nonlinear instrument, the response of which varies with frequency. Furthermore, estimates of the absolute intensity of sound by audible means are at best subjective since they are strongly influenced by the observer's frame of mind. Finally, it is well known that in the range beyond the damage limits, air blasts, while non-destructive, are observed to be extremely variable and depend critically on meteorological conditions (Cook, 1958). The fact that an LNG spill on water generates its own localized inversion layer, which is enhanced by low wind conditions, will tend to amplify the loudness and sharpness of the noise at some distance from the RPT source.

6.1.6.2. Damage Potential Estimation

The damage at any particular distance from a TNT explosion source can be estimated from the maximum overpressure at that point. The maximum overpressure can be calculated from the following empirical Equation (6.1) as addressed by Genco and Lemmon (1970). The cylindrical explosive charge of TNT is assumed in this empirical equation as analyzed by Lipsett (1966):

$$\Delta P_m = P_0 \left[\frac{11.34}{Z} - \frac{185.9}{Z^2} + \frac{19210}{Z^3} \right] \qquad (6.1)$$

where

ΔP_m = maximum overpressure, Psig

P_0 = ambient pressure, Psig

$Z = 3.96 \times (R/W)^{\frac{1}{3}}$

R = distance from the source, ft

W = TNT equivalent weight, lb

The assumption of a cylindrical charge in Equation (6.1) gives lower values for the maximum overpressure than a rectangular charge. Furthermore, it is questionable to what extent this equation is applicable to LNG-water RPT. The best guess at the moment is that Equation (6.1) will overestimate the overpressure for an LNG-water RPT since it

originates near the surface of the water. Consequently, the shock wave will be attenuated at the air-water interface and most of it will be directed upwards.
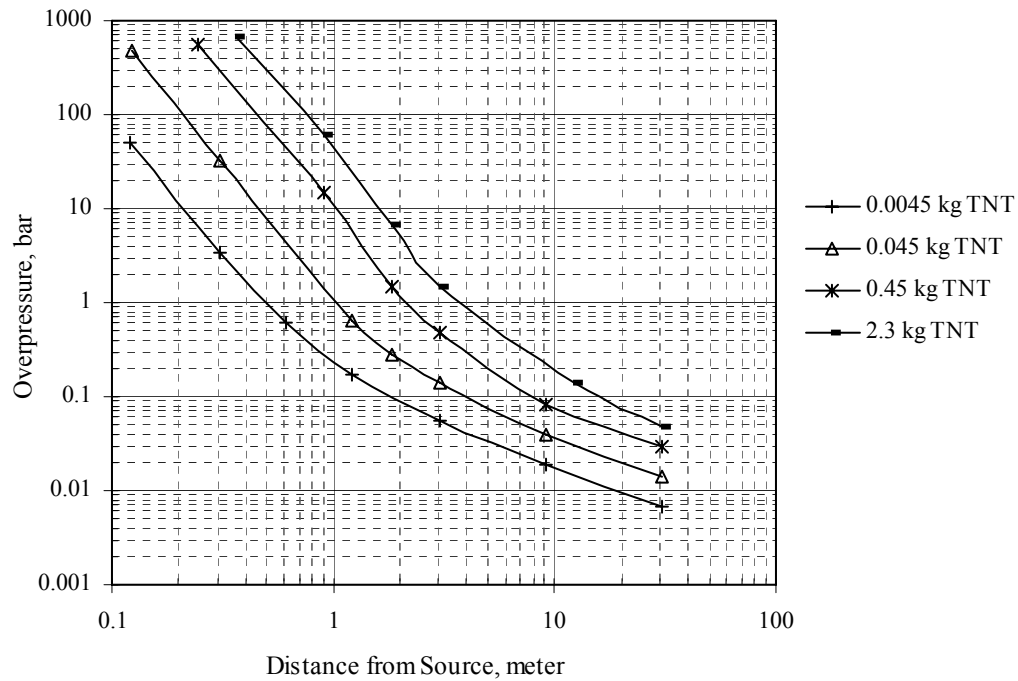
Figure 6.1. Damage potentials.

Figure 6.1 was generated from Equation (6.1). It shows the variation of peak overpressure with distance for several TNT equivalent weight parameters. Figure 6.2 is a cross-plot of Figure 6.1 and is somewhat more convenient for damage estimation. From Figure 6.2 it is evident that 4.5 kg of TNT (equivalent to 20 sticks of dynamite) would not puncture a ship's hull at a distance of 2.7 meter. These assigned distances are roughly what might be encountered in LNG tanker unloading practice.
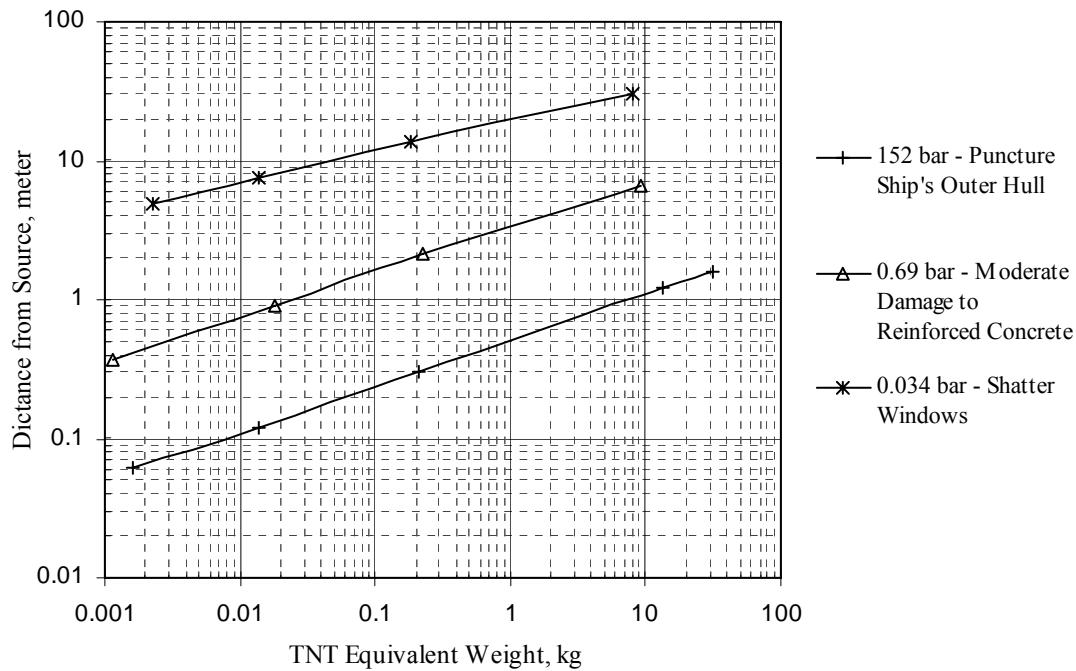
Figure 6.2. Damage potentials: cross-plot.

The highest overpressure recorded in the Shell large-scale spill tests was 14 kg/cm^2 (13.8 bar) at a distance of one meter below the liquid-liquid interface (Enger and Hartman, 1972a). From Figure 6.1 this overpressure and distance would classify the explosion as equivalent to about 0.91 kg of TNT. An LNG-water RPT of this magnitude would have to be less than 1 foot from a ship's hull to cause even minor damage to the hull structure. In this case the damage due to low temperature embrittlement by direct contact of the LNG with the hull would be a more serious threat than any LNG-water RPT.

Notice that TNT equivalent weight estimation of an explosion from peak overpressure-distance data is extremely sensitive to the distance measurement. Due to

surface penetration of the falling liquid, the distance between the explosion source and the pressure transducer in the Shell tests may be less than 1 meter. If the actual distance was 0.057 meter, the TNT equivalent of their largest blast is reduced to 0.045 kg of TNT. It should be emphasized that the majority of RPTs observed by Shell resulted in smaller maximum overpressures, further decreasing the chance of damage due to an LNG spill on water.

6.1.7. RPT Explosion Energy Release

As noted previously herein, estimates of energy release based on sound are very unreliable indicators. The available experimental data about RPT explosion energy release are shown in Table 6.1, and only those data recorded by sensors are illustrated in the Table. Experimental data on blast pressures for LNG-water RPT are not in abundant supply, and some overpressure data were not clearly noted in the reference. In Table 6.1 the TNT equivalents are derived from Figure 6.1 or Equation (6.1) on the basis of measured overpressures at known distances from the spill points.

The largest overpressure recorded by Conoco was 24.8 bar at about 0.15 meter from RPT source. This is estimated to be equivalent to 0.0045 kg of TNT. In one series of tests, a plexiglass container was destroyed by RPT and one 0.0026 m^2 remnant was found 42.7 meter from the point of detonation. By calculation of the force required to hurl this piece of plexiglass, an estimate of the peak overpressure can be made. The calculated value was 26.6 bar. The important point is that this value provides an

independent check on the order-of-magnitude of the data recorded by the pressure transducers.

Table 6.1

Summary of RPT explosion energy release[*]

Test	Spill Size	Maximum RPT Overpressure vs. Distance to source	TNT Equivalence
U. S. Bureau of Mines	6 liters	4.1 bar at 0.076 m	< 0.0045 kg
Conoco [a]	/	24.8 bar at 0.015 m	0.0045 kg
University of Maryland [b]	200 ml	28.4 bar	$\cong$ 0.0045 kg
MIT	350 ml	13.8 bar at 0.1 m	< 0.0045 kg
Shell [a]	/	13.8 bar at 1 m	0.91 kg
Burro Tests	24 m^3	0.05 bar at 30 m	3.5 kg
Coyote Tests	28 m^3	0.09 bar at 24.3 m	3.0 kg

[*] Overpressure data that could not be validated according to the measured overpressure gauge and the corresponding distance to source are not included in this table, including that from Gaz de France.

[a] The corresponding spill size was not clearly noted.
[b] The distance to measure the overpressure was not specified clearly in the reference; it was stated that "a miniature pressure transducer was fixed above the surface of the liquid sample". A distance of 0.15 meter from the source is assumed to assess the corresponding TNT equivalence.

6.1.8. Scale-up

The TNT equivalent of a large spill cannot be estimated simply by a linear scaling of the volumes of the small scale spills for which RPT has been observed. The

LNG-water explosion is highly dependent on the amount of liquid-liquid contact area, which is available for heat transfer. This heat transfer area does not increase in direct proportion to LNG spill volume. Burgess, Biordi, and Murphy (1972) developed equations for predicting the spreading rate of LNG on water. These equations can be used to show that the possible heat transfer contact area is relatively limited even for large spills. Another aspect of increased heat transfer contact area is the time required for the larger spill to reach this available surface area. It seems reasonable that a number of distinct RPTs at various times would be more likely in a large spill than one large simultaneous release. The fact that larger spills require larger distributions over time and space reinforce the probability of multiple weak RPT.

Timing and spatial configuration of any explosive source are critically important parameters. Explosive demolition of urban buildings takes advantage of these factors. Using a timed sequence of distributed explosions, a building can be razed without damage to neighboring facilities. If, however, the same amount of explosive were detonated at the same time and in one location, the resultant overpressure could do extensive damage to surrounding property.

The following Equation (6.2) provides a method for estimating the distributed effect of TNT explosions:

$$W = W_N \left(\rho_d / \rho_N \right)^{1/4} \qquad (6.2)$$

where

W = actual TNT equivalent weight

W_N = normal density TNT equivalent of the dispersed explosive

ρ_d = density of the dispersed explosive

ρ_N = normal density of the explosive

Compare the explosive power of 0.45 kg of TNT distributed over 2.83 m^3 with the same 0.45 kg of TNT concentrated at the center of this explosive volume. The normal density of TNT is about 1603 kg/m^3. The density of the distributed explosive is 0.16 kg/m^3. Equation (6.3) shows that:

$$W = (1.0)\left(\frac{0.01}{100}\right)^{0.25} = 0.1 lbs \qquad (6.3)$$

One lb of TNT, that is 0.45 kg of TNT, distributed over 2.8 m^3 is equivalent in damage potential to 0.045 kg of TNT concentrated at the center of the explosive volume. This result is in line with observed behavior; damage done by a distributed source is always less than an equivalent amount of explosive concentrated at one point.

6.1.9. RPT Impact on LNG Leak Contacting Ship Ballast

No studies have addressed the potential for damage from an RPT which results from the leak of LNG upon contact with the ballast water. Most comments on this subject have assumed that only a small leak would occur, with the resulting RPT assumed to be very minor. RPT following a major terrorism event has been dismissed as irrelevant considering the major impact of an intentional LNG sabotage scenario.

6.1.10. Varied Opinion in RPT Reported Incidents: **Badak, Indonesia, December 1992**

6.1.10.1. Quoting Directly from an Paper

The following is quoted directly from the paper of Nedelka, Sauter, Goanvic, and Ohba (2003).

"An LNG leak occurred when starting a liquefaction train, and the decision was made to operate the train despite the leak. Protective water curtains were used to reduce the effects of the vapor cloud produced. Approximately 11 hours after the plant was started, RPTs occurred in a drainage channel covered by a concrete slab. The drainage channel and concrete slab were broken, adjacent pipe was damaged, and some concrete blocks were thrown approximately 100 m. No personnel were injured because the area had been evacuated because of the leak." This simplified quote has many erroneous statements

6.1.10.2. Quoting from an Eyewitness

The rundown line from Train E had a stub with a valve and blind flange installed for the future tie in of Train F. The incident in question occurred when the valve that had been repaired was ready for re-installation prior to the tie in being made for Train F. the maintenance crew prepared to remove the blind flange and re-install the valve. Because of the existence of some residual LNG in the LNG rundown line, a small amount of liquid started to come out the bottom of the flange when the flange was spread. The leaking LNG was channeled to an area where there was a closed storm water drain that fed into a central closed storm water drain that ran down the center of the process area. It

was here that the RPT occurred due to there being a significant amount of water in the drain and then the LNG coming into contact with this water and rapidly vaporizing causing the 30" drain pipe to lift out of the ground. The actual explosion occurred underground and not in the open storm water sewer system (Harris, et. al., 1992)

6.1.10.3. Quoting Directly from Bontang Safety Manager

The following is quoted directly from John Boone, the Bontang safety manager.

"Some people believe that the damage was caused by the RPT phenomena, but many others later realized that the over-pressurization of closed drains (which did not have any pressure relief) could also be an explanation. There were many local RPTs on the surface, which made the observers focus on the RPT explanation." Figure 6.3 provides a visual sketch of the situation.
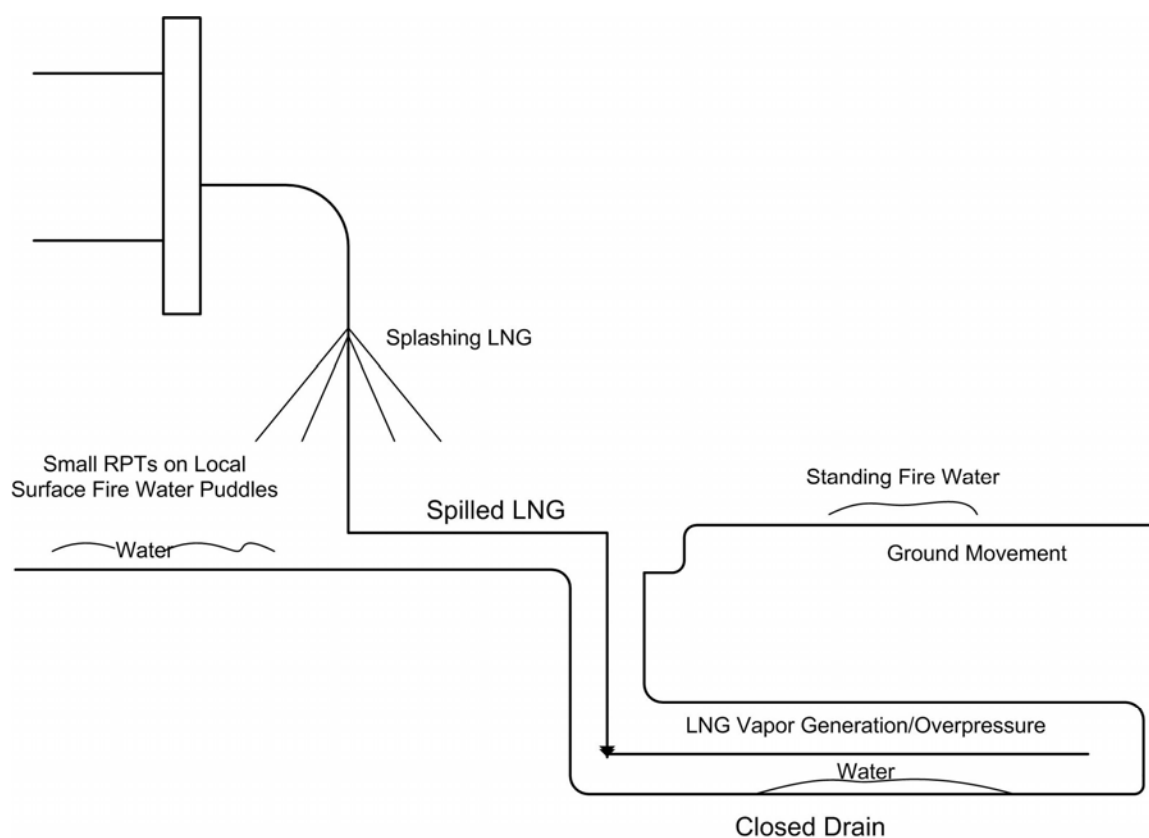
Figure 6.3. Badak, Indonesia incident, December 1992: was it RPT or unrelieved overpressure?
(Based on Harris, et. al., 1992)

6.1.11. Conclusion on RPT

Experimental and theoretical studies that have been carried out about LNG – water RPT are review. Even though RPT is a rare occurrence as shown by the experiments reviewed in this article, it did occur when some conditions were fulfilled. The effects for RPT have been explored based on early studies, and the well-accepted vapor mechanism has been described. Such understanding is beneficial for LNG tanker

transportation since the possibility of RPT occurrence could be reduced by avoiding those conditions that favor RPT.

It has been emphasized that larger LNG spills will not likely constitute a significantly larger damage potential than what has already been observed in the experimental tests by various investigators, although scale factors for LNG-water RPT cannot be developed without further experimental work and mathematical modeling. In the early LNG industry development, a concern that RPT could initiate an Unconfined Vapor Cloud Explosion prompted many of the tests that are reported herein. However, the potential for UVCE has been proved to be not feasible.

Out of all the many RPT tests, the Falcon 5 test shows a unique anomaly. It appears that an RPT may have been the ignition source of the downwind vapor. While that was a very unique event, it indicates that downwind vapor dispersion of a large LNG spill on water has an even smaller likelihood due to the potential for RPT based ignition.

Some theoretical models have been developed to predict the maximum overpressure resulting from RPT, but much more data on RPT with better pressure and distance measurements would be required to provide input for eventual model validation.

6.2. Assessment of Variables' Effect on Consequences of LNG Spillage onto Water

In this section we will focus on the flammable vapor clouds dispersion process. The related processes, including LNG spillage and pool spread and evaporation, will

also be considered. The effects of tank conditions, release scenarios and environmental conditions on the LNG spillage, spread and dispersion processes will be evaluated.

6.2.1. Background

6.2.1.1. Experimental Test about LNG Spillage onto Water

Quantitative data began to emerge from the Lake Charles experimental project in the 1950s. In 1968 and 1969, the U. S. Bureau of Mines Safety Research Center at Pittsburgh conducted LNG spill tests up to about 16.6 ft^3 (0.47 m^3) on a quiescent pond (Burgess, Murphy, and Zabetakis, 1970; Burgess, Biordi, and Murphy, 1972). Esso Research and Engineering Company carried out LNG spillage on water testS to obtain the downwind dispersion data characteristics of a marine environment (Feldbauer, et. al., 1972). Most of the tests were conducted at two sizes—about 250 gallons and about 2500 gallons. In 1980 Maplin Sands tests, involving spilling quantities of refrigerated gas of up to 20 m^3, were performed by the National Maritime Institute and were sponsored by Shell to obtain dispersion and thermal radiation data (Blackmore, Eyre and Summers, 1982). The Burro tests were conducted by the Lawrence Livermore National Laboratory and the Naval Weapons Center in 1980 (Koopman, et. al., 1982). A total of nine LNG releases onto water were performed, with spill volumes ranging from 24 to 39 m^3. In 1987, the Falcon tests were conducted in Nevada to provide a database on LNG vapor dispersion from spills involving obstacles and to assess the effectiveness of vapor fences for mitigating dispersion hazards (Shin, Meroney, and Neff , 1991). The highest spillage volume during the tests was 66.4 m^3.

6.2.1.2. LNG Source Term Calculations

Fay (2003) presented two models to assess the LNG release processes from the cargo tank ruptures, one for scenarios with holes above the seawater level, and the other for scenarios with holes below seawater level. Further analysis in his paper was based only on the former model.

In May 2004, under the contract with the Federal Energy Regulatory Commission (FERC), ABS Consulting Inc. developed consequence assessment methods for incidents involving releases from LNG carriers (ABS, 2004). FERC (2004) updated the ABS report in June 2004. An orifice model was used in ABS/FERC report to evaluate the rate of LNG release from the tank. Currently almost all authors use the orifice model, but variations exist in assumed initial conditions and orifice coefficient.

6.2.1.3. LNG Vaporization Rate on Water

LNG vapor generation is calculated based on the heat transferred from the water into the spilled LNG pool. In the model developed by Otterman (1975), which is the most widely accepted LNG evaporation model, the vaporization rate of 0.04 lb ft^{-2} s^{-1} (that is about 0.20 kg m^{-2} s^{-1}) was based upon the experimental data from the Bureau of Mines. Sometimes vaporization rates were reported as thickness regression rates, with a typical value of 1 inch per minute. Opschoor (1980) derived an evaporation rate of 0.01 lb ft^{-2} s^{-1} (0.05 kg m^{-2} s^{-1}) from the convective heat flux equations. However, FERC (2004) recommended using the value of 0.034 lb ft^{-2} s^{-1} (0.17 kg m^{-2} s^{-1}), which

corresponds to a heat flux of about 26,954 BTU hr^{-1} ft^{-2} (85 kW/m^2). This value was obtained during the Burro tests.

6.2.1.4. LNG Pool Spread on Water

Early spread models were based on the steady state Bernoulli equation and axisymmetric spread on water (Enger and Hartman, 1972a; Gideon and Putnam, 1977). With this approach, spread is driven strictly by gravity, and the rate is given as a function of pool height only. Raj and Kalelkar (1973) derived a different spreading relationship by equating gravitational force and inertial resisting force. Otterman (1975) derived the spread model based on the oil spill experiment data, and concluded that those three methodologies yield almost identical predictions for the maximum pool radius.

Bosch and Weterings (1997) employed a method based on self-similar solutions of the shallow water equations and lubrication theory. This method is called Webber's method. This approach accounts for the resistance to spreading as a result of turbulent or laminar friction. Because Webber's method has a much sound theoretical basis and accounts for friction effects, a majority of researchers believe that it is more realistic than other simpler models that ignore friction effects; thus, FERC recommended using Webber method.

Although wave action is expected to affect both the shape and rate of spread of LNG on water, little effort has been expended in defining this relationship. Quest (2003) has made some initial attempts to quantify this effect, but the lack of experimental data has made validation difficult.

6.2.1.5. Flammable Vapor Dispersion

Modeling of flash fires is primarily a matter of applying a dispersion model. The most well known codes to model LNG dense gas dispersion are FEM3, SLAB, HEGADAS and DEGADIS. FEM3 is based on Navier-Stokes, and the model computationally solves time-averaged, three-dimensional, turbulent transport equations that come from conservation of mass, species, momentum and energy balances. The other three models, SLAB, HAGADAS and DEGADIS, are one-dimensional integral models, and they use similar profiles that assume a specific shape for the crosswind profile of concentration and other properties. The downwind variation of spatially averaged crosswind values is determined by using the conservation equations in the downwind direction only.

In 1992, the American Gas Association, under provisions of 49 CFR 193, petitioned the Department of Transportation to specify the use of DEGADIS for calculation of the gas dispersion protection zones in the regulation. FERC also recommended using DEGADIS to model the LNG vapor cloud dispersion process.

6.2.2. Hazard Assessment Methodology

6.2.2.1. FERC Models for Assessing LNG Carrier Spills on Water

The orifice model was employed by FERC (2004) to assess the LNG release process. This model calculates the flow from a circular hole in the side of a cargo tank that allows the LNG to flow directly from the tank into the water, using the following equation:

$$Q = C_d \pi \rho_l R^2 \sqrt{2gH} \tag{6.4}$$

where

Q = mass flow rate, lb s^{-1}

C_d = discharge or orifice coefficient

ρ_l = density of LNG, lb f^3

R = radius of hull breach, ft

H = static head above hull breach, ft

g = gravitational acceleration, 32.2 ft s^{-2}

It is worthwhile to note that static head consists of both the liquid height and the ullage pressure. For the fixed volume release from a cargo tank, the flow rate will drop as the liquid level above the breach drops. The discharge orifice coefficient is assumed to be 0.65 as recommended by FERC.

As described in the background, Webber's method was recommended by FERC to model the LNG pool spread. A value of 85 kW/m^2 for heat flux was adopted by FERC. The DEGADIS model was employed by FERC to assess the vapor dispersion process. For flash fires, the level of concern is typically defined as the Low Flammability Limit (LFL) for the substance. The downwind distance to LFL and the time to reach LFL were derived from the DEGADIS model.

6.2.2.2. FERC Scenario for Cargo Tank Vapor Dispersion

The base scenario modeled by FERC is:

- **LNG properties**:

  LNG composition: Methane

  LNG density: 422.5kg m^{-3} (26.38 lb ft^{-3})

- **Release scenario**:

  Volume of vessel: 883,000 ft^3 (25,000 m^3)

  Percent of cargo tank volume spilled: 50%

  Total spill quantity: 441,500 ft^3 (12,500 m^3)

  Hole diameter: 3.3 ft (1 m)

  Initial liquid height above hole: 43 ft (13 m)

  Pool shape: semi-circular

- **Environmental conditions**:

  Air temperature: 71 °F (22 °C)

  Relative humidity: 70%

  Wind speed: 6.7 mph (3.0 m s^{-1}) and 4.5 mph (2.0 m s^{-1})

  Pasquill-Turner stability class: D and F

  Surface roughness: 0.03 ft (0.01 m)

  Averaging time: 1 min

- **Heat transfer parameters**:

  Heat transfer parameters:

  Film boiling heat flux to pool: 26,900 BTU hr^{-1} ft^{-2} (85 kW/m^2)

Evaporation mass flux: 0.034 lb ft^{-2} s^{-1} (0.17 kg m^{-2} s^{-1})

The results of LNG pool spreading and vapor dispersion for the above scenario were reported by FERC as shown in Table 6.2.

Table 6.2

Computed results using FERC methodology for LNG release base scenario

PARAMETERS	FERC RESULTS
Initial spill rate	7,600 lb/s (3,400 kg/s)
Total spill duration	51 min
Maximum pool radius	418 ft (127 m)
Wind speed and stability class	6.7 mph (3.0 m/s) and D stability
Downwind distance to LFL	6,500 ft (2,000 m)
Time LFL reaches maximum distance	16 min
Wind speed and stability class	4.5 mph (2.0 m/s) and F stability
Downwind distance to LFL	11,000 ft (3,400 m)
Time LFL reaches maximum distance	29 min

6.2.2.3. WinFERC Model for Scenario Assumptions Sensitivity Analysis

The FERC/ABS spill/spread models are employed in this paper to analyze the sensitivity of scenario assumptions to the LNG hazard assessment (Qiao, West, Mannan, Johnson, and Cornwell, 2006). A Fortran program was developed to compute the spill

and spread of LNG on water and to produce a suitable input file for use with the DEGADIS vapor dispersion model. The Fortran program was carefully tested against the results produced by the MathCad version of the FERC/ABS report. This model, which will be referred to as WinFERC, was used to perform the portions of the parametric study dealing with the spill and spread of LNG on water. The WinFERC interface is shown in Figure 6.4.

Figure 6.4. WinFERC model interface.

The vapor dispersion process is then modeled by DEGADIS model, with the data provided by WinFERC as input to DEGADIS.

The effects of different scenario assumption variables on the LNG hazard assessment results, especially the hazardous vapor cloud dispersion, are analyzed by using WinFERC and DEGADIS models. Those affecting variables include breach

diameter, ullage pressure, weather conditions and surface roughness. The base scenario to model in this paper is the same as the FERC scenario as described earlier. During the sensitivity analysis processes, almost all the variables will be the same as those in the base FERC scenario, and change is only allowed for the variable that is under sensitivity analysis, or unless specified.

6.2.3. Sensitivity of Scenario Assumptions to the LNG Hazard Assessment

6.2.3.1 Breach Diameter

The results shown in Figures 6.5 and 6.6 illustrate the effects of breach diameter on the release results, including the time to empty vessel and pool size. The time to empty vessel decreases dramatically with the increase of hole diameter as shown in figure 6.5. In figure 6.6, initially the LNG pool radius increases in correlation with increases in the breach diameter, but the pool radius reaches an asymptotic value when the breach diameter is larger than 5 m.

Figures 6.7 and 6.8 also show the effect of breach diameter on the LNG vapor dispersion process at two sets of atmospheric conditions. The distance to reach LFL follows a similar curve as the LNG pool radius.

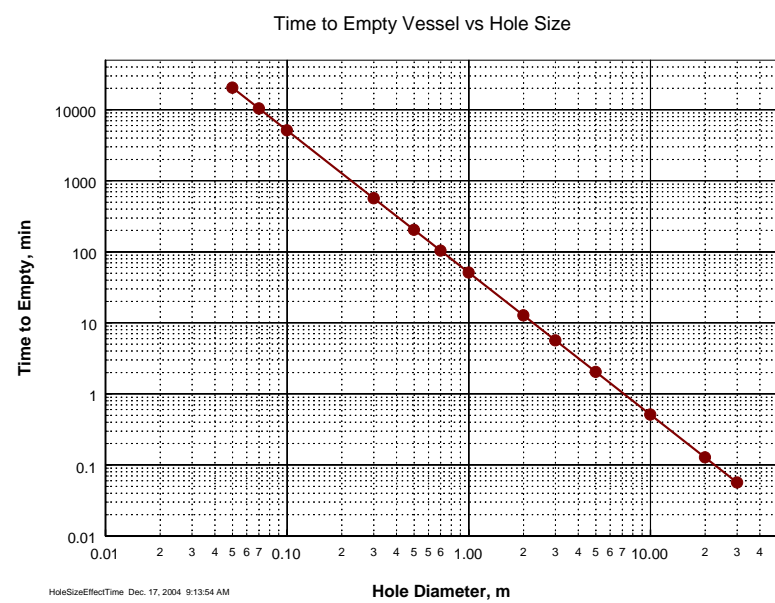Time to Empty Vessel vs Hole Size

Figure 6.5. Time to empty vessel vs. hole diameter.
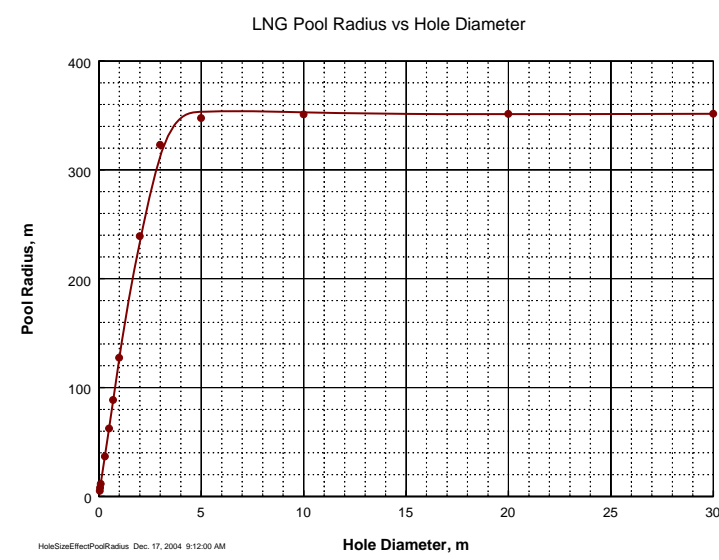
LNG Pool Radius vs Hole Diameter

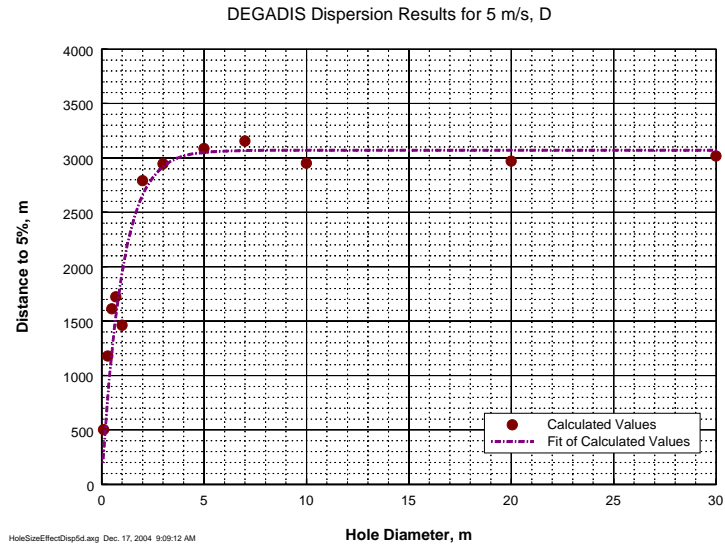Figure 6.6. LNG pool radius vs. hole diameter.

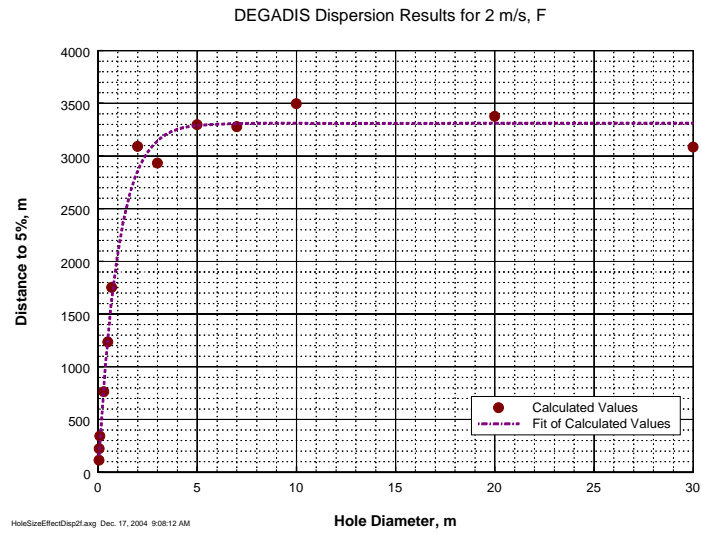Figure 6.7. LNG vapor dispersion results at 5m/s wind speed and D stability.

Figure 6.8. LNG vapor dispersion results at 2m/s wind speed and F stability.

6.2.3.2. Wind Stability Class and Wind Speed

Figures 6.7 and 6.8 illustrate that the LFL downwind distance is increased when the wind stability class changes from D to F and the wind speed decreases from 5 m s^{-1} to 2 m s^{-1}. When the wind stability class transforms from neutral class D to moderately stable class F, the atmosphere turbulence tends to be weak, so that the LFL downwind distance increases. The decrease of wind speed also diminishes the turbulence level to some degree, so the LFL downwind distance will be increased. The difference in Figure 6.7 and 6.8 presents the combined effects of wind stability and speed on the LNG vapor dispersion process. It is interesting to note that, although the distances to the LFL at small breach diameters are different, the LFL distances for breach diameters above five meters are similar.

6.2.3.3. Cargo Tank Ullage Pressure

The cargo tank ullage pressure in an LNG tanker is usually less than 2 psig. For sensitivity assessment purpose, the maximum ullage pressure considered here is 4 psig. According to Equation (6.4), the spill rate is proportional to the square root of static head above the breach, thus the time to empty vessel would be decreased with an increase of ullage pressure, as shown in Figure 6.9. Figure 6.10 illustrates that the pool radius is enlarged with the increase of ullage pressure. The vapor dispersion process is also influenced by the change of ullage pressure. As shown in Figure 6.11, when the hole diameter is 1 m, the LFL downwind distance is increased as the ullage pressure is increased from 0 psig to 2 psig, but LFL downwind distance is not strongly affected

when ullage pressure is higher than 2 psig. For LNG released from 5 m diameter hole,

the LFL downwind distance remains constant with the increase of ullage pressure.
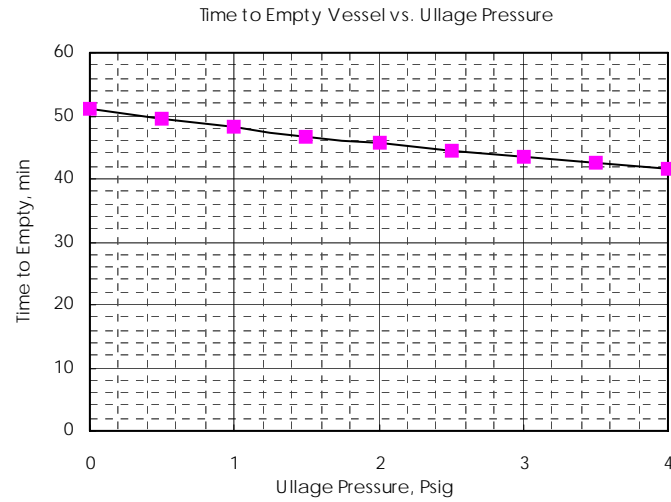
Figure 6.9. Time to empty vessel for spilled LNG vs. ullage pressure.
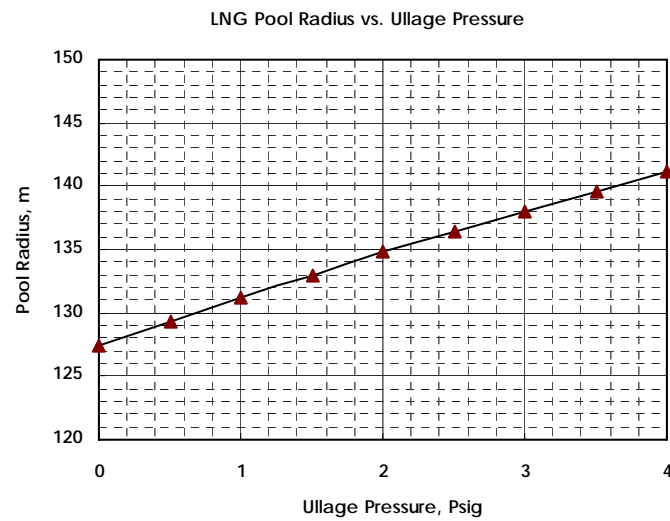
Figure 6.10. LNG pool radius vs. ullage pressure.
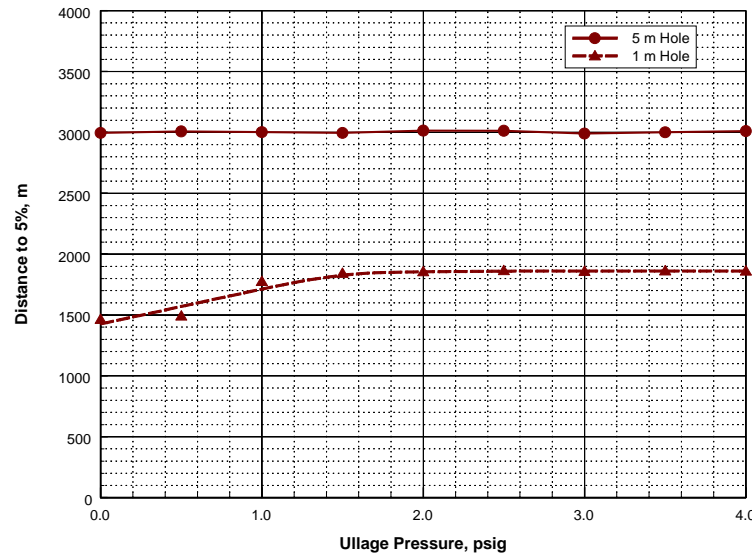
Figure 6.11. LNG vapor dispersion vs. ullage pressure.

6.2.3.4. Surface Roughness

Figure 6.12 illustrates the effect of surface roughness on the dispersion. When the surface roughness is high, the LFL downwind distance is decreased with the increase of surface roughness. However, when the surface roughness is less than 0.003 m, there is little change in the distance to reach the LFL. We could expect that the increase in surface roughness would increase the degree of atmospheric turbulence near grade, which would decrease the downwind extent of vapor clouds that would form and disperse near grade. Such kind of influence is similar to that of atmospheric stability. Based on the DEGADIS model calculations, the initial gravity that induced spreading of

the heavy LNG vapors might overwhelm the changes in surface roughness below a roughness level of 0.003 m.

Effect of Surface Roughness on Dispersion Distances (5 m/s, D)
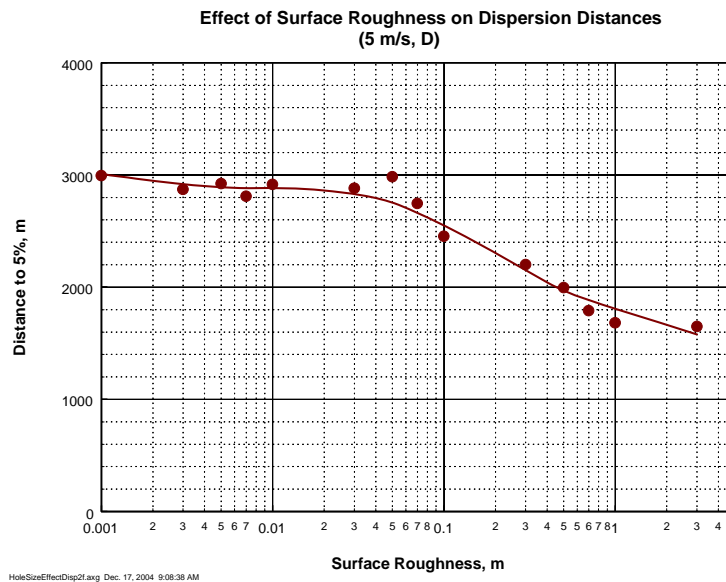
Figure 6.12. Effect of surface roughness on dispersion distances.

6.2.3.5. Tank Configuration

A typical membrane square tank and a typical Moss spherical tank were analyzed to determine the effect of tank configuration on the spillage process. The implicit tank configuration in most consequence analysis software is cylinder or square, with a constant cross sectional area. The spill of LNG from a spherical tank can not be assessed by this kind of software. The commercial program MatLab was used to compare the spillage difference for a membrane square tank and a Moss spherical tank.

The typical modern size of LNG vessels is 135,000 m^3 in 4-6 cargo tanks, so here a cargo tank volume of 25,000 m^3 is assumed. The diameter is 36.28 m for a Moss spherical tank, and the height is 29.24 m for a membrane square tank. The breach is assumed to be 30% from the bottom of each tank, resulting in an initial liquid level of 10.88 m above tank bottom for a spherical tank and 8.77 m for a square tank. So the initial liquid height above breach hole is 25.4 m for a spherical tank and 20.47 m for a square tank. By running the MatLab program, the spill rates versus time for these two kinds of tanks are modeled, and the results are shown as Figure 6.13.

The initial spill rate is higher for a spherical tank because of its higher static head above hull breach. The spill process is determined by the tank geometry. The spill rate decreases linearly with time for a square tank, while for a spherical tank, the spill rate decreases very quickly at the beginning, and decreases a little slowly after that.

Spillage Rate vs. Time for Spherical Tank and Square Tank
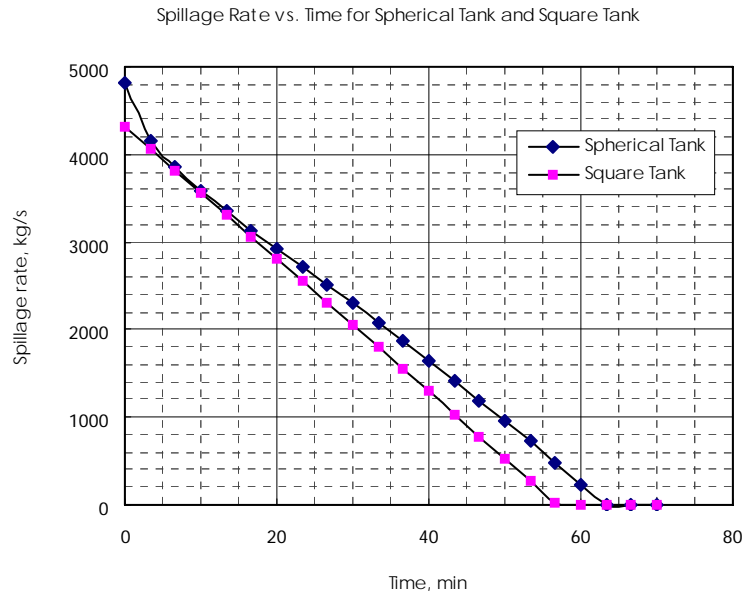
Figure 6.13. Spillage rate vs. time for spherical tank and square tank.

6.2.4. Discussion

6.2.4.1. Model Validation against Available Experimental Test Data

Experimentation has generally been performed on a fairly small scale. The largest spillage volume to date was 66.4 m^3, which was also the largest scale tested during Falcon tests in 1987 (Shin, Meroney, and Neff, 1991). However, the consequence models validated with these small scale experimental data are being used for spill scenarios of 25,000 m^3 and larger. Jones and McGugan (1978) proposed that the minimum area required to enable a spill to be scaled up reliably to the dimensions of a realistic spill of tens of meters across is 1 m^2. The scale up factor of more than 350 to 1

(25,000 m^3 to 66.4 m^3) in LNG spill modeling process has left the scale up process under question for its reliability.

As a number of experiments were performed at small scale and their relevance to real-life large spills is uncertain, a reasonable scale up factor needs to be determined and evaluated so that it is possible to test models and, subsequently, to permit any necessary modification based on the data gathered from a series of carefully controlled experiments that are at an adequately large scale.

6.2.4.2. LNG Spillage Process

It can be seen from Equation (6.4) that the mass flow rate is the direct function of the square root of the static head, the area of the breach hole, and the data of discharge coefficient.

A value of 1.0 for the discharge coefficient, which is for ideal frictionless case, is not reasonable in the case of a rough, irregular hole that would be expected in a spill from an LNG carrier. The International LNG Alliance and the International Gas Union suggested a value of 0.65, and the Center for LNG suggested a reasonable, conservative estimate of discharge coefficient ranges from 0.6 to 0.8, thus FERC recommended 0.65, which can be defended as a reasonable estimate.

In this paper, a hole diameter of 1 m is selected as the base release scenario. Pitblado, et. al. (2004) at DNV proved that 0.25 m will be a credible hole diameter for a puncture type event, the maximum credible hole from accidental operational events will be 0.75 m, and 1.5 m from terrorist events. With the hole size changing in a wider range,

from 0.5 m to 30 m, Figure 6.6 illustrates that the time to empty the vessel is changed linearly with the logarithm of the hole size as determined by Equation (6.4).

The static head incorporates both the liquid height above the breach and the ullage pressure in the tank. The ullage pressure is dependent on the LNG composition and cargo tank design, and can vary from about atmospheric pressure to about 2 psig. The time to empty the vessel is approximately a linear function of the ullage pressure as shown in Figure 6.9. The assumed location of the breach opening will affect the time to empty the vessel in the same way, since the breach location will determine the liquid height given the fixed tank volume and configuration. Most analysts assume the breach occurs at the waterline for modeling purpose.

The tank configuration is not a direct factor in computing the release rate in Equation (6.4), but it does have an effect on the release scenario as shown in Figure 6.13. The spill rate can be expressed as:

$$Q = \rho \times dV/dt = \rho \times A \times dh/dt \tag{6.5}$$

In Equation (6.5) A is uniform for the square tank, while for a spherical tank, A is changing during the whole release process. The cross area is so small at the top of the spherical tank that the height drops rapidly initially and the spill rate declines quickly at the beginning. The cross area in the middle of the tank becomes larger and changes less, so the spill rate decline more slowly than the beginning.

6.2.4.3. Sensitivity of Pool Spreading Process

The LNG will spread on the water and continuous evaporation will take place if LNG spillage occurs. The LNG pool will continue to spread until the minimum layer thickness corresponding to the maximum pool diameter is reached. The vapor production will increase during the spreading simply by virtue of the increasing area of the evaporating liquid. This will reach a maximum when the pool has reached a size corresponding to the equilibrium LNG quantity.

Otterman (1975) described the spreading process for an axi-symmetric pool through the following equation:

$$\frac{dr}{dt} = \left[2g\Delta_1 h\right]^{\frac{1}{2}} \tag{6.6}$$

Where

$$h = \frac{V}{\pi r^2}$$

V = LNG volume on water, ft^3

r = pool radius, ft

$$\Delta_1 = \frac{\rho_1 - \rho}{\rho_1}$$

ρ_1 = density of water, lb f^3

ρ = density of LNG, lb f^3

g = gravitational acceleration, 32.2 ft s^{-2}

Through this equation, spread is driven only by gravity and the pool reaches the maximum with the pool layer thickness at the minimum. Webber's method accounts for the friction effects, and the maximum pool size should occur when the pool is in the minimum thickness and the gravity driven force and the turbulent or laminar resistance force are in equilibrium.

For a long term release, the pool will spread until the evaporation rate matches the rate of spillage. Thus the detailed modeling of pool spreading is not necessary. The pool area can be estimated from the spill rate divided by the evaporation rate per unit area.

The change of maximum pool size with the hole size in Figure 6.6 can be explained by the combined effects of long term release scenario and instantaneous spill scenario. When the breach hole diameter is less than 4 m, the LNG spillage can be viewed as long term release process. With the hole size becoming larger, the spill rate is higher, resulting in a larger pool. When the breach hole diameter is larger than 4 m, the spill process can be simplified as instantaneous spill, and the maximum pool size is independent of the hole size.

As illustrated in Figure 6.9, when the tank ullage pressure is less than 4 psig and the breach hole diameter is 1 m, the time to empty the vessel declines linearly with the ullage pressure. The spill process can be assumed as long term release when tank ullage pressure is less than 4 Psig. The increment of the ullage pressure increases the spill rate, so the maximum pool size increases with the increasing of ullage pressure accordingly.

6.2.4.4. Sensitivity of Vapor Dispersion Process

Blackmore, Eyre and Summers (1982).found that plume dispersion behavior is dependent on source conditions, especially for continuous LNG spills. The results illustrated in Figures 6.7 – 6.11 prove that the hole size and ullage pressure affect the dispersion process.

Increasing breach hole size and ullage pressure has similar effects in enlarging the spreading pool. A larger pool size means that the overall evaporation rate will increase. As the evaporation rate increases, the downwind distance to a given concentration increases. When the increase of the spill rate can not enlarge the pool size and the subsequent evaporation rate, the downwind distance to LFL will not change any more as shown in Figures 6.7, 6.8 and 6.9.

The wind stability class is an indicator of atmosphere turbulence level. A higher turbulence level will increase the dilution of the LNG plume with the air. So the downwind distance to LFL will increase when the turbulence level degrades. The decreases of the surface roughness and the wind speed have the similar effects on the vapor dispersion process. In Maplin Sands tests, liquid propane was continuously released from a tank at an average spill rate of 2.3 m^3/min. When the win speed is 5.5 m/s and 3.8 m/s, the observed dispersion distances to LFL were 215 m and 400 m, respectively (Blackmore, Eyre and Summers, 1982). The same trend has been found in our model results shown in Figures 6.7 and 6.8.

6.2.5. Conclusions

When an LNG cargo tank is ruptured, the LNG flows out of the hole onto the surface of water, in an amount and at a rate depending on the tank size, dimension, location of the rupture and ullage pressure. The spilled fluid spreads on the water surface, eventually evaporating entirely, mixing with air and dispersing downwind.

The FERC modeling algorithms were employed in this paper to analyze the LNG spillage consequences. The computed results illustrate that the changes of breach size and ullage pressure will change not only the spill duration and pool size, but also the dispersion process. Variations of tank configuration affect the spill process. The wind stability, wind speed and surface roughness affect the vapor dispersion process for breach diameters less than 4 m, but have a smaller effect on spills from breach diameters larger than 5 m.

CHAPTER VII

CONCLUSIONS AND RECOMMENDATIONS

7.1. Conclusions

This research is aimed at developing a practical and efficient TRA methodology to support the operations of HazMat transportation. A quantitative risk assessment methodology is provided in this dissertation to measure the risk profile. The basic idea of the proposed methodology is to capture the matching of data/databases availability with TRA techniques and to set up an applicable framework to assess transportation risk step by step.

Risk components, including incident frequency, release probability, consequence scenario, and fatality, are carefully observed to determine their contributing factors and to figure out the proper data/databases for analysis. Given the conditions where no enough data exist, some mathematical methods including fuzzy logic are employed to incorporate human's linguistic information. Then these components are assessed based on the analysis on available data/databases, commercially available software, and expert knowledge. Mathematical models and risk analysis techniques like ETA are employed for each risk component assessment.

The measure of the overall risk level considers the interaction between the transportation network, the vehicle or traveling risk source, and the impact area.

Numerical models are presented to measure individual risk and societal risk caused by HazMat transportation.

By matching the available data with the model set up, the TRA methodology can be applied directly in the decision support system to guide the operations of HazMat transportation.

The overall methodology is developed from available data/databases, which makes it an applicable and accountable tool in the decision support system to guide the operations of HazMat transportation. This generic method could be applied for most of TRA within the scopes defined therein. Decision makers could modify the methodology when dealing with different HazMat. The methodology could be simplified or elaborated further based on the requirement of users.

7.2. Recommendations

This work is proposed based on the analysis on available data/databases. An abundant supply of data/database will facilitate the improvement of accuracy and practicality of our methodologies. In recent years, especially after September 11, 2001, fewer institutes, agencies, or organization would like to disclose incident data to the public, even to our researcher. It is recommended that institutes associated with HazMat transportation (e.g., American Petroleum Institute and Chlorine Institute) grant the accessibility to transportation incident databases, so that the changes in HazMat transportation in recent years could be tracked, and TRA methodology can be proposed with a solid background.

GIS has proved to be helpful in TRA. Many environmental features necessary for TRA are attainable in GIS, but some important features may not be there. For example, the number of highway lanes, which is critical to the risk measurement, could not be found in GIS. It also happens to wind direction probability and other parameters. More effort could be devoted to collecting data on crucial parameter outside of GIS and merging that information with GIS. By this way, all the environmental information needed for TRA can be pulled out directly from GIS, and the TRA process will be more efficient.

Our methodology is developed to assess the transportation risk over a year. However, the risk for any certain given transportation scenario should be analyzed to take account of the effect of time varying parameters. Our model for incident frequency assessment has considered the time varying parameters like weather and driver experience. More work needs to be performed to assess other risk components taking into consideration the effect of time varying parameters.

If more incident data are accessible, e.g., transportation institutes of all states could standardize their data collection and provide the incident data on more highways, a global model could be built in the similar way as presented in this dissertation. A user friendly computer program could then be compiled. By coupling this model with a more powerful GIS, the risk associated with any route could be easily assessed.

In our optimum routing models, it has been proved that TRA is important in guiding the route selections of HazMat transportation. Transportation decision support system is a complex system. More actions could be facilitated by utilizing TRA results.

Further research is recommended to explore the application of TRA in emergency response and other actions made in decision support system to mitigate transportation hazard and ensure a safer environment.

REFERENCES

Abkowitz, M. P. and Cheng, P.D-M (1988). Developing a risk/cost framework for routing truck movements of hazardous materials, *Accident Analysis and Prevention*, *20*(1), 39-51.

ABS Consulting, Inc. (ABS) (2004). *Consequence assessment methods for incidents involving releases from liquefied natural gas carriers*, Report for the Federal Energy Regulatory Commission. http://www.ferc.gov/industries/gas/indus-act/lng-model.pdf.

Advisory Committee on Dangerous Substances (1991). *Major hazard aspects of the transportation dangerous aubstances*. London: Health and Safety Commission.

Anderson, R. and Armstrong, D. (1973). Comparison between vapor explosion models and recent experiment results. *Fourteenth National Heat Transfer Conference*, Atlanta, GA, 1-62.

Ang, J. B. (1989). *Development of a systems risk methodology for single and multimodal transportation systems,* Final Report. Washington, DC: Office of University Research, US DOT.

Atallah, S. (1997). *Rapid phase transitions,* GRI-92/0533. Chicago, IL: Gas Research Institute.

Battelle (2001). *Comparative risks of hazardous materials and non-hazardous materials truck shipment accident/Incident*. Washington, DC: Federal Motor Carrier Safety Administration, US DOT.

Baumeistor, K., Hendrick, R., and Hamill, T. (1966). *Metastable Leidenfrost states,* NASA Technical Note D-3226. Cleveland, OH: Lewis Research Center.

Blackmore, D., Eyre, J. and Summers, G. (1982). Dispersion and combustion behavior of gas clouds resulting from large spillages of LNG and LPG onto the sea. *Transactions of the Institute of Marine Engineers*, *94*, paper 29.

Bosch, C. and Weterings, R. (1997). *Methods for the calculation of physical effects,* TNO yellow book (3rd edition*)*. The Netherlands: The Hague.

Brown, D. and Dunn, W. (2000). *A national risk assessment for selected hazardous materials in transportation,* ANL/DIS-01-1. Argonne, IL: Argonne National Laboratory.

Bubbico, R., Cave, S., and Mazzarotta, B. (2002). A GIS-supported transportation risk analysis approach. *17th International Conference and Workshop*, Center for Chemical Process Safety, American Institute of Chemical Engineers, 361-374.

Bubbico, R., Cave, S., and Mazzarotta, B. (2004a). Risk analysis for road and rail transport of hazardous materials: A GIS approach. *Journal of Loss Prevention in the Process Industries, 17*, 483-488.

Bubbico, R., Cave, S., and Mazzarotta, B. (2004b). Risk assessment for land transportation of hazardous materials in Italy. *11th International Symposium: Loss Prevention and Safety Promotion in the Process Industries*, Praha, Czech Republic, 4297-4304.

Burgess, D., Biordi, J. and Murphy, J. (1972). *Hazards of spillage of LNG into water,* PMSRC Report No. 4177. Washington, DC: Bureau of Mines, US Department of the Interior.

Burgess, D., Murphy, J. and Zabetakis, M. (1970). *Hazards associated with the spillage of liquefied natural gas on water,* R#17448. Washington, DC: Bureau of Mines, US Department of the Interior.

California Energy Commission (2003). *Liquefied natural gas in California: History, risks, and sitting.* http://www.energy.ca.gov/reports/2003-07-17_700-03-005.PDF.

Cameron, A. and Trivedi, P. (1998). *Regression analysis of count data.* Cambridge, UK: Cambridge University Press.

Center for Chemical Process Safety (CCPS) (1995). *Guidelines for chemical transportation risk analysis.* New York: American Institute of Chemical Engineers.

Center for Chemical Process Safety (CCPS) (2000). *Guidelines for chemical process quantitative risk analysis.* New York: American Institute of Chemical Engineers.

Chlorine Institute (2003). *Letter from Chlorine Institute to Yuanhua Qiao at Mary Kay O'Connor Process Safety Center.* Arlington, VA.

Cleaver, P., Dahlsveen, J, and Heiersted, R. (1998). Rapid phase transition of LNG. *Twelfth International Conference & Exhibition on Liquefied Natural Gas,* Perth, Australia. 6.5-1—6.5-13.

Cook, M. (1958). *Science of explosives.* New York: Reinhold Publishing Co.

Crane, R. K. (2005). *Rain rates.*

http://my.athenet.net/~multiplx/cgi-bin/pics/rain_rate.html.

Crowl, D. A. (2002). *Chemical process safety: Fundamentals with applications*. NJ: Prentice-Hall.

Enger, T. and Hartman, D. (1972a). Explosive boiling of liquefied gases on water, *Conference on LNG Importation and Terminal Safety,* Boston, 5-24.

Enger, T. and Hartman, D. (1972b). Rapid phase transformation during LNG spillage on water. *Third International Conference on Liquefied Natural Gas,* Washington, D. C. Section v, Paper 2.

Erkut, E. and Ingolfsson, A. (2005).Transportation risk models for hazardous materials: revisited. *Operations Research Letters*, *33*, 81-89.

Erkut, E., and Verter, V. (1995). A framework for hazardous materials transport risk assessment. *Risk Analysis, 15*(5), 589-601.

Erkut, E. and Verter, V. (1998). Modeling of transport risk for hazardous materials, *Operation Research*, *46*(5), 625-642.

Fabiano, B., Curro, F., Palazzi, E., and Pastorino, R. (2002). A framework for risk assessment and decision-making strategies in dangerous good transportation, *Journal of Hazardous Materials, 93*, 1-15.

Fauske, H. (1974). Some aspects of liquid-liquid heat transfer and explosive boiling. *Topical Meeting of Fast Reactor Safety,* Beverly Hills, CA, 992-1005.

Fay, J. (2003). Model of spills and fires from LNG and oil tankers. *Journal of Hazardous Materials*, *96*(2-3), 171-188.

Federal Energy Regulatory Commission (FERC) (2004). *Notice of availability of staff's responses to comments on the consequence assessment methods for incidents*

involving releases from liquefied natural gas carriers, Docket No. AD04-6-000. Washington, DC: Office of Energy Project.

Fedra, K. (1998). Integrated risk assessment and management overview and state of the art. *Journal of Hazardous Materials*, *61*, 5-22.

Feldbauer, G., Heigl, J., McQueen, W., Whipp, R. and May, W. (1972). *Spills of LNG on water-vaporization & downwind drift of combustible mixtures,* Report No. EE61E-72. Linden, New Jersey: Esso research & engineering company.

Gabillard, M., Dahlsveen, J. and Cronin, P. (1996). Rapid phase transition of liquefied gas. *European Applied Research Conference, Trondheim, Norway*.

Garland, F. and Atkinson, G. (1971). *The interaction of liquid hydrocarbons with water,* Report on contract No. DOT-CG-11, 911A. College Park, MD: Maryland University.

Genco, J. and Lemmon, A. (1970). Physical explosions in handling molten slags and metals", *American Foundry Society Transactions*, *57*, 317-323.

Gideon, D. and Putnam, A. (1977). Dispersion hazard from spills of LNG on land and on water. *Cryogenics*, *17*(1), 9-15.

Goldwire, H., Rodean, H., Cederwall, R., Kansa, E., Koopman, R., McClure, J., McRae, T., Morris, L., Kamppinen, L., Kiefer, R., Urtiew, P. and Lind, C. (1983). *Coyote series data report: LLNL/NWC 1981 LNG spill tests, dispersion, vapor, and rapid-phase-transition,* UCID-19953. Livermore, CA: Lawrence Livermore National Laboratory.

Harris, C., Boone, J., Irving, G., Hunter, P., and Solis, T (1992). Personal emails from witnesses and investigators.

Harwood, D. and Russell, E. (1990). *Present practices of highway transportation of hazardous materials,* FHWA/RD-89/013. Washington, DC: Federal Highway Administration, US DOT.

Harwood, D. W., Viner, J. G., and Russell, E. R. (1993). Procedure for developing truck accident and release rates for HAZMAT routing. *Journal of Transportation of Engineering-ASCE*, *119*(2), 189-199.

Iakovou, E. T. (2001). An interactive multiobjective model for the strategic maritime transportation of petroleum products – risk analysis and routing. *Safety Science*, *39*, 19-29.

Jones, C. and McGugan, P. (1978). An investigation into the evaporation of volatile solvents from domestic waste. *Journal of Hazardous Materials, 2*(3), 227-233.

Kara, B., Erkut, E. and Verter, V. (2003). Accurate calculation of hazardous materials transportation risks. *Operations Research Letters, 31*, 285-292.

Katz, D. (1972). Superheat-liquid explosions. *Chemical Engineering Progress*, *68*(5), 68-69.

Katz, L. and Sliepcevich, C. (1971). LNG/water explosions: cause and effect. *Hydrocarbon Processing*, *50*(11), 240-244.

Koopman, R, Cederwall, R., Ermak, D., Goldwire, Hogan, W., McClure, J., McRae, T., Morgan, D., Rodean, H. and Shinn, J. (1982). Analysis of Burro series 40-m^3 LNG spill experiments. *Journal of Hazardous Materials*, *6*(1-2), 43-83.

Leonelli, P., Bonvicini, S., and Spadoni, G. (1999). New detailed numerical procedures for calculating risk measures in hazardous materials transportation. *Journal of Loss*

Prevention in the Process Industries, *12*, 507-515.

Lepofsky, M., Abkowitz, M., and Cheng, P. (1993). Transportation hazard analysis in integrated GIS environment. *Journal of Transportation of Engineering-ASCE*, *119*(2), 239-254.

Lipsett, S. (1966). Explosions from molten materials and water. *Fire Technology*, *2*, 118-126.

List, G. and Mirchandani, P. (1991). An integrated network/planar multiobjective model for routing and siting for hazardous materials and wastes. *Transportation Science*, *25*(2), 146-156.

LNG Research Center, MIT (1977). *Flameless vapor explosions final report contract BR87-5*. Washington, DC: American Gas Association.

McRae, T., Goldwire, H., and Koopman, R. (1984). *Analysis of large-scale LNG/water RPT explosions,* UCRL-91832. Livermore, CA: Lawrence Livermore National Laboratory.

Nakanishi, E. and Reid, R. (1971). Liquid natural gas-water reactions. *Chemical Engineering Progress*, *67*(12), 36-41.

National Climate Data Center (2005). *Rainfall statistics*.

http://www.ncdc.noaa.gov/oa/climate/online/ccd/nrmpcp.txt.

National Propane Gas Association (NPGA) (2005). *Consumer information*.

http://www.npga.org/i4a/pages/index.cfm?pageid=462.

Nedelka, D., Sauter, V., Goanvic, J. and Ohba, R. (2003). Last developments in rapid phase transition knowledge and modeling techniques. *2003 Offshore Technology Conference,* Houston, OTC 15228:1-7.

Office of Hazardous Materials Safety (OHMS) (2005a). *CFR 49*. http://www.myregs.com/dotrspa/.

Office of Hazardous Materials Safety (OHMS) (2005b). *Hazardous materials transportation guides*. http://ntl.bts.gov/DOCS/hmtg.html.

Office of Hazardous Materials Safety (OHMS) (2005c). *Reported hazardous materials incident*. http://hazmat.dot.gov/enforce/spills/spills.htm

Opschoor, G. (1980). Spreading and evaporation of LNG-spills and burning LNG-spills on water. *Journal of Hazardous Materials*, *3*(3), 249-266.

Otterman, B. (1975). Analysis of large LNG spills on water. 1. Liquid spread and evaporation. *Cryogenics*, *15*(8), 455-460.

Parfomak, P., (2003). *Liquefied natural gas (LNG) infrastructure security: Background and issues for congress,* CRS Report for Congress. http://www.energy.ca.gov/lng/documents/CRS_RPT_LNG_INFRA_SECURITY.PDF.

Pitblado, R., Baik, J., Hughes, G., Ferro, C. and Shaw, S. (2004). Consequences of LNG marine incidents. *19th International Conference and Workshop*, Center for Chemical Process Safety, American Institute of Chemical Engineers.

Porteous, W., and Reid, R. (1976). Light hydrocarbon vapor explosions. *Chemical Engineering Progress*, *72*(5), 83-89.

Purdy, G. (1993). Risk analysis of the transportation of dangerous goods by road and rail, *Journal of Hazardous Materials*, *33*, 229-259.

Qiao, Y., West, H., Mannan, M., Johnson, D., and Cornwell, J. (2006). Assessment of the effects of release variables on the consequences of LNG spillage onto water using FERC models. *Journal of Hazardous Materials*, in press.

Quest Consultants, Inc. (Quest) (2003). Modeling LNG spills in Boston Harbor, *Letter from John Cornwell of Quest to Don Juckett of the U. S. Department of Energy; and letter from John Cornwell of Quest to Clifford Tomaszewski of the Office of Natural Gas & Petroleum Import & Export Activities. Norman, OK.*

Raj P. and Kalelkar, A. (1973). Fire hazard presented by a spreading burning pool of liquefied natural gas on water. *Combustion Institute (USA) Western States Section Meeting,* El Segundo, CA.

Rausch, A. and Levine, A. (1973). Rapid phase transformations caused by thermodynamic instability in cryogens. *Cryogenics*, *13*(4), 224-229.

Rhyne, W. (1994). *Hazardous materials transportation risk analysis: Quantitative approaches for truck and train*. New York: Van Nostrand Reinhold.

Rowe, W. D. (1983). *Risk assessment procedures for HazMat transportation*. Transportation Research Board national cooperative highway research program synthesis of highway practice report 103. Washington, D.C.: Transportation Research Board, National Research Council.

Sandia National Laboratories (Sandia) (2004). *Guidance on risk analysis and safety implications of a large liquefied natural gas (LNG) spill over water,* SAND2004-

6258. Albuquerque, NM.

Shin, S., Meroney, R. and Neff, D. (1991). *LNG vapor barrier and obstacle evaluation: Wind-tunnel simulation of 1987 Falcon spill series,* Final report, GRI-91/0219. Chicago, IL: Gas Research Institute.

Spadoni, G., Leonelli, P., Verlicchi, P., and Fiore, R. (1995). A numerical procedure for assessing risks from road transport of dangerous substances. *Journal of Loss Prevention in Process Industry, 8*(4) 245-252.

US Census Bureau (2004). *2002 commodity flow survey*. http://www.census.gov/prod/ec02/ec02tcf-tx.pdf

US Department of Transportation (US DOT) (1998). *Biennial report on HazMat transportation report*. http://hazmat.dot.gov/pubs/biennial/96_97biennial.rpt.pdf

US Department of Transportation (US DOT) (2005).*Incidents, deaths, and injuries by mode and incident year*. http://hazmat.dot.gov/pubs/inc/data/tenyr.pdf.

Vayiokas, N. and Pitsiava-Latinopoulou, M. (2004). Developing a framework for assessing risks involved in the transportation of dangerous goods. *11th Internatinal Symposium: Loss Prevention and Safety Promotion in the Process Industries*, Praha, Czech Republic, 4495-4503.

Verter, V. and Kara, B. Y. (2001). A GIS-based framework for hazardous materials transportation risk assessment. *Risk Analysis, 21*(6), 1109-1120.

West, H., Qiao, Y., and Mannan, M. (2005). LNG-water rapid phase transition: A literature review. *LNG Journal*, *May*, 21-24.

Yang, K. (1973). Explosive interaction of liquefied natural gas and organic liquids. *Nature*, *243*(May), 221-222.

Yen, J. and Langari, R. (1999). *Fuzzy logic: Intelligence, control, and information.* Upper Saddle River, NJ: Prentice-Hall.

Zhang, J., Hodgson, J. and Erkut, E. (2000). Using GIS to assess the risks of hazardous materials transportation in networks. *European Journal of Operational Research, 121*, 316-329.

Zografos, K. G. and Androutsopoulos, K. N. (2004). A heuristic algorithm for solving hazardous materials distribution problems. *European Journal of Operation Research*, *152*, 507-519.

VITA

Yuanhua Qiao was born in Jianping, Liaoning, China, and in 1998 she obtained B. En. degree in Chemical Engineering from Tianjin University, Tianjin, China.

After graduating she was recommended to graduate school without taking the entrance examination, and her research is the nanocarbon production from nickel-based catalysts. In 2001 she received her M. S. degree in Chemical Engineering from Tianjin University, Tianjin, China.

In August 2001 she enrolled at Chemical Engineering Department at Texas A&M University as a Ph.D. student. In January 2002 she joined the Mary Kay O'Connor Process Safety Center and worked under the guidance of Dr. M. Sam Mannan.

Her permanent address is: Kalaqin, Jianping County, Liaoning, P. R. China